ปฏิกิริยาออกซิเดชันของแอลกอฮอล์บนตัวเร่งปฏิกิริยา TS-1

นางสาวเกศสุดา ชัยรัตน์

วิทยานิพนธ์นี้เป็นส่วนหนึ่งของการศึกษาตามหลักสูตรปริญญาวิศวกรรมศาสตรมหาบัณฑิต
สาขาวิชาวิศวกรรมเคมี ภาควิชาวิศวกรรมเคมี
คณะวิศวกรรมศาสตร์ จุฬาลงกรณ์มหาวิทยาลัย
ปีการศึกษา 2547

ISBN 974-53-1416-1

OXIDATION REACTION OF ALCOHOLS OVER TS-1 CATALYST

Miss Kedsuda Chairat

A Thesis Submitted in Partial Fulfillment of the Requirements
for the Degree of Master of Engineering in Chemical Engineering
Department of Chemical Engineering
Faculty of Engineering
Chulalongkorn University
Academic Year 2004

ISBN 974-53-1416-1

Thesis Title	OXIDATION REACTION OF ALCOHOLS OVER TS-1 CATALYST
By	Miss Kedsuda Chairat
Field of Study	Chemical Engineering
Thesis Advisor	Associate Professor Tharathon Mongkhonsi, Ph.D.

Accepted by the Faculty of Engineering, Chulalongkorn University in Partial Fulfillment of the Requirements for the Master's Degree

……...Dean of the Faculty of Engineering
(Professor Direk Lavansiri, Ph.D.)

THESIS COMMITTEE

…….. Chairman
(Associate Professor Suttichai Assabumrungrat, Ph.D.)

…….…. Thesis Advisor
(Associate Professor Tharathon Mongkhonsi, Ph.D.)

…….. Member
(Joongjai Panpranot, Ph.D.)

…….. Member
(Amornchai Arpornwichanop, D.Eng.)

เกศสุดา ชัยรัตน์ : ปฏิกิริยาออกซิเดชันของแอลกอฮอล์บนตัวเร่งปฏิกิริยา TS-1
(OXIDATION REACTION OF ALCOHOLS OVER TS-1 CATALYST)
อ.ที่ปรึกษา : รศ.ดร.ธราธร มงคลศรี, 115 หน้า. ISBN 974-53-1416-1

งานวิจัยนี้ทำการศึกษาสมบัติออกซิเดชันของตัวเร่งปฏิกิริยาไทเทเนียมซิลิกาไลต์-1 สำหรับปฏิกิริยาออกซิเดชันของแอลกอฮอล์ต่างๆ ได้แก่ 2-โพรพานอล, 1-โพรพานอล, เอทานอล และเมทานอล ที่มีความเข้มข้น 5% โดยปริมาตร นอกจากนี้งานวิจัยได้ทำการศึกษาผลของความเข้มข้นของออกซิเจนในสายป้อนในช่วง 0-21% โดยปริมาตร ต่อค่าการเปลี่ยนของแอลกอฮอล์และค่าการเลือกเกิดของผลิตภัณฑ์ ปฏิกิริยาทดสอบทดลองโดยใช้ตัวเร่งปฏิกิริยา 0.1 กรัม บรรจุในเครื่องปฏิกรณ์ขนาดเล็ก ทำปฏิกิริยาในช่วงอุณหภูมิ 100 ถึง 500 องศาเซลเซียส ที่ความดันบรรยากาศ งานวิจัยนี้พบว่าตัวเร่งปฏิกิริยาไทเทเนียมซิลิกาไลต์-1 สามารถแสดงสมบัติตัวเร่งปฏิกิริยาที่ดีสำหรับปฏิกิริยาออกซิเดชันของแอลกอฮอล์ในวัฏภาคก๊าซ และสมบัติการทำปฏิกิริยาของตัวเร่งปฏิกิริยาไทเทเนียมซิลิกาไลต์-1 ขึ้นอยู่กับชนิดของสารตั้งต้น สำหรับปฏิกิริยาออกซิเดชันของ 1-โพรพานอล และ 2-โพรพานอล พบว่าอัตราการเกิดปฏิกิริยาออกซิเดชันสูงกว่าอัตราการเกิดปฏิกิยาดีไฮเดรชัน สำหรับปฏิกิริยาออกซิเดชันของเอทานอลพบว่าอัตราการเกิดปฏิกิริยาออกซิเดชันเทียบเคียงได้กับอัตราการเกิดปฏิกิริยาดีไอเดรชัน อย่างไรก็ตามปฏิกิริยาออกซิเดชันมีส่วนสำคัญต่อค่าการเปลี่ยนของเอทานอลในช่วงอุณหภูมิที่ทำปฏิกิริยามีค่าต่ำ (200 ถึง 400 องศาเซลเซียส) สำหรับปฏิกิริยาออกซิเดชันของเมทานอลพบว่าปฏิกิริยาการเผาไหม้มีส่วนสำคัญต่อค่าการเปลี่ยนของเมทานอล

ภาควิชา.....วิศวกรรมเคมี..... ลายมือชื่อนิสิต.....
สาขาวิชา.....วิศวกรรมเคมี..... ลายมือชื่ออาจารย์ที่ปรึกษา.....
ปีการศึกษา.....2547.....

##4670228021: MAJOR CHEMICAL ENGINEERING
KEY WORD: TITANIUM SILICALITE-1/ ALCOHOL/ OXIDATION

KEDSUDA CHAIRAT: OXIDATION REACTION OF ALCOHOLS OVER TS-1 CATALYST. THESIS ADVISOR: ASSOC.PROF. THARATHON MONGKHONSI, Ph.D. 115 pp. ISBN: 974-53-1416-1

This research investigates the oxidation properties of titanium silicalite-1 (TS-1) catalyst for the oxidation of alcohols, such as 2-propanol, 1-propanol, ethanol and methanol at concentration 5 vol%. In addition, the concentration of oxygen in the feed gas from 0-21 vol% is studied to determine the effect of oxygen concentration on the conversion of alcohols and product selectivities. The catalytic test reaction was carried out with 0.1 gram of catalyst packed in a microreactor at temperature ranging from 100 to 500˚C and atmospheric pressure. The research found that the TS-1 can play role as an effective catalyst for alcohol oxidation reactions in gas phase and the oxidation property of the TS-1 catalyst depends on reactant. For 1-propanol and 2-propanol, the oxidation rate is much higher than the dehydration rate. For ethanol, the oxidation rate is quite comparative to the dehydration rate. The oxidation reaction, however, dominates the conversion of ethanol in low reaction temperature region (200-400°C). For methanol, the combustion reaction dominates the conversion.

Department……Chemical Engineering… Student's signature……
Field of study….Chemical Engineering… Advisor's signature……...
Academic year……2004……...

ACKNOWLEDGEMENTS

The author would like to express her greatest gratitude and appreciation to her advisor, Associate Professor Tharathon Mongkhonsi for his invaluable guidance, providing value suggestions and his kind supervision throughout this study. In addition, she is also grateful to Associate Professor Suttichai Assabumrungrat, as the chairman, Dr. Joongjai Panpranot and Dr. Amornchai Arpornwichanop, who have been member of thesis committee.

Many thanks for kind suggestions and useful help go to Miss Patta Soisuwan, Miss Pimporn Chaiyasit, Miss Patchanee Chammingkwan, Miss Wasana Jamsak, Miss Amonrut Muanpug, Miss Cheunkamol Kamolsawat and many friends in the petrochemical laboratory who always provide the encouragement and co-operation along the thesis study.

Finally, she would like to dedicate the achievement of this work to her parents, who have always been the source of her support and encouragement.

CONTENTS

PAGE

CHAPTER **PAGE**

PAGE

LIST OF TABLES

LIST OF FIGURES

FIGURE **PAGE**

CHAPTER I

INTRODUCTION

Selective oxidation is an important reaction that is widely used in several processes to produce chemical intermediates of use in many downstream industries. Oxidation of alcohols into carbonyl compounds is one of the most important functional group transformations in organic synthesis. In recent years, selective oxidation of alcohols using different catalysts is interested [Pestryakov and Lunin (2000), Scire et al. (2003)]. In particular, researches have been carried out to develop suitable heterogeneous catalysts that can be used. Most attention has been given to noble metal and to transition metal oxide catalysts, which are effective for the oxidation of alcohols.

Using an alcohol as a reactant for the oxidation process is an interesting reaction. It is known that C1-C4 alcohols can be converted into alkenes by dehydration reaction or lose a-hydrogen to form aldehydes or ketones depends on reactants by the oxidation or dehydrogenation reactions. The conversion of a low alcohol concentration feed into a more expensive product is more interesting. In this case, the gas phase oxidation is preferred because the process already requires a low reactant concentration to avoid creating explosive mixture.

Previous studies discovered that unsupported Co-Mg-O and supported Co-Mg-O systems can be selectively oxidized alcohols to aldehydes [Mongkhonsi et al. (2001), (2002)]. During the oxidation, the hydroxyl group of alcohol is oxidized to form an aldehyde group.

Titanium silicalite-1 (TS-1) is a zeolite catalyst like ZSM-5 structure containing framework titanium atoms instead of aluminium atoms. TS-1 was first discovered by Taramasso in 1983. The invention of TS-1 material opened a new route in heterogeneous catalyst for several reactions such as hydroxylation and oxidation. TS-1 is usually synthesized by using tetraethyl orthotitanate (TEOT) as Ti source, tetraethyl orthosilicate

(TEOS) as Si source and tetrapropylammoniumhydroxide (TPAOH) as template. TS-1 has two notable advantages: firstly, it is hydrophobic and consequently aqueous hydrogen peroxide can be used as oxidant, and secondly, it is very stable under typical reaction conditions and Ti-leaching is minimal for well prepared samples. Therefore, it has been tested as a catalyst for several important reactions. For example, the hydroxylation of benzene by H_2O_2, the epoxidation of propylene with molecular oxygen and the ethylene epoxidation have been studied. The gas phase selective oxidation of organic reactants using TS-1 has yet to be explored.

In this study, the main objectives of this research were to investigate the oxidation properties of Titanium Silicalite-1 (TS-1) catalyst in gas phase oxidation reactions of alcohols, such as methanol, ethanol, 1-propanol and 2-propanol, and to determine the effect of oxygen concentration in the feed gas on the conversion of alcohol and product selectivities. This research has been scoped as follows:

1) Preparation of TS-1 catalysts by using the hydrothermal method.

2) Characterization of TS-1 catalysts by using the following techniques.

- Determination of bulk composition of Si/Ti by Atomic Adsorption Spectroscopy (AAS).
- Determination of specific area by N_2 adsorption based on BET method (BET).
- Determination of structure and crystallinity of catalysts by X-ray Diffractrometer (XRD).
- Determination of incorporation of Ti atoms as a framework element by Infrared Spectroscopy.
- Determination of oxygen species of an oxide catalyst by Temperature Programmed Reeduction (TPR)

3) Catalytic reactions (of alcohols) in gas phase oxidation at 100 - 500°C and atmospheric pressure.

This present work is organized as follows:

The background and scopes of the research are described in chapter I.

Chapter II presents literatures related to TS-1 catalysts and oxidation of alcohols on various reaction in the past and comments on previous work.

The theory of this research, studies about the oxidation reaction and its possible mechanism, and the properties of TS-1 catalysts are presented in chapter III.

Chapter IV consists of procedures of catalyst preparation, catalyst characterization and catalytic reaction in gas phase oxidation of alcohols.

The experimental results of the characterization of TS-1 catalysts, and the methanol, ethanol, 1-propanol and 2-propanol oxidation reactions over these catalysts, including an expanded discussion, are described in chapter V.

Chapter VI contains the overall conclusion emerging from this research and some recommendations for future work.

Finally, the sample of calculation of catalyst preparation, external diffusion limitations, calculation of specific surface area, calibration curves from area to mole of alcohols, alkenes, ketones and the others, and data of the experiments which had emerged from this research are included in appendices at the end of this thesis.

CHAPTER II

LITERATURE REVIEW

The invention of TS-1 catalyst, opened a new field in heterogeneously catalyzed various oxidation reaction such as the epoxidation of alkenes, the oxidation of alcohols, the phenol hydroxylation etc. in both gas and liquid phases. Some TS-1 catalyzed processes are advantageous from the environmental point of view as the oxidant is aqueous H_2O_2, which turns into water, and the reactions, operated in liquid phase under mild conditions, show very high selectivities and yields reducing problems and cost of by-product treatment. In addition, TS-1 can catalyze a variety of useful oxidation reactions in the presence of O_2 as the oxidant, carried out in gas phase is also well known. Many researches have been written about the development of preparations, characterization and conditions for the oxidation reaction but no one has studied about the gas-phase oxidation of the alcohols over TS-1 by using oxygen as the oxidant before.

This chapter divides the reviewed works into two parts, i.e., (a) the preparation, characterization of the TS-1 catalyst and the oxidation of organic compound over the TS-1, and (b) The oxidation of organic compounds by using the various catalysts. An attempt will also be made to summarise the present knowledge and understanding of various factors influencing the conversion of the oxidation of organic compounds (such as alkenes, alcohols). In the last section of this review, comments on previous studies that have directly influenced the aims of this study are given.

2.1 Literature reviews

2.1.1 The preparation, characterization of the TS-1 catalyst and the oxidation of organic compound over the TS-1.

Taramasso et al. (1983) invented a new catalyst material constituted by silicon and titanium oxide. The material was given the name titanium silicalite-1 or TS-1, and corresponds to the following formula $xTiO_2.(1-x)SiO_2$. The material was

prepared by using a source of silicon oxide and a source of titanium oxide. The reaction took place in an aqueous phase at a temperature of 130°C to 200°C, and the solid product obtained was calcined in air at 550°C.

Kraushaar-Czarnetzki and van Hooff (1989) reported that TS-1 could also be obtained from [Al]ZSM-5 by dealumination and subsequent treatment with titanium tetrachloride. The obtained TS-1 exhibited the same catalytic properties as hydrothermally synthesized TS-1 of high purity. Moreover, their experimental result showed that the selectivity of their catalyst was strongly affected by the presence of small amounts of non-framework titania.

Van der Pol et al. (1992) synthesized and investigated TS-1 samples of different particle size. Smaller particles were more active than larger particles. From calculation of the Weisz modulus it could be concluded that large zeolite particle were not fully utilized because of pore diffusion limitations. The product distribution was also influenced by particle size.

Duprey et al. (1997) characterized two titanium silicalite-1 samples (A and B) which similar particle size by powder X-ray diffraction, FT-IR and FT-Raman spectroscopy, UV-visible diffuse reflectance spectroscopy (DRS), transmission electron microscopy with X-ray energy dispersion spectrometry, and xenon-129 NMR. The activity and selectivity for the epoxidation of the oct-1-ene by phosphate-free 30% aqueous hydrogen peroxide have been investigated. The critical factors concerning the activities of the samples with molar rations Si:Ti ~ 39 (sample A) and 32 (sample B) were reported to be the distributions of titanium within the microporous materials and within the extraframework titania. They found that Xenon-129 NMR chemical shifts depended dramatically on extraframework impurities and Ti(IV) dispersion. Pure silicalite and nearly perfect TS-1 were not differentiated by xenon-129 NMR, a fact which was tentatively attributed to the “atomic dispersion” of the titanium in the nearly perfect TS-1, as evidenced by X-ray EDS and by the channel dimension.

Davies et al. (2001) compared the study of the crotyl alcohol using hydrogen peroxide and *tert*-butyl hydroperoxide as oxidants with TS-1, Ti-β, Ti-MCM-41 and Ti-grafted-MCM-41 as catalysts. With hydrogen peroxide as oxidant, significant Ti-leaching was observed with all the catalysts except TS-1 (Ti-Alβ > Ti-grafted-MCM-41 > Ti-MCM-41 > Tiβ > Ti-Al-MCM-41 >> TS-1). For Ti-Alβ, Ti-grafted-MCM-41 and Ti-Al-MCM-41, initial heterogeneously catalyzed formation of the epoxide was observed. The formation of a Ti-species in solution was shown to contribute to competing homogeneously catalyzed formation of ether diols and triol. Using *tert*-butyl hydroperoxide as oxidant the Ti-leaching was minimized and selective epoxide formation was observed with Ti-β, Ti-Alβ Ti-MCM-41 as heterogenous catalysts, although, with Ti-Alβ, the ether diols and triol products dominated due to acid catalyzed sovolysis of the epoxide.

Schuster et al. (2001) investigated the activity of titanium and vanadium containing zeolitic and non-zeolitic materials in the oxidative dehydrogenation of propane to propene. Using TS-1 as the catalyst showed the optimum performance. The propane and oxygen partial pressure had no influence on the selectivity, and the mass transport limitation in the macro- and mesopores could be neglected. The addition of water caused a decrease in the conversion, but increased the selectivity, probably due to a competitive adsorption of the water molecules and the reactant molecules on the active site. They assumed that the reaction probably took place on the outer surface of the TS-1 crystallites on Lewis acid sites, the exact reaction mechanism nor the exact active site are not yet clear. In addition, increasing the Lewis acidity by a sulfation of TS-1 in both the gas phase and the liquid phase prior to the reaction resulted in an increase of the conversion of up to 17% with a selectivity about 74% which are the best results up to now.

Wang et al. (2003) investigated the effect of preparation, treatment method of the Ag/TS-1 catalyst and the reaction conditions on propylene epoxidation using oxygen as the oxidant in a fixed-bed quartz glass reactor. The results of effect of preparation condition were divided into three parts. The first one was the effect of Ag loading, showed the amount of Ag loading had an important effect on the catalytic properties. With an increase in the Ag loading, the propylene conversion increased

significantly, and then leveled off, but the selectivity to propylene oxide decreased significantly with an excessive increase of Ag loading. The optimum catalytic activity for Ag loading was 2%. The second one was the effect of support, showed that the different supports loaded with 2 wt.% Ag were prepared such as Ag/TiO_2, Ag/SiO_2, Ag/silicalite-1, Ag/HZSM-5, and Ag/TS-1. Their catalytic activities for the epoxidation of propylene were different. Only TS-1 was the suitable support, and there was a synergy between Ag and TS-1 in the gas phase epoxidation of propylene. The third one was the effect of Si/Ti ratio of TS-1, they found that the Si/Ti ratio of TS-1 had a great effect on the propylene epoxidaton. With an increase in the Si/TI ratio of TS-1, both the propylene conversion and the selectivity to propylene oxide increased. The Si/Ti ratio was 64, the catalyst exhibited optimum performance, 0.92% propylene conversion and 91.21% propylene oxide selectivity.

Moreover, they studied the effect of pretreatment condition of Ag/TS-1 catalysts. The results showed that an increase in the calcination temperature, both the propylene conversion and the selectivity to propylene oxide increased. The catalyst was calcined at 450°C, exhibited the optimum performance. In case of the effect of calcinations methods of Ag/TS-1 catalysts, they presented that calcinations methods had an important effect on the reaction. The optimum activity showed when the catalyst was calcined in air at 450°C. The optimum Ag/TS-1 catalyst, by passing a reactant mixture of C_3H_6, O_2, H_2, and N_2 at 150°C at a volume ratio of 1:2:3:12 with a space velocity of 4,000 h^{-1}, exhibited the best result. At this condition, after 70 min reaction the conversion of propylene and the selectivity to propylene oxide was 1.37 and 93.51%, respectively. The results of the characterization showed that the oxidized Ag species without single electrons played an important role in the epoxidation of propylene.

Yap et al. (2004) studied the direct vapor-phase epoxidation of propylene using hydrogen and oxygen over gold particles prepared by the deposition-precipitation (DP) method on various modified titanium silicalite- (TS-1) supports. The reaction carried out over a reaction time of 24-36 hrs at a space velocity of 7000 ml $g_{cat}^{-1}h^{-1}$ and temperatures of 140, 170, and 200°C. The results showed that gold deposition at pH 9-10 allowed for a consistent amount of 1-3 wt% of the gold

available in solution to be deposited, while still maintaining gold particle diameters in the 2-5 nm range, as observed by TEM. Au/TS-1 catalysts achieved propylene conversions of 2.5-6.5% and propylene oxide selectivities of 60-85% at 170ºC, with dilute Au and Ti catalysts. They explained that propylene oxide rates were not highly influenced by the TS-1 particle size and are thus not proportional to the specific external surface area of the support.

The conclusion that activity may reside in the channels of the TS-1 was supported by the finding that the observable gold particles decorating the TS-1 particle only account for about 30% of the total gold content of the catalyst. Increasing the gold loading up to 0.74 wt% did not increase the propylene oxide rates proportionally, suggesting that the active Au-Ti propylene oxide-forming centers were limited. In contrast to the prevailing interpretation of this catalyst that a critical Au particle diameter of 2-5 nm was essential for propylene oxide activity, their results were consistent with a molecular cluster model where extremely small gold clusters located near Ti sites inside the TS-1 pores or on the external surface are active for propylene epoxidation.

Wang et al. (2004) investigated the effect of calcination atmospheres of Ag/TS-1 catalyst and other Ti-containing supports on propylene epoxidation in the presence of hydrogen and oxygen. The results showed that the calcination atmospheres had an important effect on the catalytic properties. The catalyst, which was calcined in air, exhibited the optimum catalytic activity 0.43% propylene conversion with 92.75% propylene oxide selectivity. However, the catalyst, which was calcined in nitrogen or hydrogen, exhibited obviously activity decrease. The framework titanium species played an important role in the reaction, but the extra framework titanium species also had weak epoxidation activity. They concluded that excessive extra framework titanium species (hexahedral) could decrease the propylene oxide selectivity and the oxidized silver ions are the main active sites for the gas-phase epoxidation of propylene.

2.1.2 The oxidation of organic compound by using the various catalysts.

Yao (1984) studied the catalytic oxidation of ethanol at low concentrations by Pt, Pd, Rh, Ag and the first row transition metal oxide catalysts supported on Al_2O_3. The results presented $CuO/\gamma\text{-}Al_2O_3$ and $Mn_2O_3/\gamma\text{-}Al_2O_3$ gave the highest activity for total oxidation to CO_2. Ethylene was found to be the only product over $\gamma\text{-}Al_2O_3$. The amount of acetaldehyde formed was generally higher with the base metal oxide catalysts than with Pt or Pd. Dehydration by $NiO/\gamma\text{-}Al_2O_3$ produced ethylene was predominant.

Ozkan et al. (1990) reported the oxidation of methanol over transition metal oxide catalysts (oxides of Cr, Mn, Fe, Co, Ni, Cu) which supported on $\gamma\text{-}Al_2O_3$. The results showed that all the catalysts exhibited similar activities for methanol conversion but Cu catalyst was found to be considerably more selective to CO_2.

Rekoske and Barteau (1997) determined the steady-state kinetics of 2-propanol decomposition on oxidized anatase TiO_2 at temperatures ranging from 175 to 325°C and 2-propanol partial pressures from 8.9 to 102.7 Torr. The effects of the addition of O_2 and water to the carrier gas were also investigated. The steady-state reaction resulted primarily in the formation of a dehydration product, propylene, and a dehydrogenation product, acetone, with small amounts of carbon oxides also being observed. Depending on the reaction conditions, the selectivity to either propylene or acetone could range between 5 and 95%. The rate of dehydrogenation increased dramatically with the addition of both O_2 and water, while the dehydration rate was unaffected by their presence. Accordingly, the kinetics of 2-propanol decomposition were investigated using both air and an inert carrier. Using air as the carrier gas, the dehydration and dehydrogenation reactions were determined to be approximately one-half order with respect to 2-propanol partial pressure. The activation energies determined for the two processes were substantially different, 68 kJ mol^{-1} for dehydrogenation and 130 kJ mol^{-1} for dehydration, as evidenced by the strong temperature dependence of the decomposition selectivity. Using an inert carrier, the reaction kinetics depend in a complex fashion on the conversion of 2-propanol. The dependence on conversion was found to arise from the influence of water on the

dehydrogenation kinetics. The presence of water, whether produced by 2-propanol dehydration or added independently, was found to increase the rate of 2-propanol dehydrogenation. The results of the present study can be reconciled with previously reported steady-state and temperature-programmed desorption investigations of 2-propanol on TiO_2 by recognizing the influence of both surface hydroxyls and the use of an oxidizing carrier gas on the dehydrogenation and dehydration pathways at steady state.

Mongkhonsi et al. (2000) investigated the selective oxidation reaction of ethanol and 1-propanol over V-Mg-O/TiO_2 catalyst. Ethanol and 1-propanol could be selectivity oxidized to ethanal and propanal, respectively. Aldehyde yield up to 73% and 66% for ethanal and propanal, respectively, were achieved in the temperature range 200-250^{o}C. The catalyst was rather inactive for the further oxidation of aldehyde products to carboxylic acid.

Pestryakov and Lunin (2000) studied the active electronic states of the supported metal catalysts (Ag, Cu, Au) in the processes of alcohol partial oxidation by physicochemical methods. Comparison of the obtained catalytic and spectroscopic data revealed that one-charged cations M^{+} were the active sites of the local interaction on the metal catalyst surface in the processes of alcohol oxidation. The catalyst selectivity strongly depended on the effect charge of the surface active sites.

Mongkhonsi et al. (2001) studied the reactivity of Co-Mg-O catalyst in the gas phase selective oxidation of methanol, ethanol, 1-propanol and 2-propanol by using a tubular flow reactor. The Co-Mg-O system has shown the potential as a selective oxidation catalyst for the production of aldehydes from ethanol and 1-propanol. They found that another advantage of this catalyst system is the other by-products form in a small amount and can be removed from the product stream by any conventional process. The oxidation of methanol and 2-propanol does not produce any oxygenate compound. Oxidation of methanol produced mainly CO_2 while the major products for the oxidation of 2-propanol was propene.

Mongkhonsi et al. (2002) investigated the oxidation of 1-propanol and 2propanol by Co-Mg-O catalysts supported on TiO_2 and Al_2O_3. The reaction condition carried out in gas phase by using oxygen as the oxidant. They found that the catalytic activity of the supported Co-Mg-O catalysts depended on the reactant. Propanal was the primary product of 1-propanol oxidation reaction. In the case of 2-propanol oxidation, the primary product at low reaction temperature was propene, while at high reaction temperatures, propanal began to appear as others main product. The direct oxidation of propene confirmed that the catalysts could directly oxidize propene to propanal. The sequence of cobalt and magnesium loading had no observable effect on the structure or catalytic performance of the catalysts studied.

Unnikrishnan and Endalkachew (2002) studied selective oxidation of various primary and secondary alcohols in a gas-phase photochemical reactor using immobilized TiO_2 catalyst. An annular photoreactor was used at 190°C with an average contact time of 32 second. The system was found to be specifically suited for the selective oxidation of primary and secondary aliphatic alcohols to their corresponding carbonyl compounds. Benzylic alcohols gave higher conversions, however, with more secondary reaction products. The reaction mechanism for various products formed was explained. The effects of different reaction parameters, such as O_2/alcohol ratio, water vapor, UV light, and contact time, were studied. The presence of oxygen was found to be critical for the photooxidation. Water vapor in the feed was also found to be helpful in the reaction, although it was not as critical as in hydrocarbon oxidation, where it was necessary for hydroxylating the catalyst surface and sustaining its activity. In alcohol oxidation, surface hydroxylation could be partially provided by the hydroxyl groups of the alcohol itself. Catalyst deactivation was also observed and is attributed to the surface accumulation of reaction products. However, the catalyst regained its original activity after regeneration by calcination in air for 3 hours at 450°C.

Scire et al. (2003) investigated the gold/cerium oxide catalyst, which was prepared by coprecipitation (CP) and deposition-precipitation (DP) on the catalytic combustion of some representative volatile organic compounds, such as 2-propanol, methanol and toluene by using oxygen as the oxidant. From the results, deposition-

precipitation method has been found to be more suitable than coprecipitation to obtain highly active Au/CeO_2 catalysts, because the deposition-precipitation method leads to gold nanoparticles, which are preferentially located on the surface of ceria. The high activity of the Au/CeO_2 system might be related to the capacity of gold nanoparticles to weaken the Ce-O bond, thus increasing the mobility or reactivity of the surface lattice oxygen, which is involved in the volatile organic compounds oxidation through a Mars-van Krevelen reaction mechanism.

Sato et al. (2003) investigated the selective dehydration of 1,3-diols into allylic alcohols at 300-375°C by using CeO_2 catalyst in a usual fixed bed flow reactor. In the dehydration of 1,3-propanediol over pure CeO_2, 2-propen-1-ol is produced with the maximum selectivity of 98.9 mol% at 325°C. In the dehydration of 1,3-butanediol, 2-butane-1-ol and 3-buten-2-ol were produced with the sum of the selectivity >99 mol% over CeO_2, which showed attractive catalytic performance without decay at temperature <375°C. In the reaction of 2-buten-1-ol, 1,2- and 1,4-butanediol, little dehydrated products were detected over the CeO_2.

2.2 Comment on previous works

From the previous studies about the reaction, there are many researches studied about the oxidation of organic compounds over the TS-1 and other various catalysts. From the reviewed literatures, TS-1 can be catalyzed several reactions both in gas and liquid phases. However there are only few researches about the oxidation of hydrocarbon compounds by O_2 in gas phase and some researches concerning the oxidation of alcohol by H_2O_2 in liquid phase. This review can be inferred that TS-1 could be utilized in various reactions.

Although, the oxidation of alcohol by using TS-1 has been performed before in liquid phase, the previous studies showed no research carried out in gas phase. Thus, the oxidation of alcohol such as methanol, ethanol, 1-propanol and 2-propanol by O_2 using the TS-1 as the catalysts carried out in gas phase is chosen to studied in this research.

CHAPTER III

THEORY

3.1 Reactions of alcohols

Reactions of an alcohol can involve the breaking of either of two bonds: the C-OH bond, with removal of the -OH group; or the O-H bond, with removal of -H bond. Either kind of reaction can involve substitution, in which a group replaces the -OH or -H, or elimination, in which a double bond is formed.

3.1.1 Oxidation

The oxidation of an alcohol involves the loss of one or more hydrogens (α-hydrogens) from the carbon bearing the -OH group. The kind of product that is formed depends upon how many of this α-hydrogens the alcohol contains, that is, upon whether the alcohol is primary, secondary, or tertiary.

A primary alcohol contains two α-hydrogens, and can either lose one of them to form an aldehyde,

A 1^{o}alcohol An aldehyde

or both of them to form a carboxylic acid.

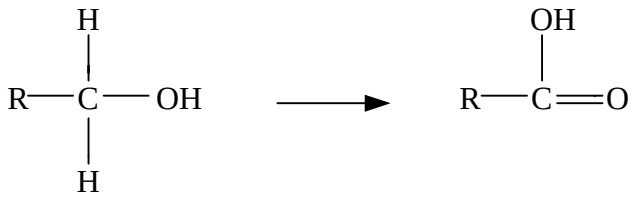

A 1^{o} alcohol A carboxylic acid

A secondary alcohol can lose its only one α-hydrogen to form a ketone.

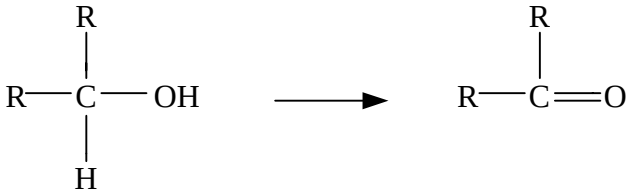

A 2^o alcohol A ketone

A tertiary alcohol contains no α-hydrogen and is not oxidized. (An acidic oxidizing agent can, however, dehydrate the alcohol to an alkene and then oxidized this).

A 3^o alcohol

3.1.2 Dehydration

Dehydration requires the presence of an acid and the application of heat. It is generally carried out in either of two ways: (a) by heating the alcohol with sulfuric or phosphoric acid; or (b) by passing the alcohol vapor over a catalyst, commonly alumina (Al_2O_3), at high temperature. An alcohol is converted into an alkene by dehydration (elimination of a molecule of water).

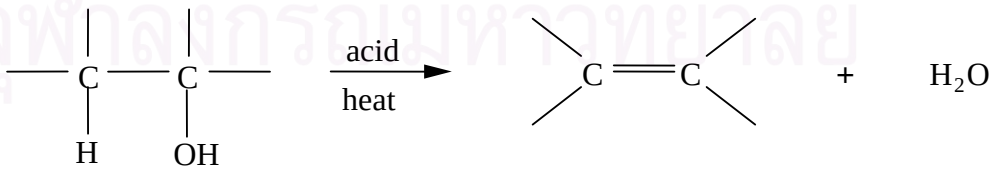

Alcohol Alkene Water

The various classes of alcohols differ widely in ease of dehydration, the order of reactivity being

Ease of dehydration of alcohol $3^o > 2^o > 1^o$

3.2 Titanium silicalite [Notari (1989)]

Titanium silicalite is an interesting material obtained by isomorphic substitution of trivalent metals or tetravalent metals in the framework of crystalline aluminosilicates or silicates. Titanium silicalites with MFI (TS-1) and MFI/MEL (TS-2) structures have been used in several oxidation reactions with H_2O_2 as the oxidizing agent [Centi et al. (2001)].

Titaniun has a stable valence of 4 and in an oxidizing medium it is very likely that this valence is maintained. An examination of the chemistry of Ti^{IV} compounds immediately shows that Ti^{IV} has a strong tendency to assume a high coordination number: with oxygen, six groups in octahedral coordination form a stable and very frequently observed configuration, but to do this Ti^{IV} must have near neighbours capable of increasing their coordination number to satisfy at the same time titanium valency of four and coordination of six. When bulky groups are linked to Ti^{IV}, tetrahedral coordination is also observed. Coordination of seven in. a pentagonal pyramidal arrangement like in peroxo compounds and of eight like in $Ti(NO_3)_4$ are also observed.

From the crystalline structure and the regular change in unit cell parameters which are consistent with isomorphous substitution of Si^{IV} with Ti^{IV} it seems justified to represent TS-l as a silicalite in which few Ti^{IV} have taken the place of Si^{IV}. The interpretation of the catalytic activity of TS-l must take into consideration the role played by these few Ti^{IV}: in fact pure silicalite is totally inactive, and other phases containing Ti have not been identified. Due to the fact that TS-l crystallizes from a homogeneous solution, it is reasonable to assume that the distribution of Ti^{IV} in the crystal lattice is at random; since the Si/Ti ratio is in the range 40 - 90 in typical preparations, most Ti^{IV} must be isolated from each other by long sequences of -O-Si-O-Si-O-. If Ti^{IV} replaces a Si^{IV} it should be tetrahedrally coordinated by $O^{=}$: however, the presence of a band at 980 cm^{-1} closely corresponds to the band observed in other titanium compounds containing the $\diagdown\!\!\diagup$ Ti = O group, whose streching frequency is 975 cm^{-1} with bond distances of 1.66 – 1.79 Å; furthermore, hydroxyl

groups are present at the surface as shown by the increase in selectivity which is obtained upon silylation.

Finally, near neighbour positions of Ti^{IV} are occupied by Si^{IV} which in a field of $O^{=}$ is stable only in tetrahedral coordination. A simple representation of the sites where substitution has occurred which takes into consideration the various pieces of experimental evidence could be

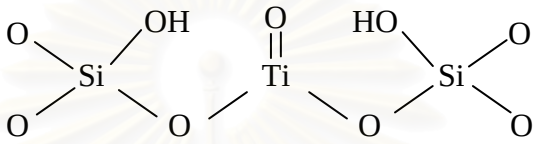

Other more elaborated and detailed representations could be given, should the present model prove inadequate to interpret all experimental facts. Ti^{IV} in TS-1 maintains the strong affinity of soluble Ti^{IV} salts for H_2O_2 and in fact the addition of H_2O_2 gives rise to a strong yellow colour which can be attributed to the formation of surface titaniunperoxocompounds which can be in the hydrated or dehydrated form and which constitutes the actual oxidants.

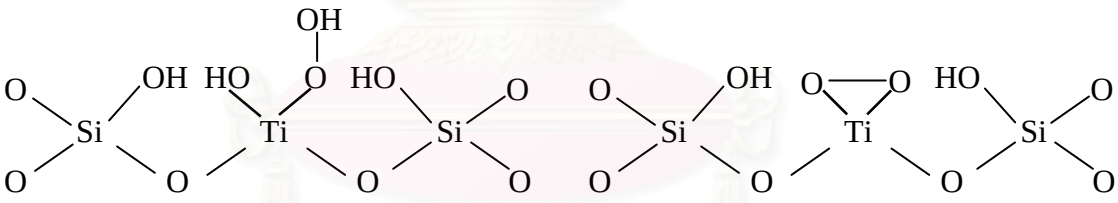

Work carried out on Mo(VI) and W(VI) peroxocompounds [Amato et al. (1986)] has demonstrated that peroxocompounds can act as oxidants in stoichiometric epoxidations involving a nucleophilic attack of the substrate to the peroxidic oxygen: in the presence of excess H_2O_2 the peroxo compound is regenerated and this accounts for the catalytic nature of the reaction. It seems reasonable to assume that a similar mechanism operates in the case of Ti(IV) peroxocompounds. The relevance of isolated Ti^{IV} and the connection with catalytic performances appears to hold also for the TiO_2/SiO_2 catalyst. In fact high epoxide selectivities are obtained when TiO_2 is distributed on high surface area SiO_2 and its concentration is limited to 2% [Sheldon, (1980)]. It is very likely that at this low concentration Ti^{IV} are isolated and surrounded by Si^{IV}. Furthermore, SiO_2 or TiO_2 alone, or physical mixtures of SiO_2

and TiO_2 or various metal titanates exhibit no significant activity. Similarly, supporting TiO_2 on carriers different from SiO_2 like Al_2O_3, MgO or ZrO_2 leads to catalysts whose activity is lower or nil. One piece of evidence seems very convincing: when the TiO_2 concentration on the catalyst is reduced from 4% to 0.4%, all other conditions being equal, an increase in epoxide selectivity is obtained. The only effect that a reduction in the concentration of TiO_2 can have is an increase in the degree of dispersion of each Ti^{IV}: chances for each Ti^{IV} of having Si^{IV} as near neighbours increase, as does the selectivity of the catalyst. The correlation between the isolated Ti^{IV} and selectivity of the catalyst in epoxidation could be due to the fact that on Ti^{IV} having other Ti^{IV} as near neighbours, a mechanism proceeding through a bimolecular interaction of surface peroxo species could be operating which would give rise to a high decomposition rate of H_2O_2 or hydroperoxides to O_2. This mechanism could not operate on perfectly isolated Ti^{IV}.

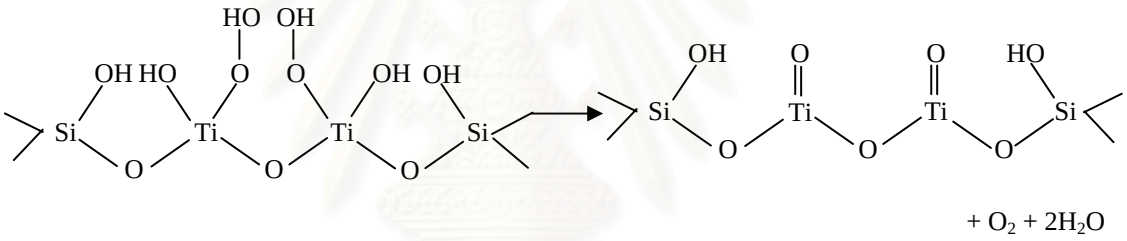

$+ O_2 + 2H_2O$

Low decomposition of H_2O_2 (or hydroperoxides as well) means greater stability of titanium peroxo compound whose reduction can only be carried out by the organic substrate with increased yields of useful oxidized products. When the different results between TS-1 and TiO_2/SiO_2 in the hydroxylation of phenol are analyzed the existence of a “restricted transition state selectivity” must be assumed to explain the small amount of tars formed.

CHAPTER IV

EXPERIMENTAL

This chapter consists of experimental systems and procedures used in this study. The chapter is divided into three sections, i.e., catalyst preparation, catalyst characterization and catalytic reaction. The chemicals, apparatus and procedures for catalyst preparation are explained in section 4.1. The composition, structure and surface properties of the catalyst characterized by various techniques such as AAS, XRD, BET, FT-IR and TPR are discussed in section 4.2. Finally, the details of the catalytic reaction are illustrated in section 4.3.

The scope of this study

The reaction conditions are chosen as follows:

Catalyst	:	Titanium silicalite-1 (TS-1)
Reactant	:	Methanol, Ethanol, 1-Propanol, 2-Propanol
Feed composition	:	Methanol 5 vol%, Oxygen 0-21 vol%, Ethanol 5 vol%, Oxygen 0-21 vol%, 1-propanol 5 vol%, Oxygen 0-21 vol%, 2-propanol 5 vol%, Oxygen 0-21 vol%, Nitrogen balance
Flow rate of reactant	:	100 ml min^{-1}
Reaction temperature	:	100-500^{o}C
Space velocity	:	60,000 ml $g^{-1}h^{-1}$

4.1 Catalyst preparation

4.1.1 Chemicals

The details of chemicals used in the preparation procedure of TS-1 are shown in Table 4.1.

Table 4.1 The chemicals used in the catalyst preparation

Chemical	Grade	Supplier
Tetrapropylammonium hydroxide, 1.0 M solution in water	-	Aldrich
Tetraethyl orthosilicate 98%	-	Aldrich
Tetraethyl orthotitanate 95%	For synthesis	Merk-Schuchardt

4.1.2 Preparation Procedures

Tinanium silicalite-1 (TS-1) was prepared according to the hydrothermal procedure.

4.1.2.1 Preparation of Solution

Tetraethyl orthotitanate was added dropwise to tetraethyl orthosilicate and then the mixture solution was stirred at 35°C. To the clear solution, tetrapropylammonium hydroxide was added with stirring and then heating at 80°C for 1 hour. The clear gel was stirred at 80°C for 3 hours to aid hydrolysis, during the procedure the volume of the mixture solution was maintained by adding de-ionized water.

4.1.2.2 Crystallization

The mixture of solution was filled in a 250 ml Pyrex glass. The glass container was placed in a stainless steel autoclave. The atmosphere in the autoclave was replaced by nitrogen gas and pressurized up to 3 kg/cm^2 gauge. The mixture was heated from room temperature to 175°C with a heating rate of 2°C/min and held at this temperature for 4 days while being stirred at 60 rpm, followed by cooling the mixture to room temperature in the autoclave overnight. The product crystals were washed with de-ionized water until the pH of the washing water decreased from about 10 to 7. Then the crystals were dried in an oven at 110°C for 24 hours.

4.1.2.3 Calcination

The dry crystals were calcined in an air stream at 550°C and held at that temperature for 6 hours, by heating them from room temperature to 550°C with heating rate 8.6°C/min. The organic templates were burned off leaving cavities and channels in the crystals. The calcined crystals were finally cooled down to room temperature and stored in a dessicator for later use.

4.2 Catalyst characterization

4.2.1 Determination of composition content of catalysts

The composition analysis of elements in the bulk of the catalyst was performed by atomic absorption spectroscopy (AAS) using Varian, Spectra A8000 at the Department of Science Service Ministry of Science Technology and Environment.

4.2.2 X-ray Diffraction (XRD)

The crystallinity and X-ray diffraction patterns of the catalysts were performed by an X-ray diffractometer, SIEMENS D5000, using Cu Kα radiation with Ni filter. The operating conditions of measurement are shown below :

2θ range of detection : 6-40^{o}

Resolution : 0.04^{o}

Number of scan 10

4.2.3 Temperature Programmed Reduction (TPR)

The reducible site was determined by measuring the amount of H_2, which reduced oxide species on the surface. The product of this reaction was water vapor, which was trapped by liquid nitrogen. The thermal conductivity detector (TCD) measured the amount of H_2 passed through the sample. The operating conditions of the TCD are shown in Table 4.2.

Table 4.2 Operating conditions of TCD for temperature programmed reduction

Detector	**TCD**
Carrier gas	5%H_2 / 95%Ar
Carrier gas flow	30 ml min^{-1}
Detector temperature	80^{o}C
Detector current	80 mA

Catalyst sample 0.2 g was placed in a sample tube. The TPR runs were started at 50^{o}C, by allowing the temperature to increase to 500^{o}C at a rate of 10^{o}C min^{-1}.

4.2.4 BET surface area measurement

4.2.4.1 Apparatus

The apparatus consisted of two gas feed lines for helium and nitrogen. The flow rate of gas was adjusted by means of a fine-metering valve. The sample cell was made from pyrex glass. The operation conditions of the gas chromatograph (GOW-MAC) are shown in Table 4.3

Table 4.3 Operation conditions of gas chromatograph (GOW-MAC)

Model	**GOW-MAC**
Detector	TCD
Helium flow rate	30 ml min^{-1}
Detector temperature	80°C
Detector current	80 mA

4.2.4.2 Procedure

The mixture of helium and nitrogen gas flowed through the system at the nitrogen gauge pressure of 0.3. The sample was placed in the sample cell, which was then heated up to 200°C and held at this temperature for 2 hours. The sample was cooled down to room temperature and ready to measure the surface area. There were three steps to measure the surface area.

(1) Adsorption step

The sample cell was dipped into a liquid nitrogen bath. Nitrogen was adsorbed on the surface of the sample until an equilibrium was reached.

(2) Desorption step

The nitrogen-adsorbed sample was dipped into a water bath at room temperature. The adsorbed nitrogen was desorbed from the surface of the sample. The desorb nitrogen caused the recorder signal to move away from the baseline. This step was completed when the recorder signal return back to the base line.

(3) Calibration step

1 ml of nitrogen gas at atmospheric pressure was injected at the calibrations port and the area was measured. The area was the calibration peak.

(4) Then BET surface area is calculated using procedures described in Appendix C.

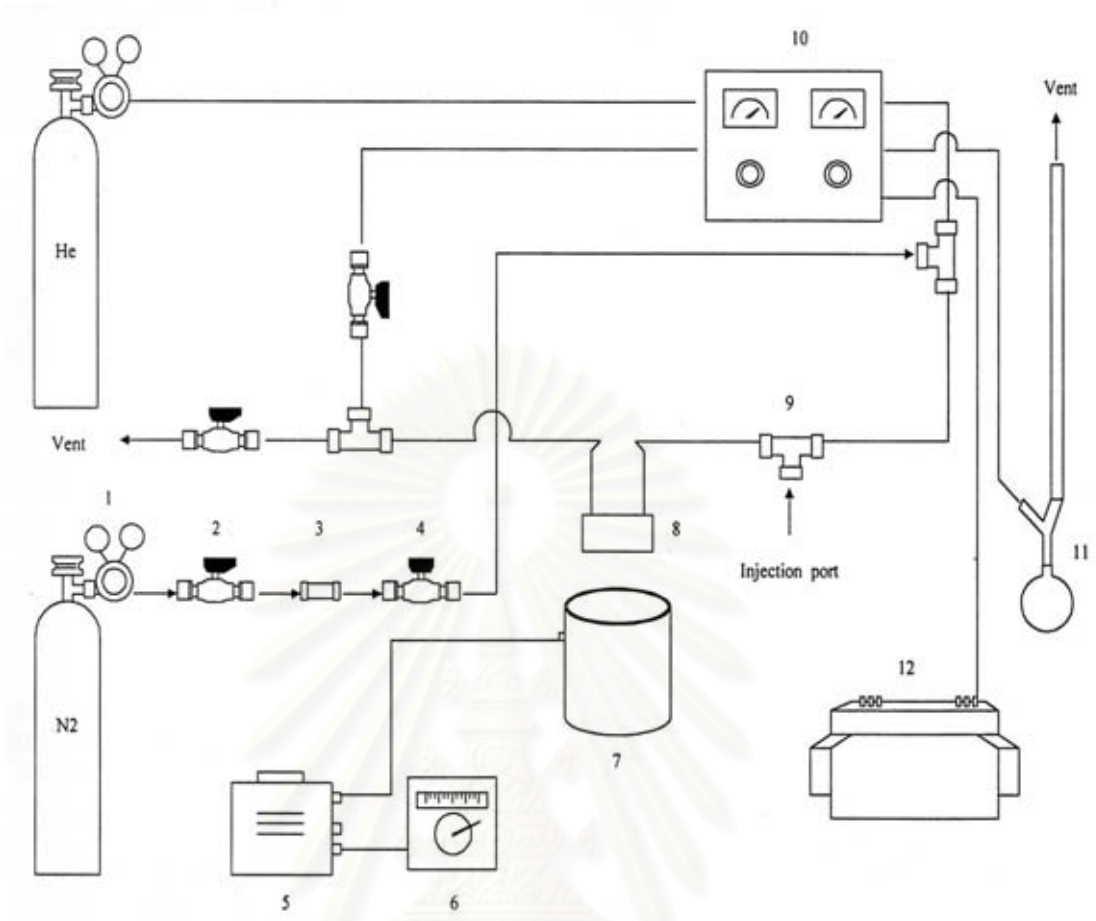

1. Pressure regulator 2. On-Off valve 3. Gas filter
4. Needle valve 5. Voltage transformer 6. Temperature controller
7. Heater 8. Sample cell 9. Three-way valve
10. Thermal Conductivity Detector 11. Bubble flow meter 12. Recorder

Figure 4.1 Schematic diagram of the single point BET specific surface area measurement

4.2.5 Fourier Transform Infrared (FT-IR)

The functional group on the catalyst surface was determined by FT-IR using Nicolet model Impact 400. Each sample was mixed with KBr with ratio of sample, KBr equal to 1:100 and then pressed into a thin wafer. Infrared spectra were recorded between 400 and 1300 cm^{-1} on a microcomputer.

4.2.5.1 Chemicals and reagents

Ultra high purity (99.99%) nitrogen suppies by TIG Ltd. and pyrindine, analytical grade supplied by Univax or Ajax chemical were used in this experiment.

4.2.5.2 Instruments and apparatus

(1) Flow diagram

The schematic diagram of the in situ FT-IR apparatus is represented in Figure 4.2 All gas lines, valves and fittings in this apparatus were made of pyrex glass except the IR gas cell and the sample disk holder, which were made of quartz glass in order to avoid the adsorption of any glass species which may remain on the inner surface of glass tube while the system was evacuated. Nitrogen was used for purging before starting the experiment. Pyridine was added to a glass tube connected which a value which can open to the glass line system. A home made electro-magnetic pump, fixed in the gas line, was used for circulating the gas (including the pyridine vapor) through the sample in order to accomplish the adsorption of gas or pyridine species on the sample surface. A Labconco 195-500 HP vacuum pump, which theoretically had capacity at 10^{-4} Torr, was used for system evacuation. Furthermore, a digital pressure indicator, attached to the gas line, measured the pressure of the system and checked leaking of the apparatus as well.

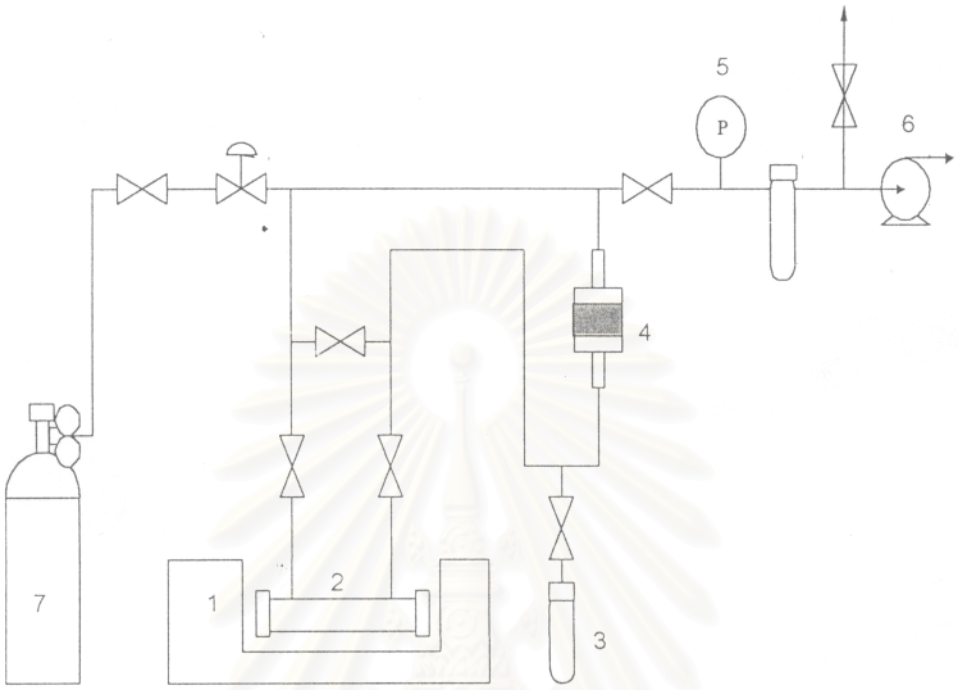

1. FT-IR analyzer
2. IR quartz gas cell
3. Pyridine tube
4. Electro magnetic circulating pump
5. Digital pressure indicator
6. Vacuum pump
7. Nitrogen gas cylinder

Figure 4.2 Flow diagram of instrument used for pyridine adsorption experiment

(2) FT-IR

The FTIR spectrometer was used as a detector in the experiment. A Nicolet model Impact 400 FT-IR equipped with a deuterated triglycine sulfate (DTGS) detector and connected to a personal computer with Omnic version 1.2a on Windows software (to fully control the functions of the IR analyzer) were applied to this study. The analyzer was place on a moveable table for conveniently adjustment.

(3) IR gas cell

The IR gas cell used in this experiment, shown in Figure 4.3, was made of quartz and covered with 32×3 mm NaCl windows at each end of the cell. Each window was sealed with two O-rings and a stainless flange fastened by a set of screws.

The cell is roughly divided into two zones; heating and cooling respect to their temperature. The function of the heating zone at the middle of the IR cell is the increase the temperature for the sample disk. The quartz sample holds for the sample disk to keep it perpendicular to the IR beam, is arranged inside the IR cell in the heating zone. A thermocouple is used to measure the sample disk temperature. The temperature is controlled by a variable voltage transformer and a temperature controller. At both end of the IR cell was cooled water. They were applied to reduce the excessive heating, which may damage O-ring seals and the windows.

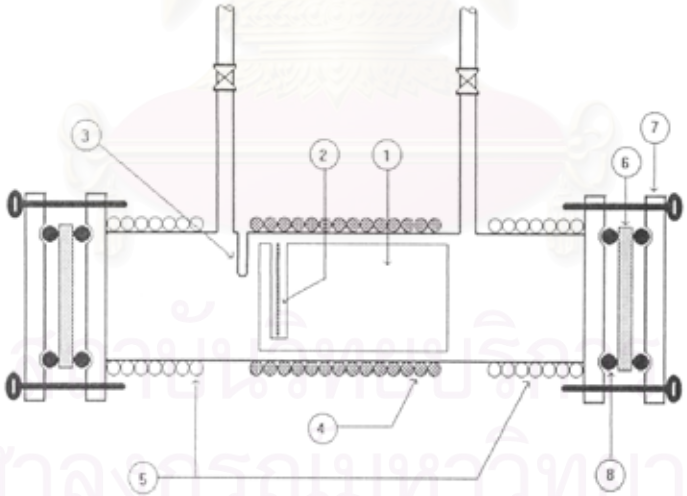

1. Sample holder
2. Sample disk
3. Thermocouple position
4. heating rod
5. Water cooling line
6. KBr window
7. Flange
8. O-ring

Figure 4.3 IR gas cell used for pyridine adsorption experiment.

4.2.5.3 Sample disk preparation

To produce a self-supporting catalyst sample disk for an IR experiment the catalyst was milled thoroughly in a small quartz mortar to obtain a very fine powder. This minimized the scattering of infrared radiation and provided a high quality of spectrum.

The die used was made of stainless steel and is shown in Figure 4.4. The most important part of this die, which is directly in contact with the sample is the so-called the support disks. The support disks are composed of upper and lower disks, each 20 mm. in diameter. The support disks are highly polished to a mirror like finish in order to overcome the sticking of sample to the surface of the die, the main problem in pressing disks. The powder sample, about 0.06-0.065g, was spread to totally cover the surface of the lower support disk placed in the die to make sample having a weight 15-20 mg cm^{-2}. If a thick sample disk was used, a poor IR would scan result and if too thin sample dick was employed, it would be easily cracked by thermal treating as well as broken itself. All part of die was put together and was pressed by a manual hydraulic press at pressure of 140-180 kg cm^{-2} for 5 minutes. The pressure should not be low so that a self-supporting disk cannot form. After pressing, the well-formed disk was carefully removed from the die and mounted in the IR cell.

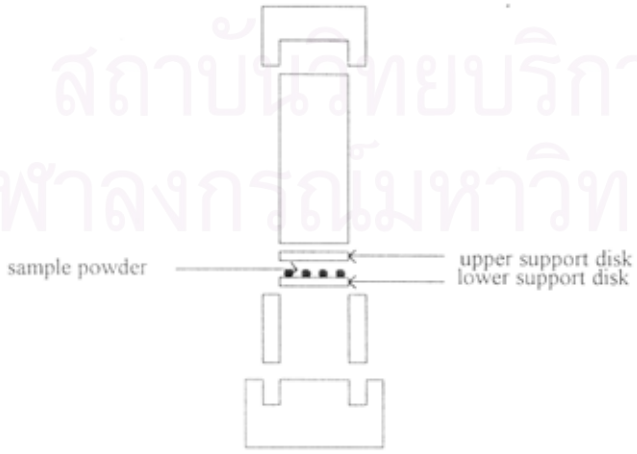

Figure 4.4 Body of the die for preparation of a self-supporting catalyst disk.

4.2.5.4 Experimental procedure

After a well-formed disk sample disk is obtained, it was placed in the sample holder and then the sample holder, including sample disk, was placed into the middle of R gas cell. The sample disk is located as close to the thermocouple probe holes as possible. Once the KBr windows were sealed of the both end of the IR gas cell and the leaks were not observed, the IR gas cell was evacuated by a vacuum pump through the gas line for at least 30 minutes to place the system under vacuum. The sample disk was evacuated in vacuum for 1 hour at room temperature. However, since no change of the IR spectrum of the sample was found during the pre-treatment, this step something ignored. Pyridine vapor was brought into contact with the disk at room temperature. Under vacuum, liquid pyridine evaporates from the pyridine tube in to the gas line leading to the IR gas cell. To achieve the maximum adsorption of pyridine, pyridine vapor was circulated though the system by the electro-magnetic pump for 1 hour or until the IR spectrum of pyridine peak did not change. After that, the IR cell and gas line were evacuated to remove not only pyridine vapor remaining in the cell and gas line but also the physicsorbed pyridine from the catalyst surface too. The vacuum pump was operated until the IR spectra peaks of pyridine vapor and physisorbed pyridine totally vanished and there was no change in any other peaks of the spectra. This normally took around 1.5 hours then, FT-IR measurement of the spectra of the pyridine-adsorbed sample started at room temperature and were repeated at elevated temperature in 50 C steps.

The vacuum pump was kept running while the sample disk and the IR gas cell were heating to remove all species desorbed from the sample surface out of the system in order to avoid disturbing the result spectra by such species. On the other hand, since the vibration would occur and bring about bad scans, the vacuum was switched off while the temperature was held constant for IR detection. The measurement was completed when all peaks of adsorbed pyridine disappeared so that the IR spectra of the sample were identical to the one before pyridine dosing.

4.3 The catalytic activity measurements

4.3.1 Equipment

Flow diagram of the reaction system is shown in Figure 4.5. The system consists of a saturator, a microreactor, an automatic temperature controller, an electrical furnace and a gas controlling system. The liquid phase reactant was filled in the saturator. N_2 or Ar is passed through the evaporator to evaporate the reactant and carried to the microreactor.

The microreactor is made from a stainless steel tube. Three sampling points are provided above and below the catalyst bed. Catalyst was placed between two quartz wool layers.

The gas supplying system consists of cylinders of ultra high purity nitrogen or argon and air, each equipped with pressure regulators (0-120 psig), on-off valves and needle valves for adjusting the flow rate of these gases.

The composition of oxygenate compounds in the feed and product streams were measured by a Shimadzu GC8A gas chromatograph equipped with flame ionization detector.

A Shimadzu GC8A gas chromatograph equipped with a thermal conductivity detector was used to analyze permanent gases and water. Two columns, a 5A molecular sieve to separate oxygen and carbon monoxide and a Porapak-Q column to separate CO_2 and water were operated in parallel. The operating conditions are shown in the Table 4.4.

Table 4.4 Operating conditions for gas chromatograph.

Gas chromatograph	Shimadzu GC8A	Shimadzu GC8A	Shimadzu GC8A
Detector	TCD	FID	FID
Column	MS-5A, Porapak-Q	15% Carbowax 1000	3% SP-1500
Carrier gas	He (99.999%)	N_2 (99.999%)	N_2 (99.999%)
Carrier gas flow	25 ml min^{-1}	25 ml min^{-1}	25 ml min^{-1}
Column temperature			
- Initial	100°C	40°C	70°C
- Final	100°C	80°C	120°C
Detector temperature	130°C	120°C	120°C
Injector temperature	130°C	120°C	120°C
Heating rate	-	4°C min^{-1}	4°C min^{-1}
Analyzed gas	CO, CO_2, H_2O	Oxygenates	Oxygenates

4.3.2 Oxidation procedure

The oxidation procedures are described in the detail below.

1. 0.1 gram of catalyst was packed in the middle of the stainless steel microreactor located in the electrical furnace.

2. The total flow rate was 100 ml min^{-1}. Flow rate of 1-propanol, nitrogen or argon and air were adjusted to the required values. The gas mixtures for oxidation reaction were 5 vol% alcohols, 0-21 vol% oxygen and balance with nitrogen (or argon in case of no O_2 in feed gas).

3. The reaction temperature was between 100-500^{o}C. The effluent gases were analyzed by using the FID and TCD gas chromatographs. The chromatograph data were changed into mole of methane, ethylene, propylene, methanol, ethanol, 1-propanol, 2-propanol, acetaldehyde, isopropyl ether, acetone CO and CO_2 by calibration curves in Appendix D.

4. The result of catalytic test was calculated in the term of

$$\%\ \text{A conversion (C)} = \frac{\text{mole of A converted}}{\text{mole of A in feed}}$$

$$\%\ \text{Selectivity (S) to B} = \frac{\text{mole of B formed}}{\text{mole of A converted}} \times \frac{\text{no. of C atom of B}}{\text{no. of C atom of A}} \times 100$$

$$\%\ \text{Yield (Y) to B} = \frac{\%\ \text{A conversion} \times \%\ \text{selectivity to B}}{100\%}$$

Where, A is reactant

B is product

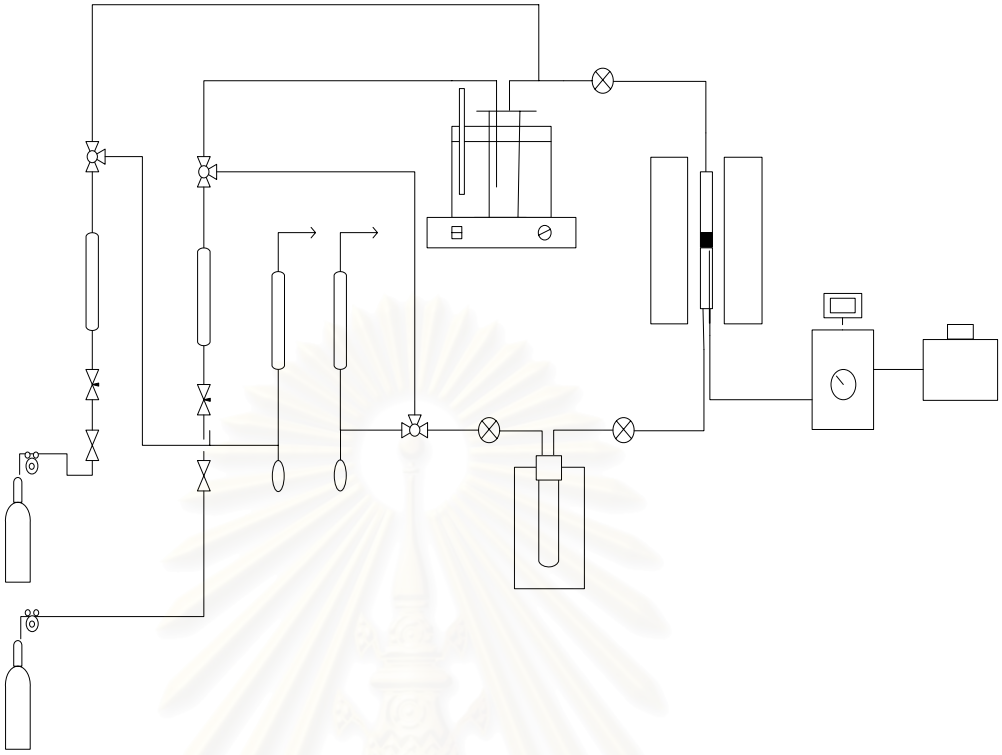

1. Air vessel
2. N_2/Ar vessel
3. Mass Flow controller
4. Three-way-valve
5. Gate valve
6. Needle valve
7. Rotary meter
8. Rubber cock
9. Sampling point
10. Condenser
11. Saturator
12. Furnace
13. Reactor
14. Catalyst bed
15. Temperature controller
16. Digital temperature indicator
17. Variable voltage transformer
18. Thermocouple/Thermometer
19. Pressure regulator
20. Water bath
21. Heating and Stirring controller

Figure 4.5 Flow diagram of oxidation reaction system.

CHAPTER V

RESULTS AND DISCUSSIONS

In this chapter, results and discussion are divided into two parts the first one is the results of characterization of TS-1 sample, such as AAS, BET, TPR, XRD and FT-IR. The second part is the results of catalytic activity of alcohol oxidation reactions.

5.1 Catalyst characterization

5.1.1 Determination of composition content and BET surface area of TS-1 sample

The results of mole ratio of Si/Ti and BET surface area of the TS-1 sample, which were analyzed by atomic absorption spectrometer and BET nitrogen adsorption method respectively, are represented in Table 5.1.

Table 5.1 The mole ratio of Si/Ti and BET surface area

Catalyst sample	Mole ratio of Si/Ti	BET surface area (m^2/g)
TS-1	34	212

5.1.2 X-ray Diffraction (XRD)

Figure 5.1 shows the XRD patterns of the synthesized TS-1. The XRD pattern showed six main characteristic peaks at 2θ as 8, 8.8, 14.8, 23.1, 24 and 29.5 degree, marked with dark circle.

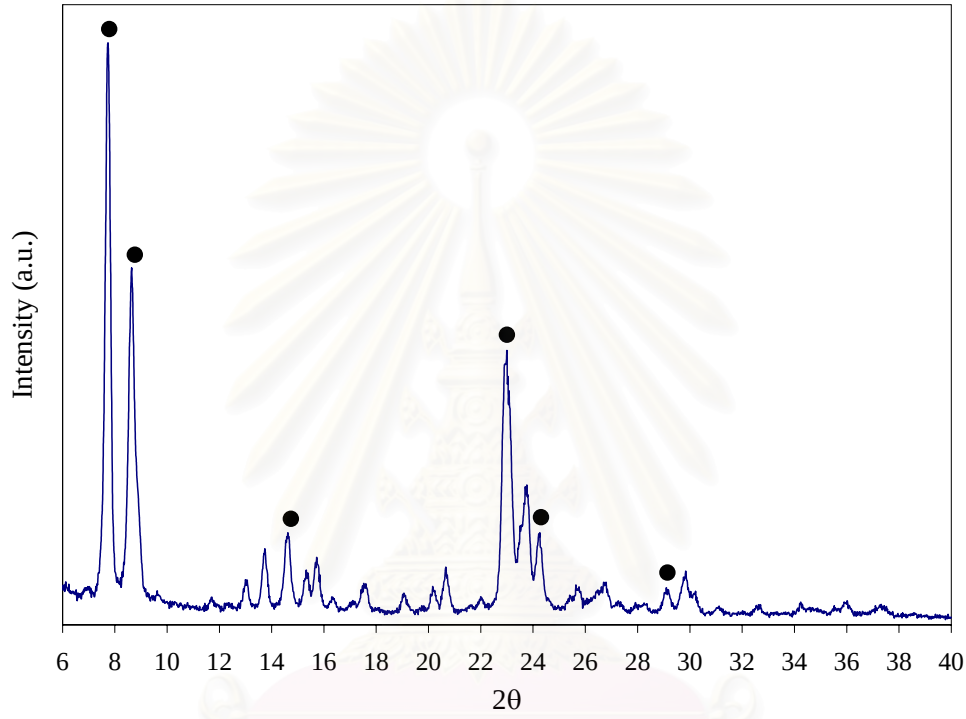

Figure 5.1 X-ray diffraction pattern of the synthesized TS-1

The pattern obtained is the pattern typical for a crystalline zeolite having a MFI structure. The result showed that the catalyst contained a well-defined single-phase XRD pattern and was consistent to those already reported for TS-1 [Taramasso et al. (1983)]. The incorporation of Ti^{4+} into the framework is indicated by the conversion of the monoclinic structure of silicalite-1 to an orthorhombic structure, evidenced by the disappearance of peaked splittings at 2θ = 24˚ and 2θ = 29.5˚ [Taramasso et al. (1983)]. Because of the low Ti content in the support materials (Ti < 3 wt%), additional TiO_2 crystalline phases, i.e., anatase (2θ = 25.5˚) and rutile (2θ = 48.2˚) [Yap et al. (2004)], did not appear in the XRD pattern.

5.1.3 Fourier Transform Infrared (FT-IR)

5.1.3.1 General character

A comparative IR spectrometric study was performed to obtain information concerning the existence of framework titanium. The spectrum obtained is exhibited in Figure 5.2. It is well known that the vibrational spectrum of TS-1 is characterized by an absorption band in the 900–975 cm^{-1} region [Taramasso et al. (1983)]. It has been suggested that the presence of a 960–975 cm^{-1} band is a necessary, but not sufficient, condition for catalytic activity [Huybrechts et al. (1991)]. Thus, defective orthorhombic silicalites, with fully hydroxylated nanocavities generated by extraction of a few adjacent (SiO_4) units, have been characterized by an extra-broad IR absorption at ca. 970 cm^{-1} [Perego et al. (1986)] as shown in Figure 5.2.

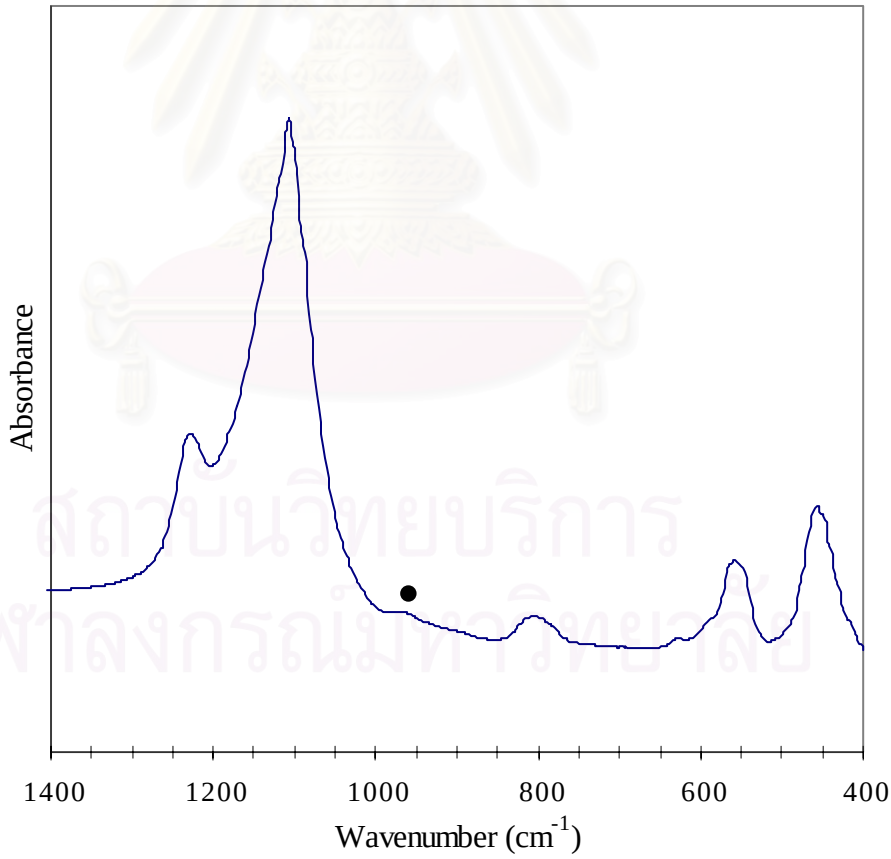

Figure 5.2 Ex- situ IR spectra of the synthesized TS-1

5.1.3.2 Surface acidity

In general, strong bases, as adsorbate, should in principle be suitable probes for the evaluation of the overall acidity of catalysts, as well as to distinguish between protonic (Brønsted) acidity and aprotic (Lewis) acidity. In this work, pyridine is used as probe molecules for acidity measurements.

Figure 5.3 demonstrates the infrared spectra obtained from the adsorption of pyridine on the synthesized TS-1 at room temperature followed by the temperature programmed desorption under vacuum up to 300ºC. It is observed that the spectrum of the adsorbed pyridine at room temperature shows obvious bands at 1445 cm^{-1} and 1490 cm^{-1}due to the adsorbed pyridine on Lewis acid sites. On the other hand, the bands at 1545 cm^{-1} and 1635 cm^{-1} representative to the pyridinium ion on Brønsted acid site cannot be detected on this catalyst. This result suggests that on the TS-1 catalyst only Lewis acid sites are present. After heating under evacuation from room temperature to 300°C, it can be seen that all bands gradually decreased with increasing temperature until hardly detectable at 300°C.

To study the acid strength of Lewis acid sites, the rate of desorption as well as the amount of desorbed pyridine on Lewis acid sites at various temperature are closely observed by focusing on the distinct bands at 1445 cm^{-1} and 1490 cm^{-1} as shown in Figure 5.3. It is found that most of the adsorbed pyridine on Lewis acid sites was dramatically released at temperature below 100ºC. Nevertheless, there was about 20% of the adsorbed pyridine remained on the catalyst surface at temperature above 150ºC. This indicated that a majority of acid sites on TS-1 catalyst behaves as the weak Lewis acid sites.

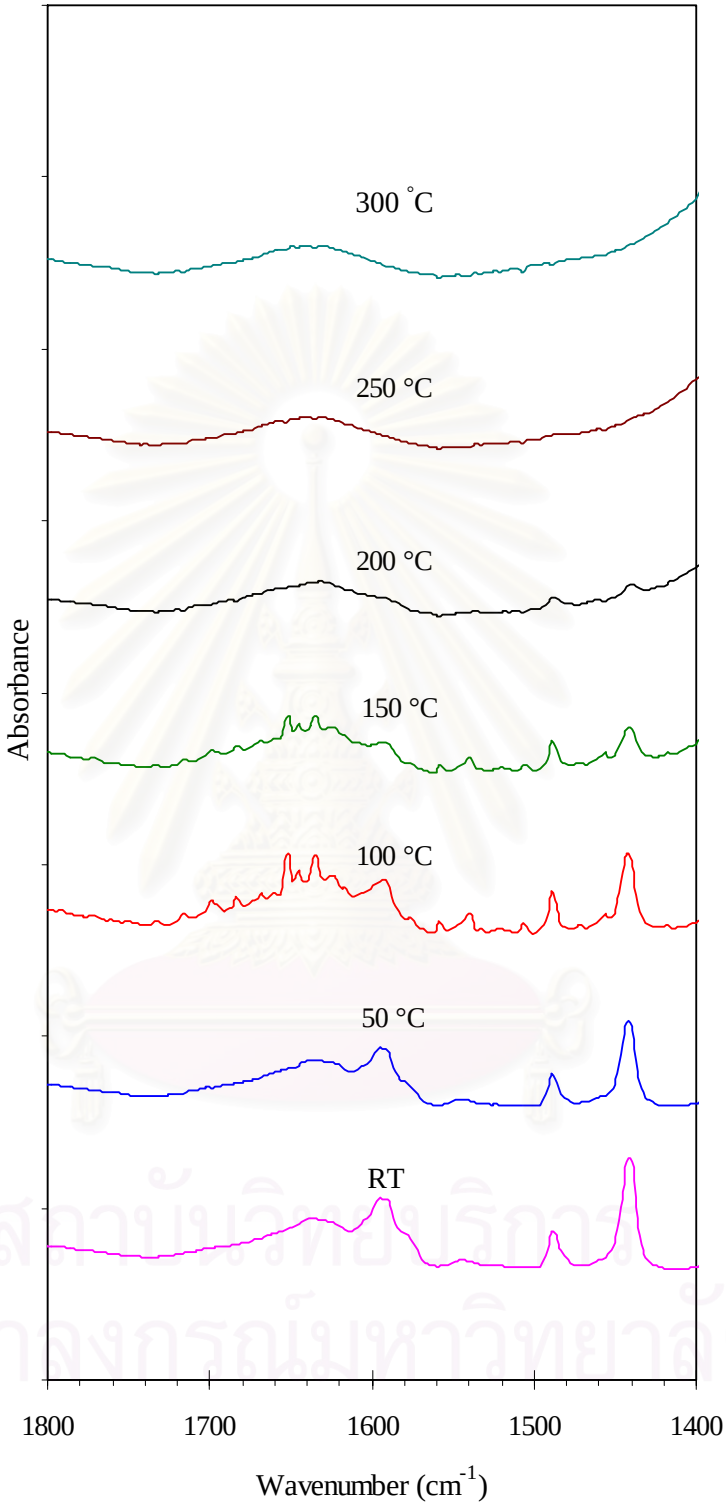

Figure 5.3 In- situ IR spectra of the synthesized TS-1

5.1.4 Temperature Program Reduction (TPR)

Temperature programmed reduction (TPR) is an important method to classify the oxygen species of an oxide catalyst. %Reducibility of a catalyst can be calculated from the area under temperature programmed reduction peaks. The temperature programmed reduction profile of the synthesized TS-1 is shown in Figure 5.4. The reduction profile composed of three main peaks with maxima at about 310°C (T1), 570°C (T2) and 800°C (T3), respectively. These peaks can be assigned to difference oxygen species, which are located in difference positions of the MFI structure. It is noticed that there are interaction of oxygen species on the surface of synthesized TS-1 catalyst. At lower temperature, a small amount of oxygen species can be removed, while the higher amount was removed at high temperature.

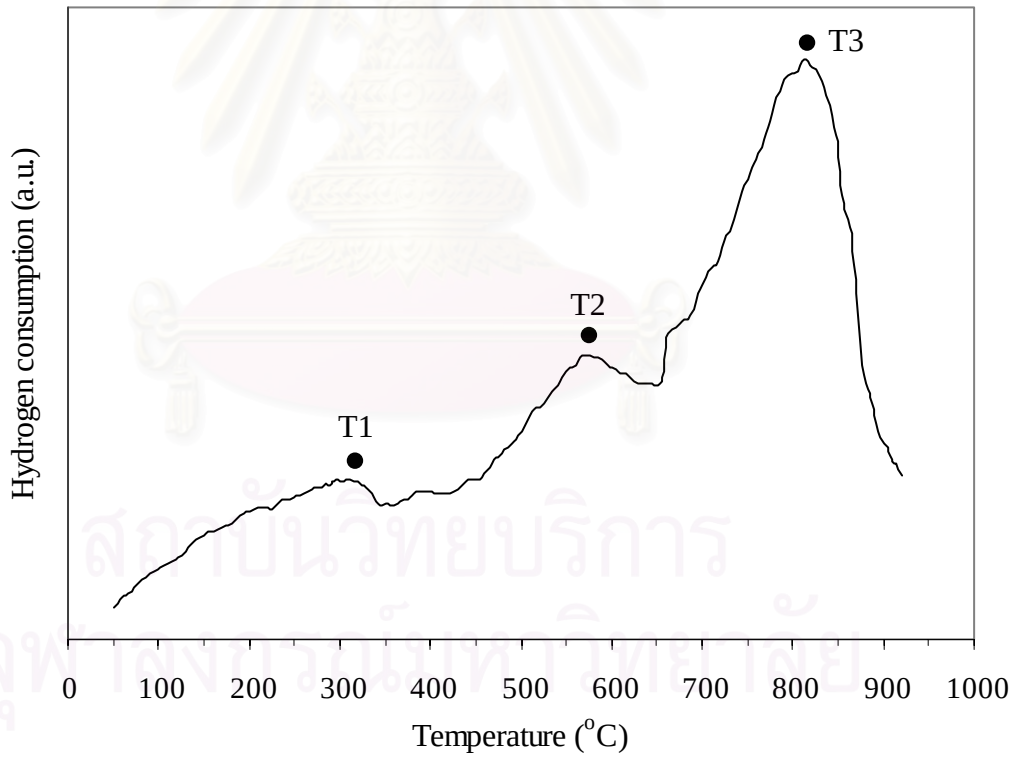

Figure 5.4 Temperature programmed reduction profile of the synthesized TS-1

5.2 Catalytic reaction

5.2.1 2-propanol oxidation

This part investigated the blank test reaction of 2-propanol for 0 vol% O_2 system, with no catalyst present in the reactor is shown in Figure 5.5.

The oxidation reaction shows the poor activity of the reaction system (the stainless steel reactor), no 2-propanol conversion was observed below the reaction temperature of 350°C. At the higher reaction temperature, however the conversion slightly increased. The products observed were propylene and acetone. The formation of propylene should be due to the dehydration of 2-propanol. The formation of acetone will be discussed later in this section.

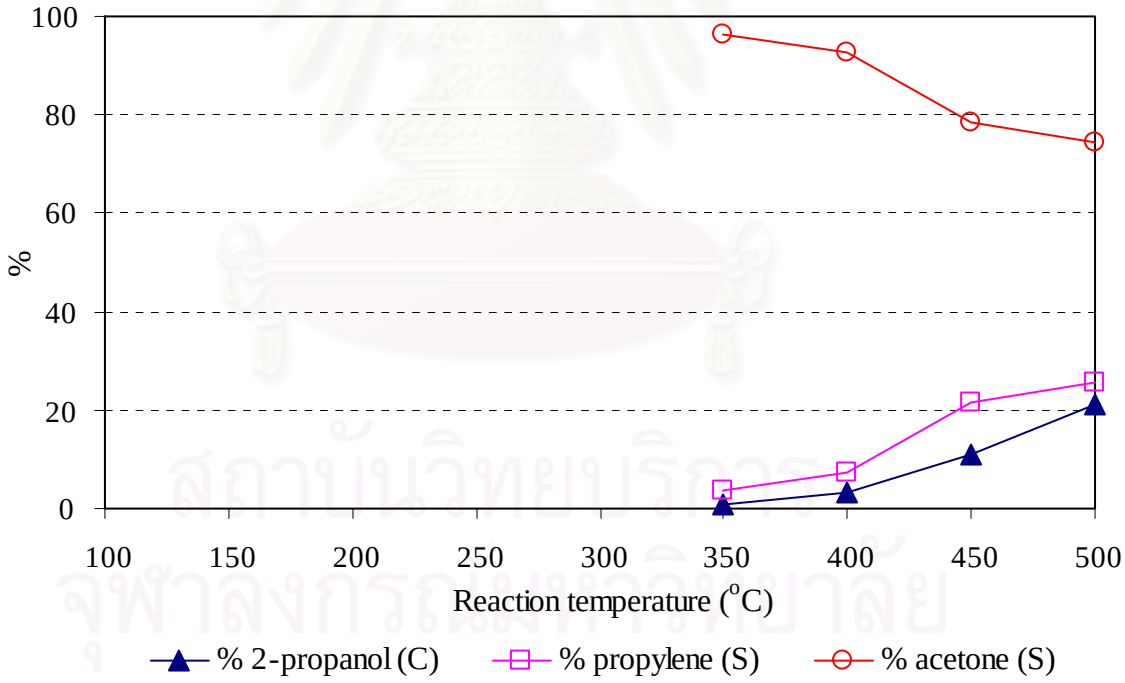

Figure 5.5 Product selectivities and conversion of 2-propanol without TS-1 for 0 vol% O_2 system (C-Conversion, S-Selectivity)

The results of conversion and product selectivities of 2-propanol oxidation are presented on Figures 5.6a-5.6d for 0 vol%, 8 vol%, 16 vol% and 21 vol% of oxygen concentration in the feed gas, respectively. Beyond 0 vol% O_2 system, the conversion of 2-propanol rapidly increased in the reaction temperature range 200-300°C. The conversion rose up to about 100% conversion at about 350°C. It is found that the main products of this system are propylene and acetone. The amount of acetone was higher in high reaction temperature range. At 500°C, the product selectivities of propylene and acetone were 72.83% and 27.71%, respectively.

While there is no doubt that propylene was formed from the dehydration of 2-propanol, the formation of acetone has yet to be verified. Acetone may be formed by the dehydrogenation (no oxygen required) or the oxidation (from oxygen leak into the system of 2-propanol). If it is the oxidation, the amount of oxygen leaked into the system should be about 0.75% to produce acetone with 25% selectivity as observed. The analysis of the feed gas confirmed that oxygen could find a way to enter the system. Another experiment (result not shown) which was performed for several days confirmed that the oxygen (reacted) in this system was not the oxygen species from the catalyst because the continuous reaction could maintain the conversion and selectivities. If the oxygen came from the catalyst, the conversion should drop with time, which was not observed.

The catalytic activity and product selectivities of 2-propanol over TS-1 catalyst for 8 vol%, 16 vol% 21 vol% of oxygen concentrations in the feed gas showed similar behavior. The conversion of 2-propanol quickly reached 100% at a reaction temperature about 350°C and then steadily at this conversion when the reaction temperature was higher than 400°C. All of these systems, acetone was the primary product with selectivity about 100% in reaction temperature range 200-400°C while carbondioxide became significant at reaction temperature above 400°C (above 350°C in case of 21 vol% O_2 system). The maximum selectivities towards carbondioxide were obtained at 500°C (97.67%, 88.46% and 98.13% for 8, 16 and 21 vol% O_2 system, respectively). This behavior indicated that carbondioxide was the secondary product produced via further oxidation of acetone. It is believed that

acetone was the oxidation product, which was produced directly from 2-propanol oxidation reactions.

In case of 8 vol% O_2 system, when the system has oxygen acetone was mainly produced (with selectivity almost 100% at 350°C) while propylene formation was extraordinary inhibited. From the result, it can be concluded that acetone can be produced from the direct oxidation of 2-propanol reaction. But the formation from the dehydrogenation was not totally excluded. The less of propylene formation shows that the oxidation well occurs than the dehydration. The reduction of propylene formation in the high reaction temperature region is possibly because of the fast oxidation of 2-propanol to acetone. Therefore, there was no enough 2-propanol to produced propylene.

The explanations for the behaviors of the 16 vol% O_2 and 21 vol% O_2 systems are similar to that of the 8 vol% O_2 system. The results showed that at the reaction temperature below 350°C, the TS-1 catalyst did not likely to destroy acetone although the amount of oxygen contains in the system is higher. Beyond 350°C, acetone was rapidly oxidized to combustion products.

The result of 0 vol% O_2 led to a suspicious that the formation of acetone by propylene oxidation (with O_2 leaked into the system) might be possible. To verify this suspicious, another experiment was performed by oxidizing propylene with oxygen over the TS-1 catalyst.

The propylene oxidation result confirmed that acetone could be formed via the oxidation of propylene. The amount of acetone formed was sufficient to explain the amount of acetone observed in the 0 vol% O_2 system. Therefore, another acetone formation route, dehydrogenation of alcohol was not likely to exist.

The catalytic activity of propylene oxidation over the TS-1 catalyst illustrates in Figure 5.7.

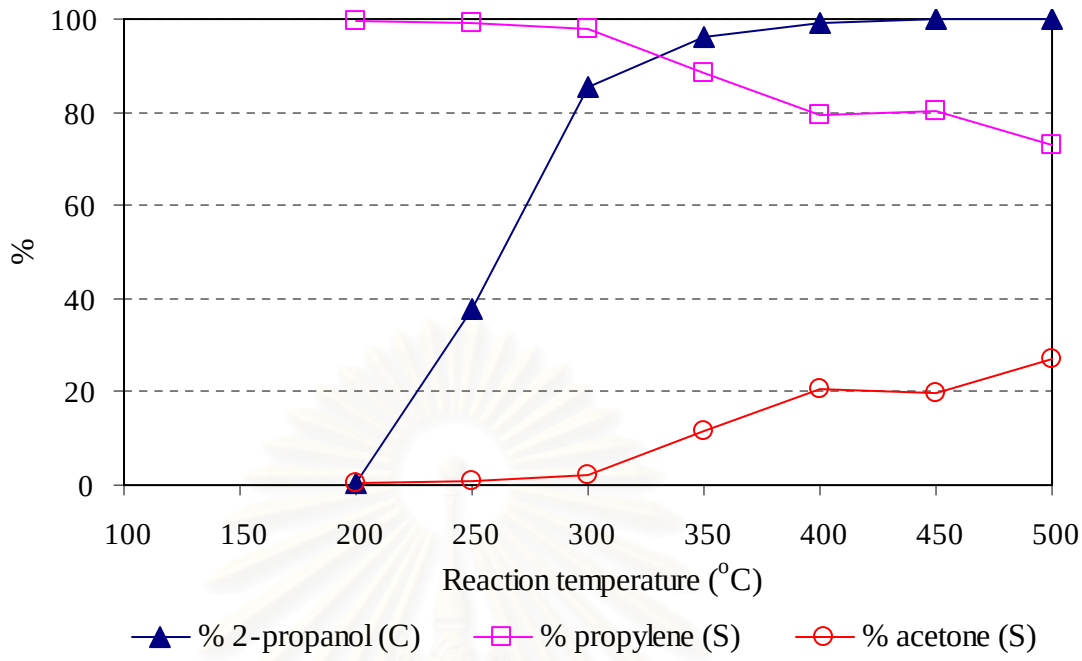

Figure 5.6a Product selectivities of 2-propanol over TS-1 for 0 vol% O_2 system

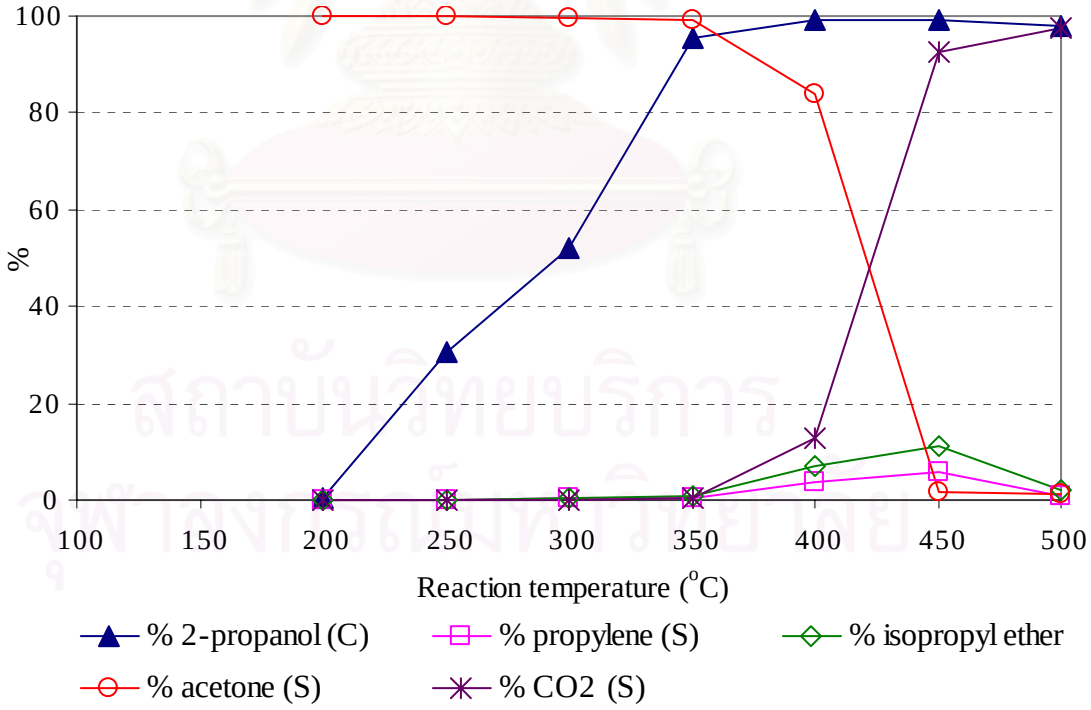

Figure 5.6b Product selectivities of 2-propanol over TS-1 for 8 vol% O_2 system (C-Conversion, S-Selectivity)

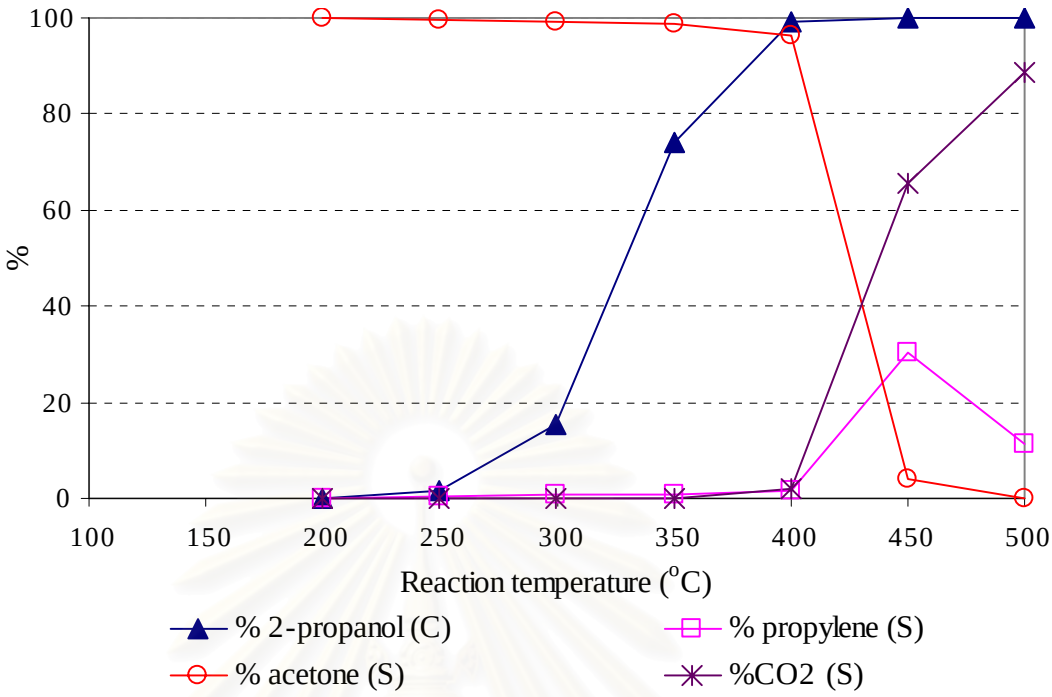

Figure 5.6c Product selectivities of 2-propanol over TS-1 for 16 vol% O_2 system

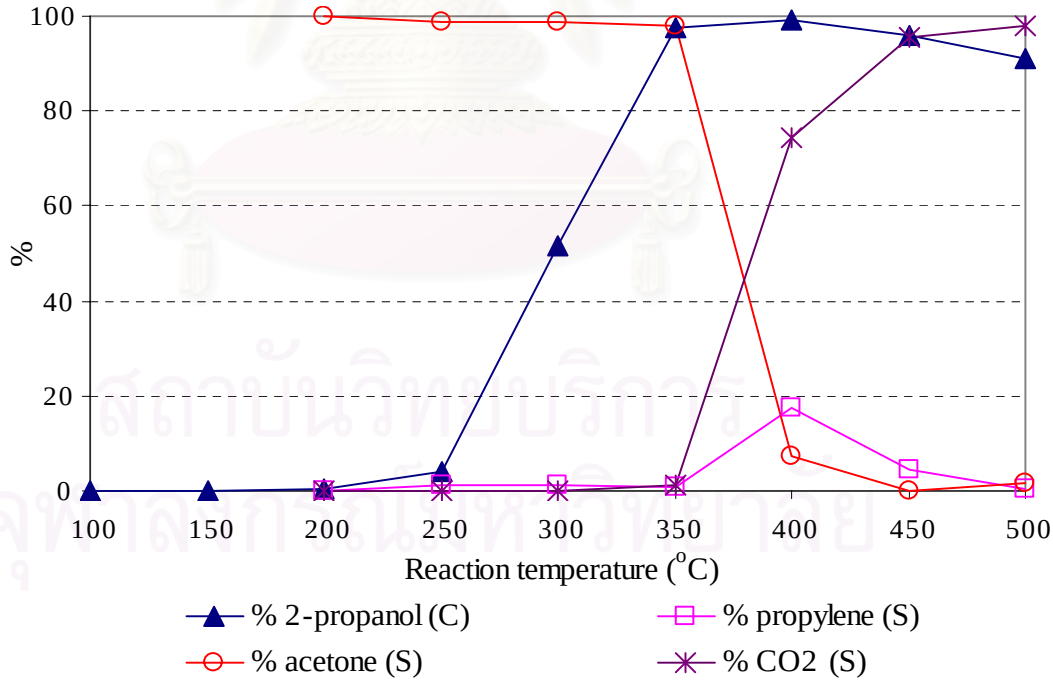

Figure 5.6d Product selectivities of 2-propanol over TS-1 for 21 vol% O_2 system (C-Conversion, S-Selectivity)

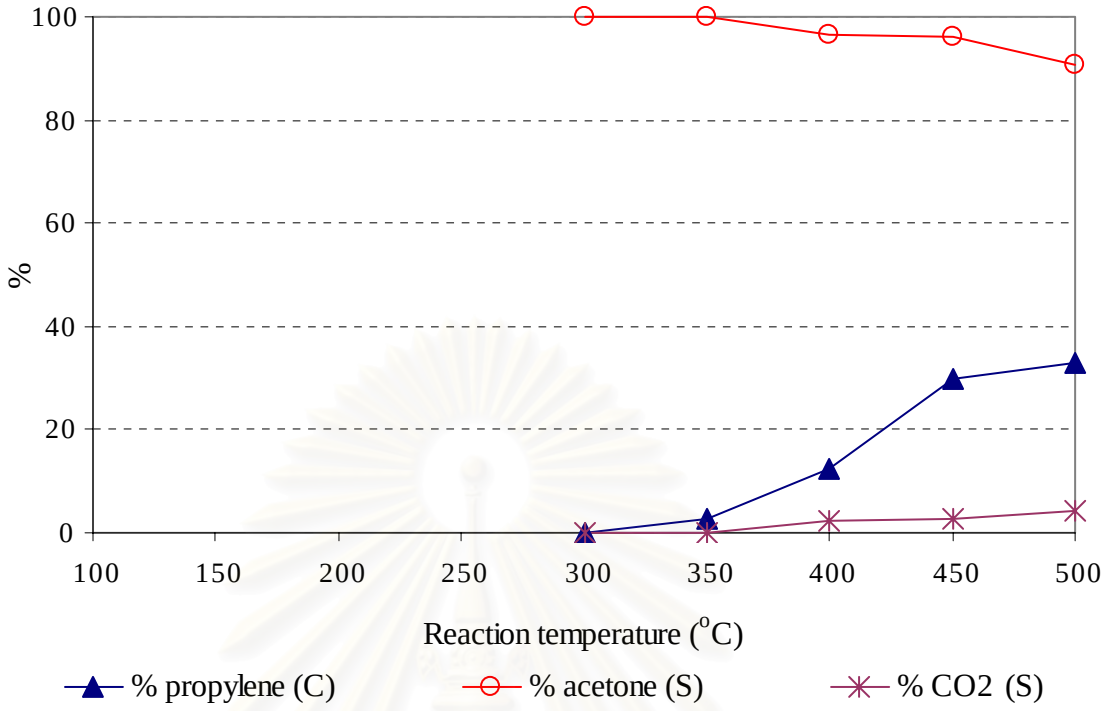

Figure 5.7 Product selectivities of propylene oxidation over TS-1 for 8 vol% O_2 system (C-Conversion, S-Selectivity)

From all of the explained experimental results the pathway of product formation in 2-propanol oxidation reaction can be summarized in Figure 5.8 below:

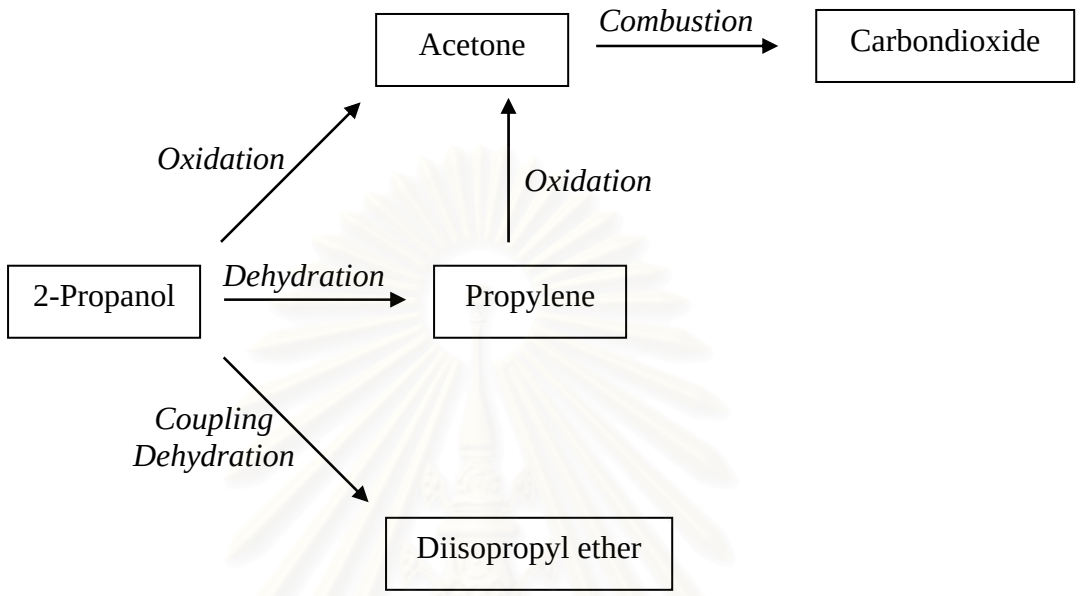

Figure 5.8 Schematic pathway of product formation in 2-propanol oxidation reaction.

5.2.2 1-propanol oxidation

The blank test reaction of 1-propanol for 0 vol% O_2 system, with no catalyst present in the reactor is shown in Figure 5.9.

The oxidation reaction shows the poor activity of the reaction system, no 1-propanol conversion was observed below the reaction temperature of 350°C. At the higher reaction temperature, however the conversion slightly increased. The maximum conversion was obtained at 500°C with 27.02%. It should be noted here that no propylene, the dehydration product, was detected. This is due to the nature of primary alcohol which prefers the oxidation reaction rather than the dehydration reaction.

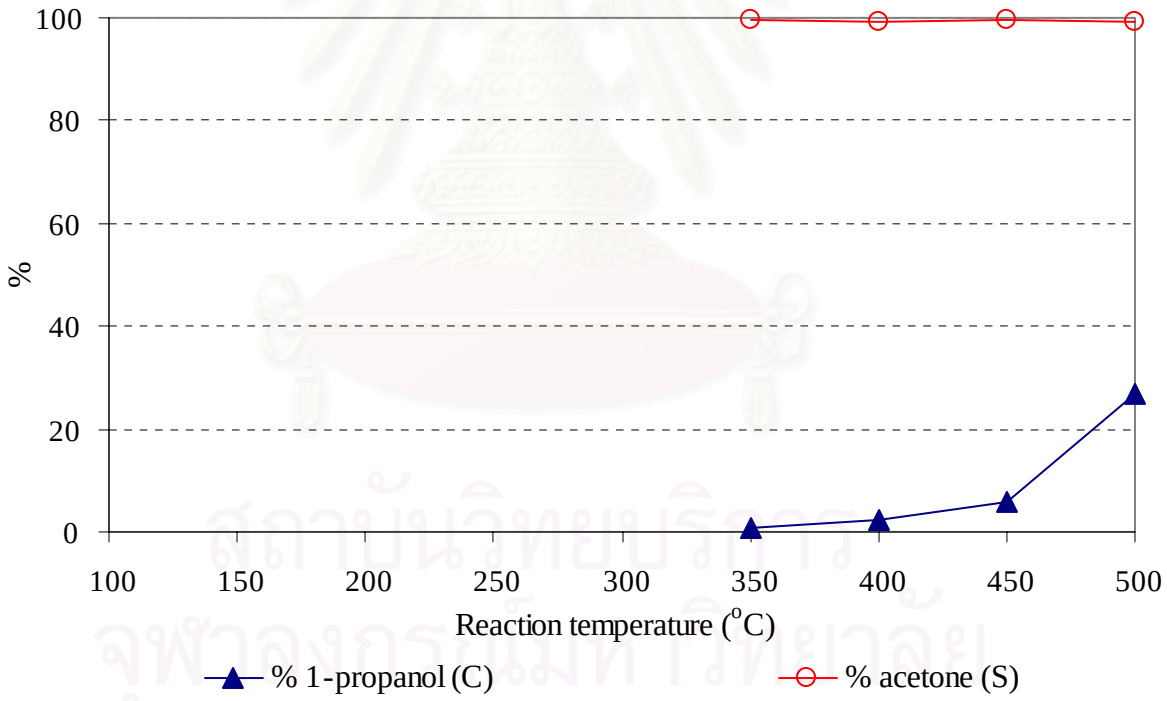

Figure 5.9 Product selectivities and conversion of 1-propanol without TS-1 for 0 vol% O_2 system (C-Conversion, S-Selectivity)

The behavior of TS-1 as catalyst for 1-propanol oxidation for 0 vol% oxygen concentration in the feed gas is illustrated in Figure 5.10a. No 1-propanol conversion was observed at reaction temperatures below 300°C. When the reaction temperature was higher than 300°C, the activity of TS-1 catalyst rose from 0.54% to 14.89% before increased dramatically up to nearly 100% at 400°C. Product selectivities of 1-propanol oxidation exhibited similar behavior to 2-propanol oxidation reaction for the same 0 vol% O_2 system, the main product was propylene with selectivity 86.40% and small amount of acetone was observed with selectivity up to 13.60%.

An increase of oxygen concentration in feed gas, such as 8 vol%, 16 vol% and 21 vol% (Figure 5.10b, 5.10c and 5.10d, respectively) resulted in different catalytic activity. For 8 vol% O_2 systems, the conversion was observed firstly at 200˚C. In the reaction temperature range of 250-350°C, the conversion increased rapidly from 0.45% to 99.60% at 350°C. The system of 16vol%O_2 and 21 vol% O_2 showed similar conversion/selectivity patterns to the system of 8 vol% O_2 system.

The result of product selectivity of 1-propanol oxidation for 8 vol% O_2 and 16 vol% O_2 showed that at low reaction temperature range 250-350°C, the main product was acetone with selectivity higher than 80% and 70% for 8 vol% O_2 and 16 vol% O_2, respectively. Also, there was some formation of propylene, n-propyl ether and trace of carbondioxide. When the reaction temperature is further increased (400-500°C) the main product was change to carbondioxide. The maximum selectivities towards to carbondioxide were also obtained at reaction temperature range 450-500°C (about 96% and 92% for 8 vol%O_2 and 16 vol% O_2, respectively).

The experimental results for 21 vol% O_2 system showed that more amount of oxygen in feed gas had no significant effect on the catalytic performance but there are a few effects on product selectivity of the TS-1 catalyst in 1-propanol oxidation. In the high 1-propanol conversion region (at above 300°C), the selectivity to acetone was higher than propylene until 450°C. When the reaction temperature was further

increased (400-500°C), acetone selectivity rapidly decreased while selectivity towards to carbondioxide gradually increased followed by rapidly rose to about 88.60% at 500°C.

The reaction pathway of 1-propanol oxidation can be discussed in the same way like 2-propanol oxidation.

Normally, the oxidation of primary alcohols should produce aldehydes. In this case, however, a different result was observed, i.e. acetone was found rather than propanal. Acetone can form from 1-propanol by 2 steps i.e. a) the dehydration of 1-propanol to propylene and b) the oxidation of propylene to acetone. As discussed earlier in section 5.2.1 (2-propanol oxidation), the TS-1 catalyst was not active enough to convert propylene to acetone to meet the amount observed during 1-propanol oxidation. Thus, another pathway for acetone formation (not propylene route) may exist. How this path proceeded is be beyond the scope of this thesis.

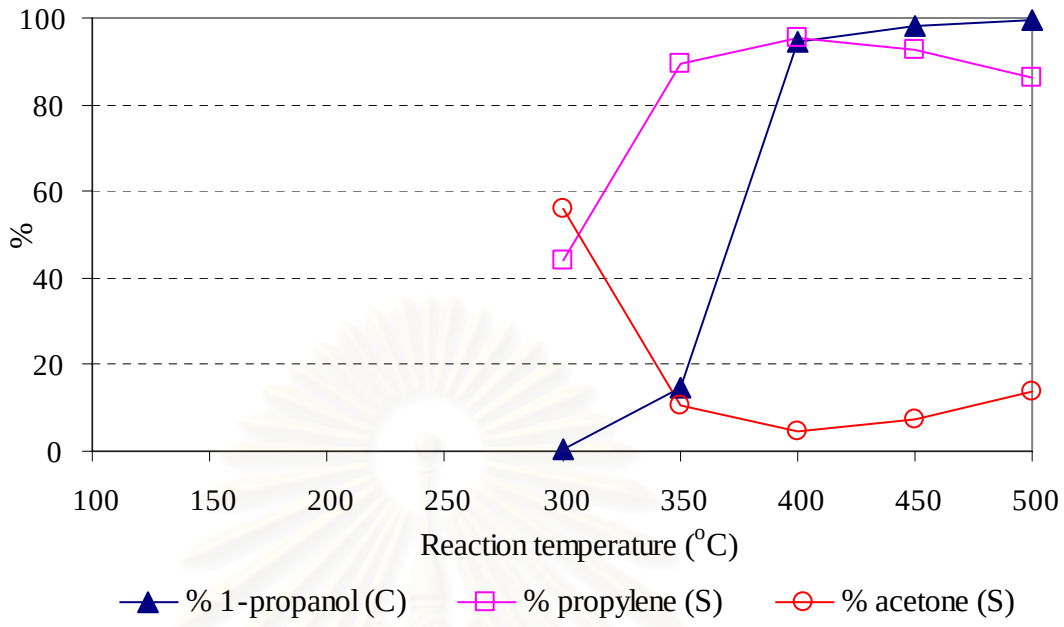

Figure 5.10a Product selectivities of 1-propanol over TS-1 for 0 vol% O_2 system

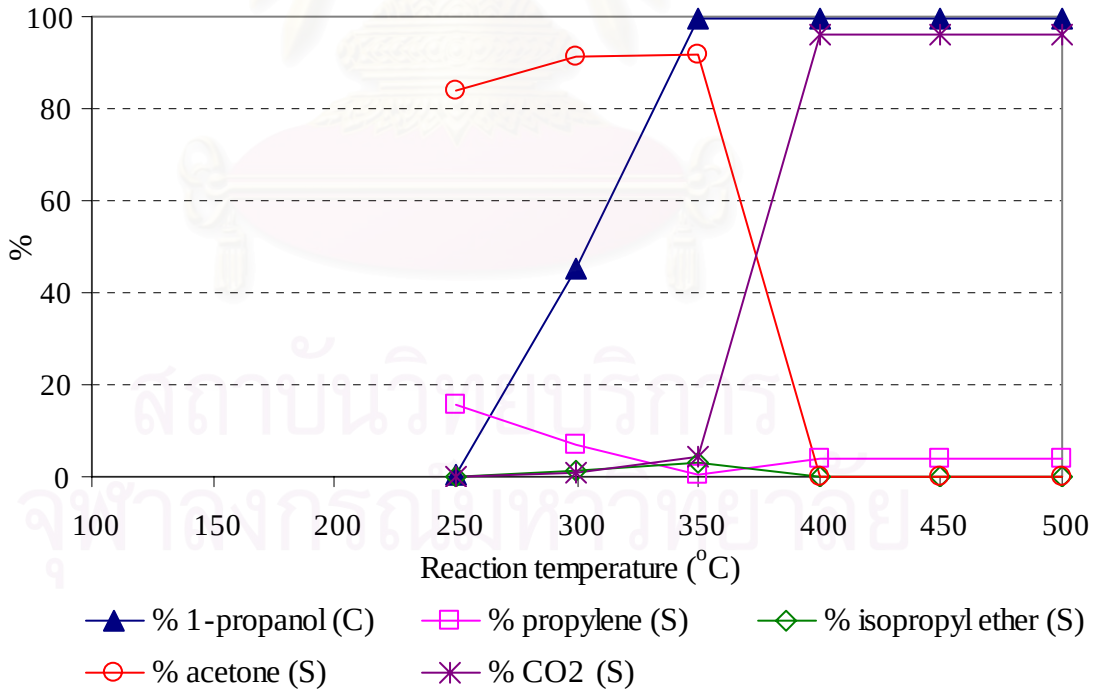

Figure 5.10b Product selectivities of 1-propanol over TS-1 for 8 vol% O_2 system (C-Conversion, S-Selectivity)

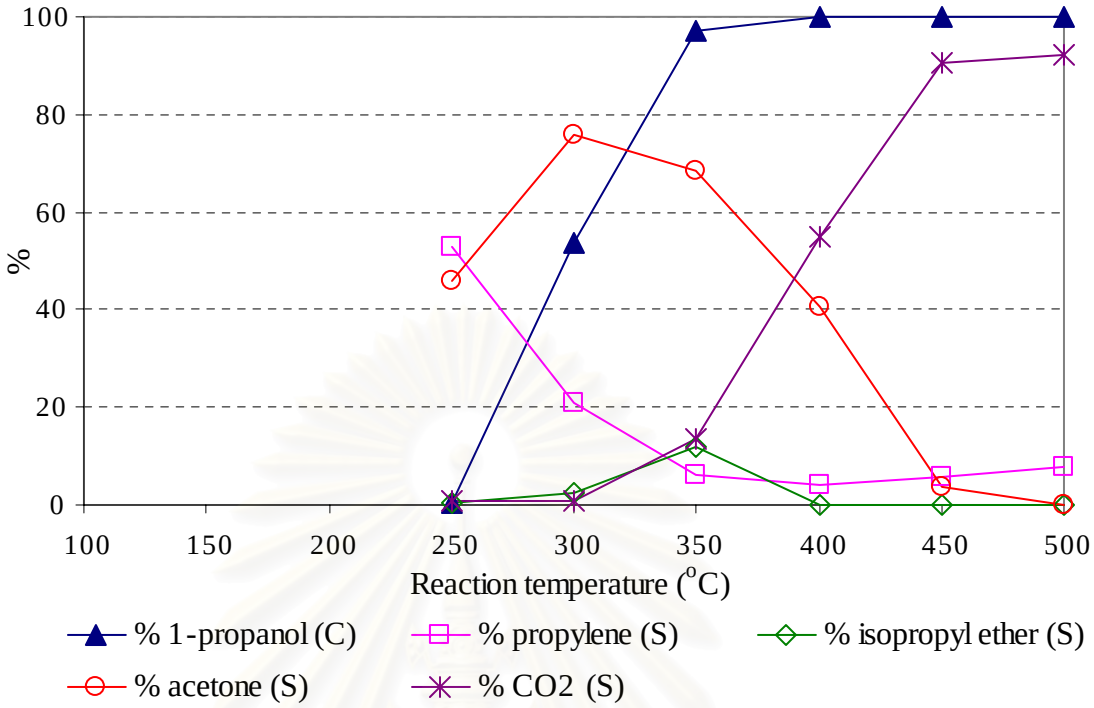

Figure 5.10c Product selectivities of 1-propanol over TS-1 for 16 vol% O_2 system

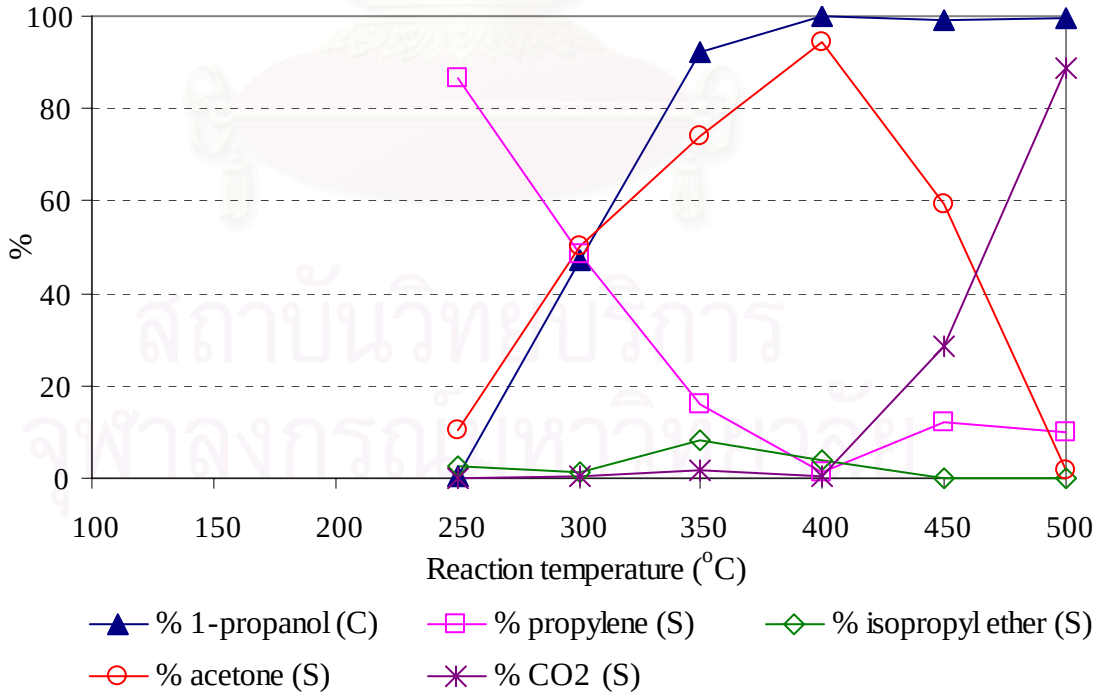

Figure 5.10d Product selectivities of 1-propanol over TS-1 for 21 vol% O_2 system (C-Conversion, S-Selectivity)

The route of product formation in 1-propanol oxidation reaction is summarized in Figure 5.11 below:

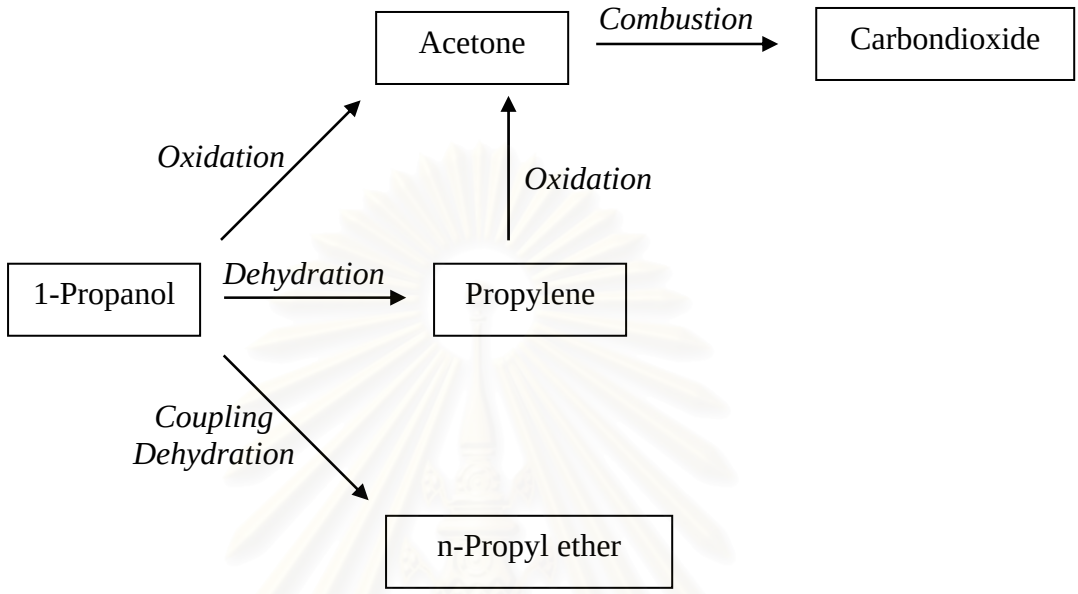

Figure 5.11 Schematic pathway of product formation in 1-propanol oxidation reaction

5.2.3 Ethanol oxidation

The reaction of ethanol for 0 vol% O_2 system, which no catalyst contained in the micoreactor is shown in Figure 5.12

The conversion was observed at 200°C, but it very poor performance. An increase of the reaction temperature was not obviously effect on the conversion. Beyond 500°C, the maximum conversion (10.51%) was detected, the main product was acetaldehyde and trace of ethylene (with selectivities 92.25% and 7.74%, respectively).

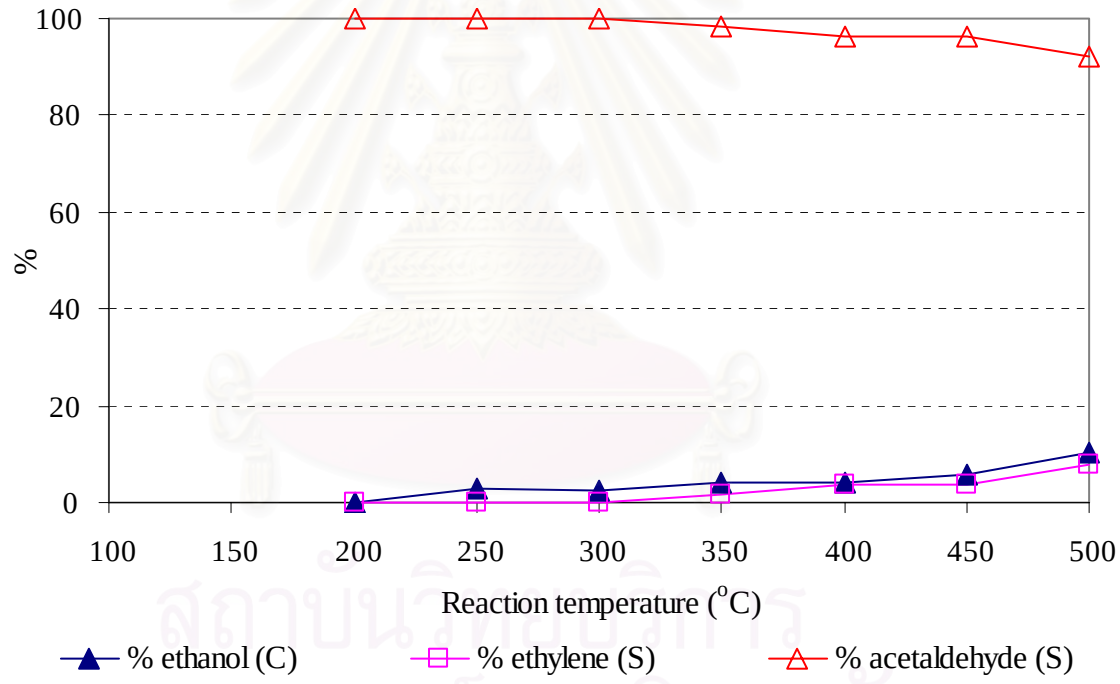

Figure 5.12 Product selectivities and conversion of ethanol without TS-1 for 0 vol% O_2 system (C-Conversion, S-Selectivity)

Figure 5.13a shows the conversion of ethanol (and the selectivities towards products) for the system, which had no oxygen contains in feed gas. The conversion was detected when the reaction temperature was higher than 300°C and rose dramatically from 0.40% to 89.14% followed by a slightly increase to about 100%in the reaction temperature range 450-500°C. At all reaction temperature, ethylene was the main product produced by the dehydration reaction with selectivity about 100% when the conversion was higher than 30%. Trace of acetaldehyde was also found in the effluent stream.

In case of 8 vol% O_2 system, the conversion was firstly observed at about 250°C and increased from 0.13 % to about 100% in the reaction temperature range 400-500°C. In the reaction temperature range 250-400°C, the major product was acetaldehyde with selectivity higher than 80%. Also, there are some amounts of ethylene and trace of carbondioxide. The amount of ethylene and carbondioxide were significant when the reaction temperature was higher than 400°C. The maximum selectivities towards ethylene and carbondioxide were also obtained at 450°C and 500°C with selectivity about 60% and 57%, respectively.

The results of 16 vol% O_2 and 21 vol% O_2 systems show the same behavior like 8 vol% O_2 system as shown in Figures 5.13c and 5.13d, respectively. The carbondioxide selectivity reached a maximum at 500°C (24.14% for 16 vol% O_2 and 42.05% vol% for 21 vol% O_2, respectively). It should be noted here that for ethanol, the dehydration product (ethylene) was quite well produced when the oxidation reaction occurs. This is different from the cases of 1-propanol and 2-propanol which the oxidation reaction is much more preferred than the dehydration reaction. Since in this case, the oxidation and the dehydration reactions did not occur at much different rates. In addition, the TS-1 catalyst does not posses high enough activity to completely oxidize alkene to combustion products. At high temperature, both ethylene and carbondioxide, therefore, appeared in the product stream.

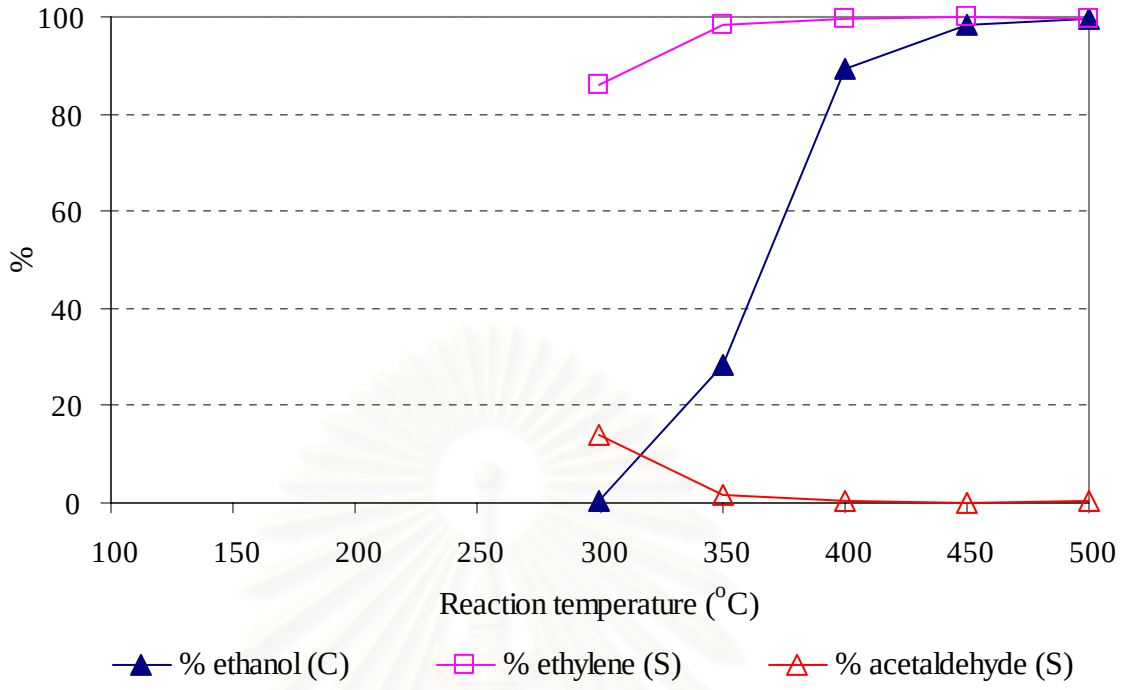

Figure 5.13a Product selectivities of ethanol over TS-1 for 0 vol% O_2 system

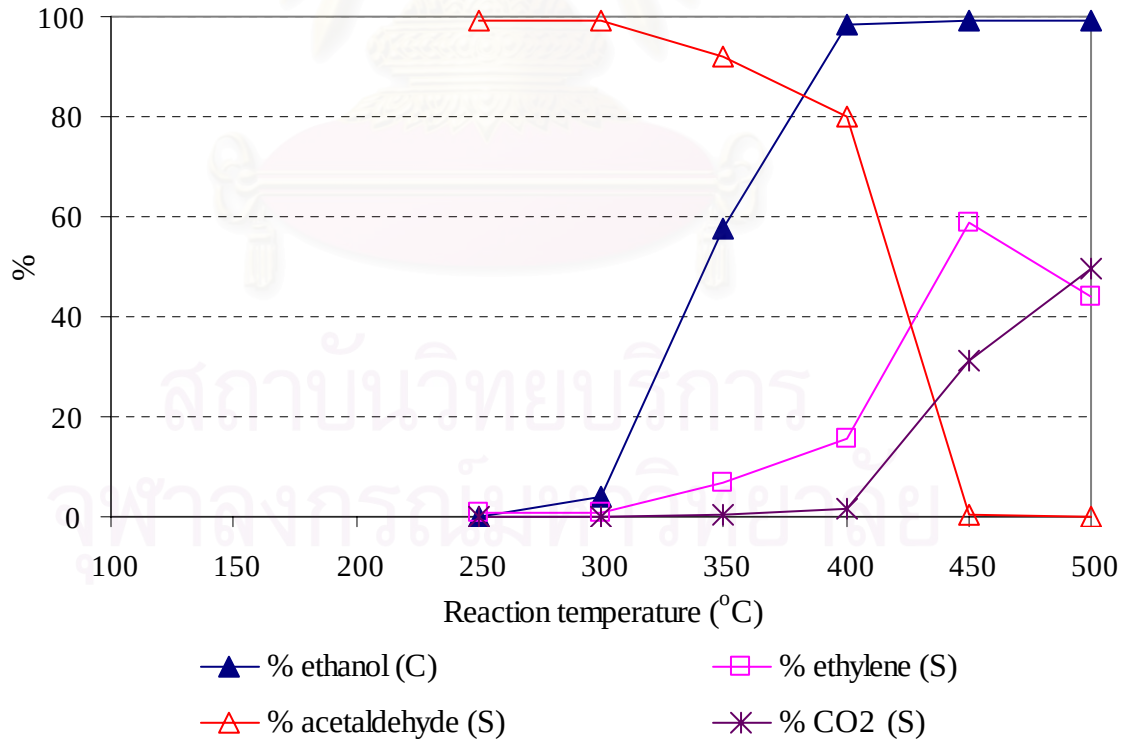

Figure 5.13b Product selectivities of ethanol over TS-1 for 8 vol% O_2 system (C-Conversion, S-Selectivity)

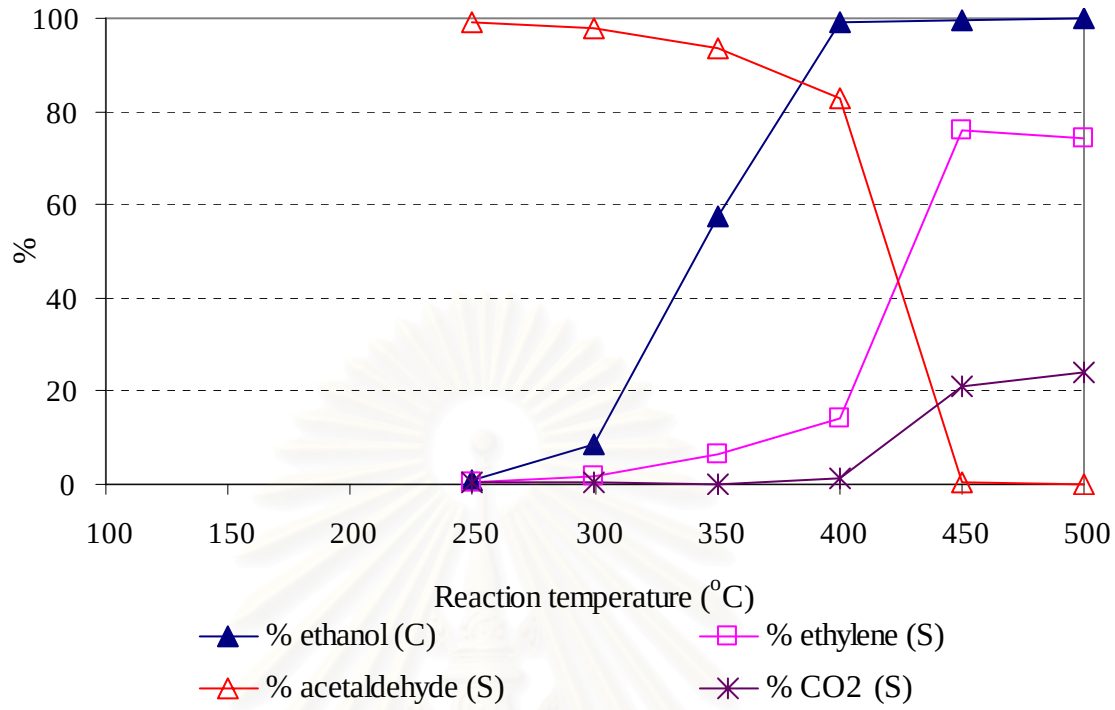

Figure 5.13c Product selectivities of ethanol over TS-1 for 16 vol% O_2 system

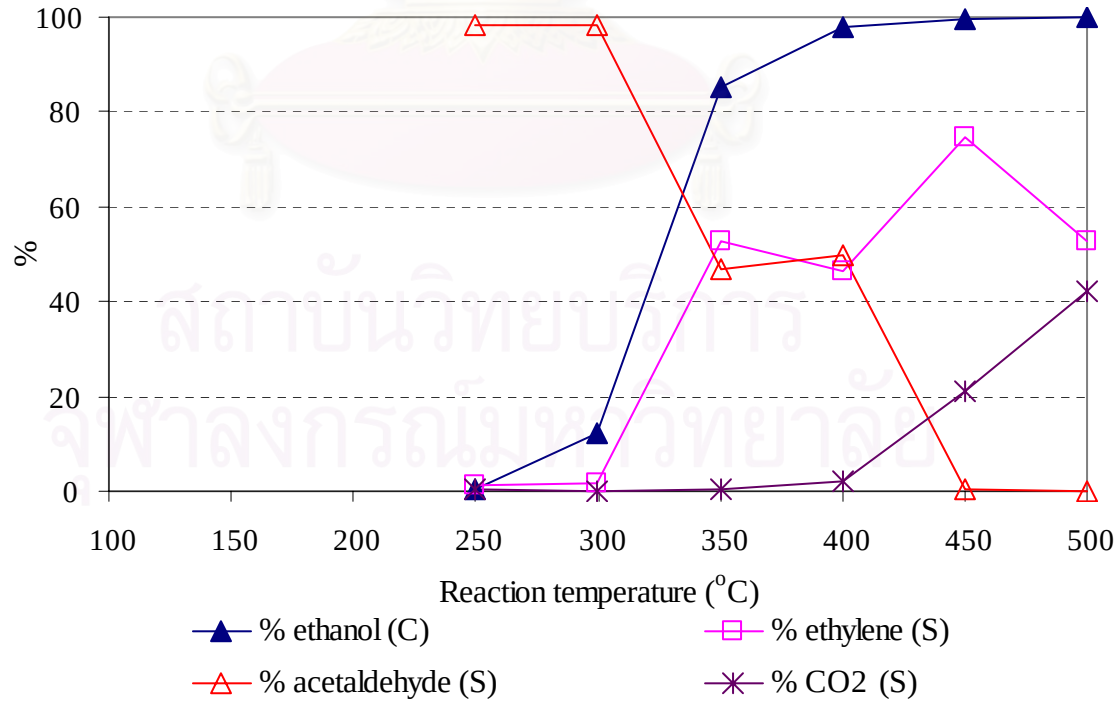

Figure 5.13d Product selectivities of ethanol over TS-1 for 21 vol% O_2 system (C-Conversion, S-Selectivity)

The route of product formation in ethanol oxidation reaction can be summarized and shown in Figure 5.14 below:

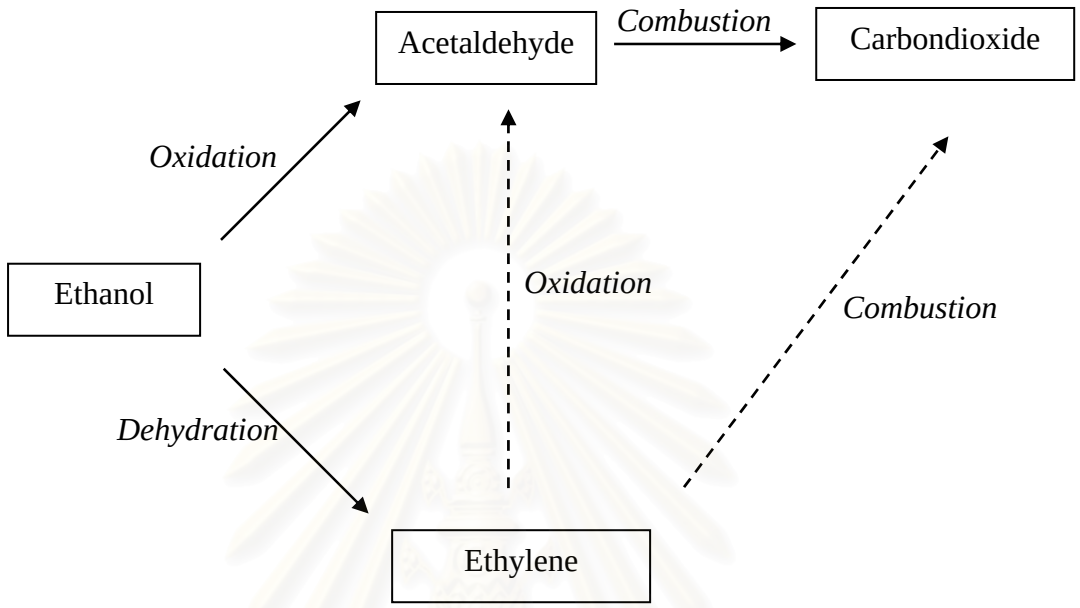

Figure 5.14 Schematic pathway of product formation in ethanol oxidation reaction
(⟶ = main route, ⇢ = possible or not likely route)

5.2.4 Methanol oxidation

The blank test reaction of methanol for 0 vol% O_2 system, with no catalyst present in the reaction is shown in Figure 5.15.

The experimental result shows the very poor activity of the reaction system, no methanol conversion was observed below the reaction temperature of 400°C. At higher reaction temperature, however, the conversion slightly increased. The maximum conversion of this system, in the reaction temperature range investigated, was obtained at 500°C with 1.19%.

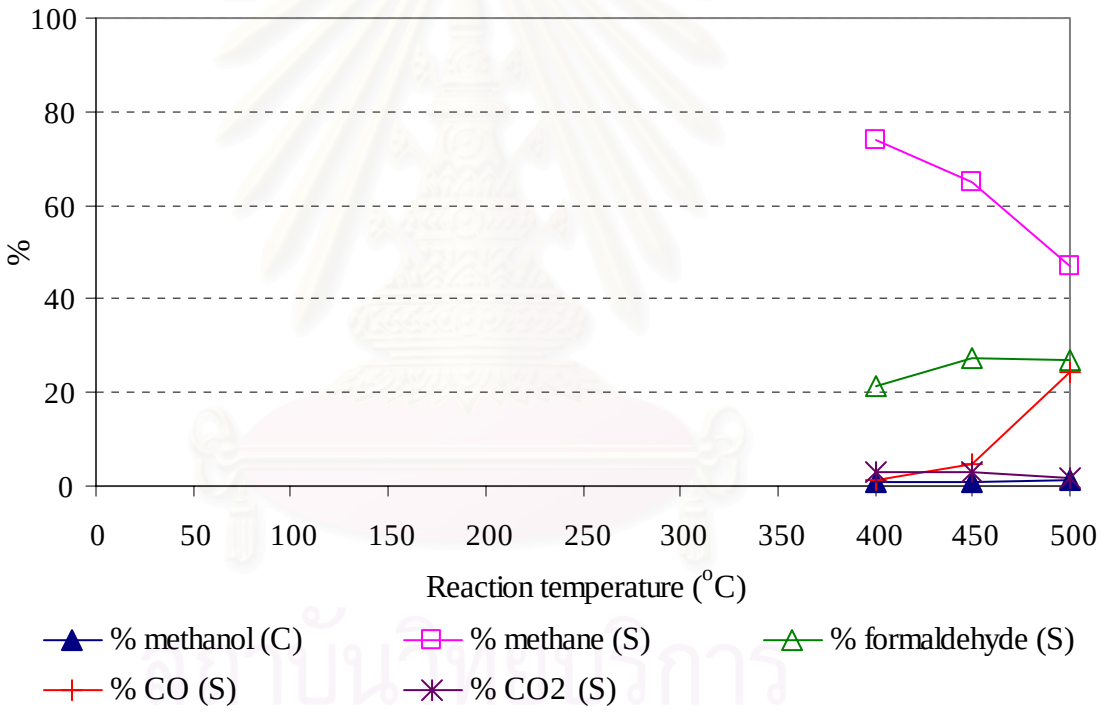

Figure 5.15 Product selectivities and conversion of methanol without TS-1 for 0 vol% O_2 system (C-Conversion, S-Selectivity)

Figures 5.16a-5.16d show the activity of TS-1 catalyst for the oxidation of methanol, which contained 0 vol% O_2, 8 vol% O_2, 16 vol% O_2 and 21 vol% O_2 in feed gas, respectively. For the system that has no oxygen contained, no methanol conversion was observed at the reaction temperature below 400°C. From 400-450°C, the conversion increased from 0.13% to 34.73% before rapidly increased to nearly 100% at 500°C. In the reaction temperature range 400-450°C, three main products were detected, i.e. such as methane, carbonmonoxide and carbondioxide. Beyond 500°C, carbonmonoxide selectivity is around 95.43% and carbondioxide selectivity is about 4.25%.

An increase of oxygen concentration in the feed gas affects the conversion of methanol, i.e. it easier to react than the 0 vol% oxygen system at all the reaction temperature. The reaction produces carbondioxide as the major product. Small amount of carbonmonoxide and trace of methane were observed for 8 vol% O_2 system.

For 16 vol% O_2 and 21 vol% O_2 systems, formaldehyde was detected at low conversion of methanol. In the reaction temperature range 350-500°C, carbondioxide was observed and became significant when the reaction temperature was further increased. It is likely that methanol was completely oxidized to carbondioxide via the formation of formaldehyde.

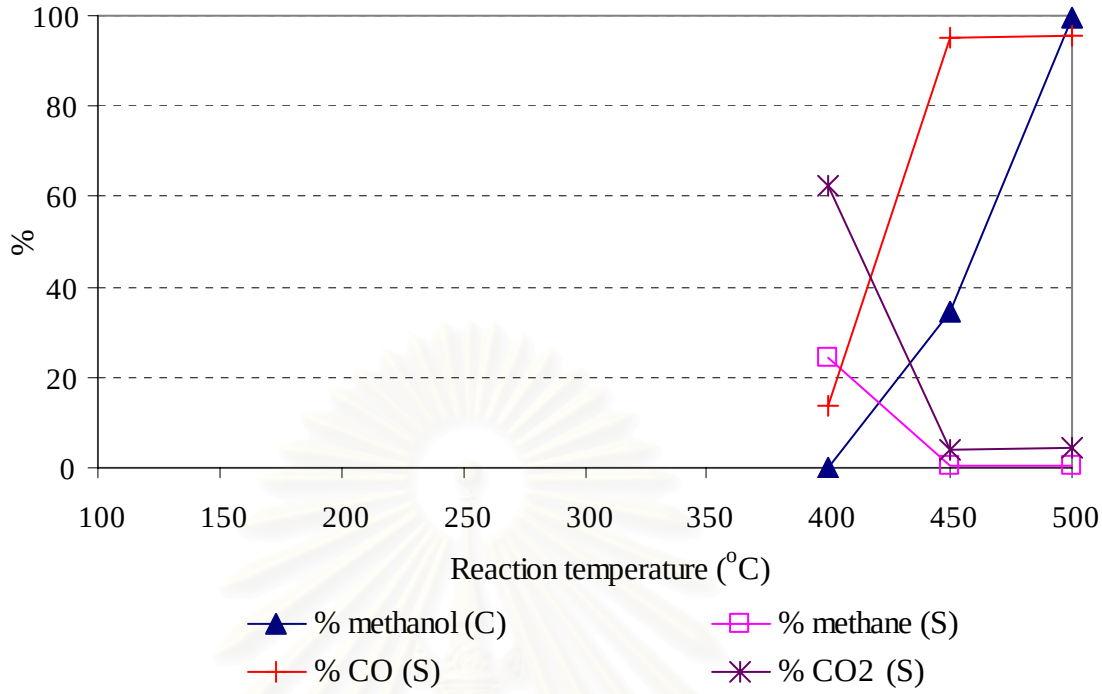

Figure 5.16a Product selectivities of methanol over TS-1 for 0 vol% O_2 system

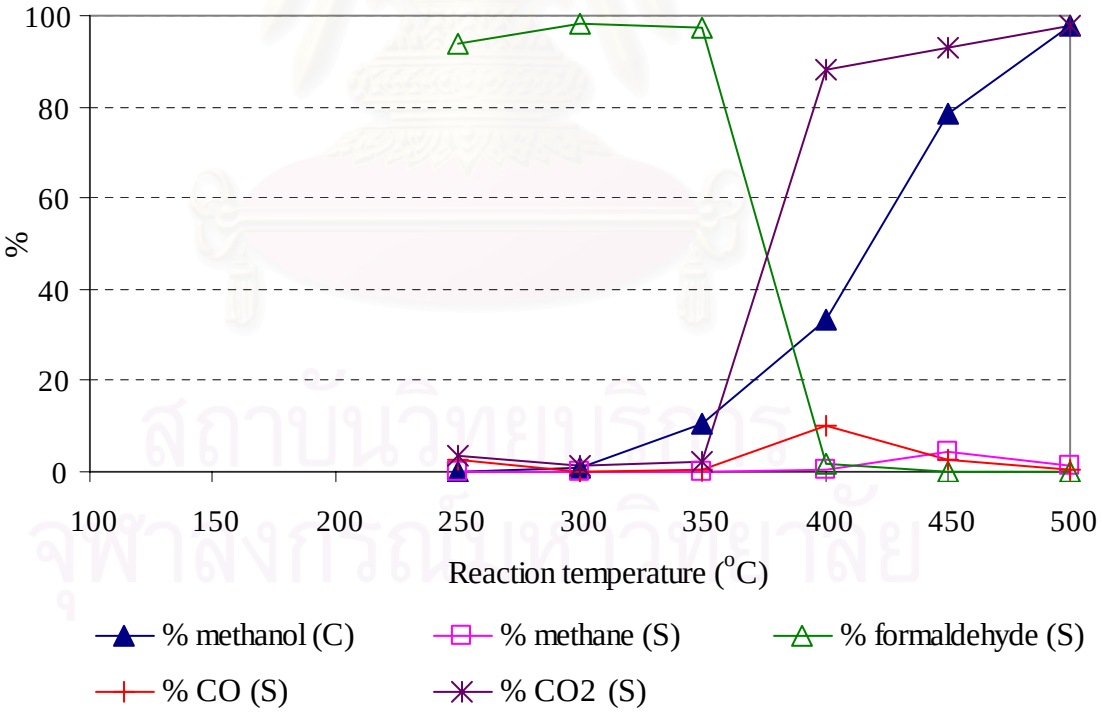

Figure 5.16b Product selectivities of methanol over TS-1 for 8 vol% O_2 system (C-Conversion, S-Selectivity)

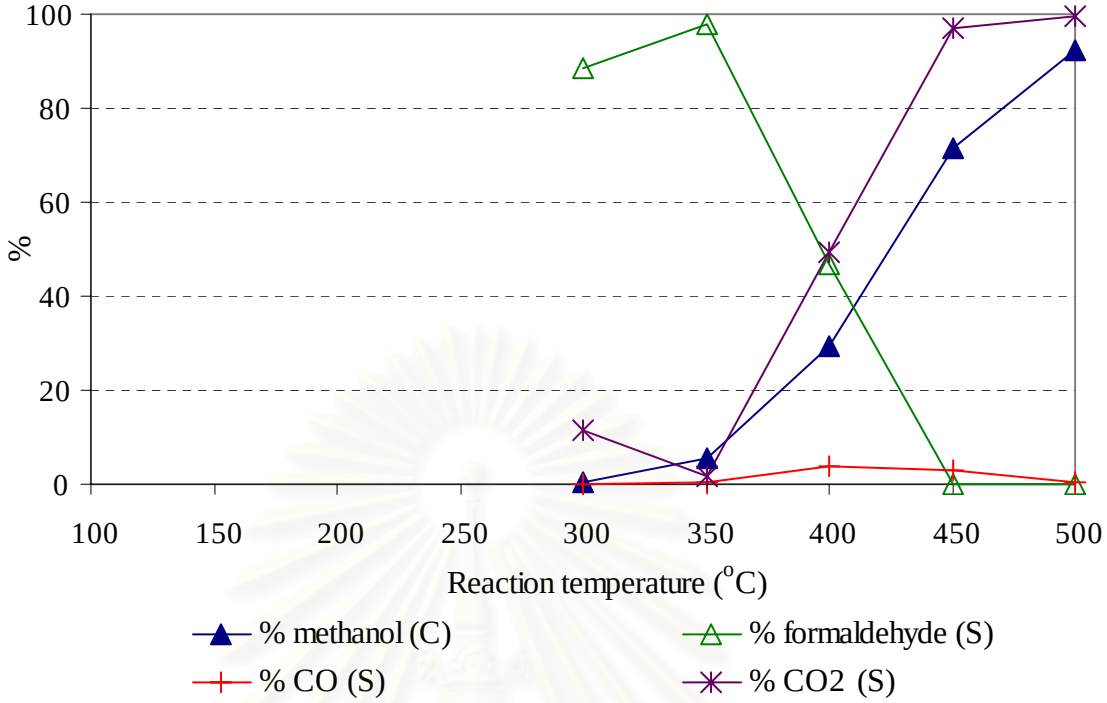

Figure 5.16c Product selectivities of methanol over TS-1 for 16 vol% O_2 system

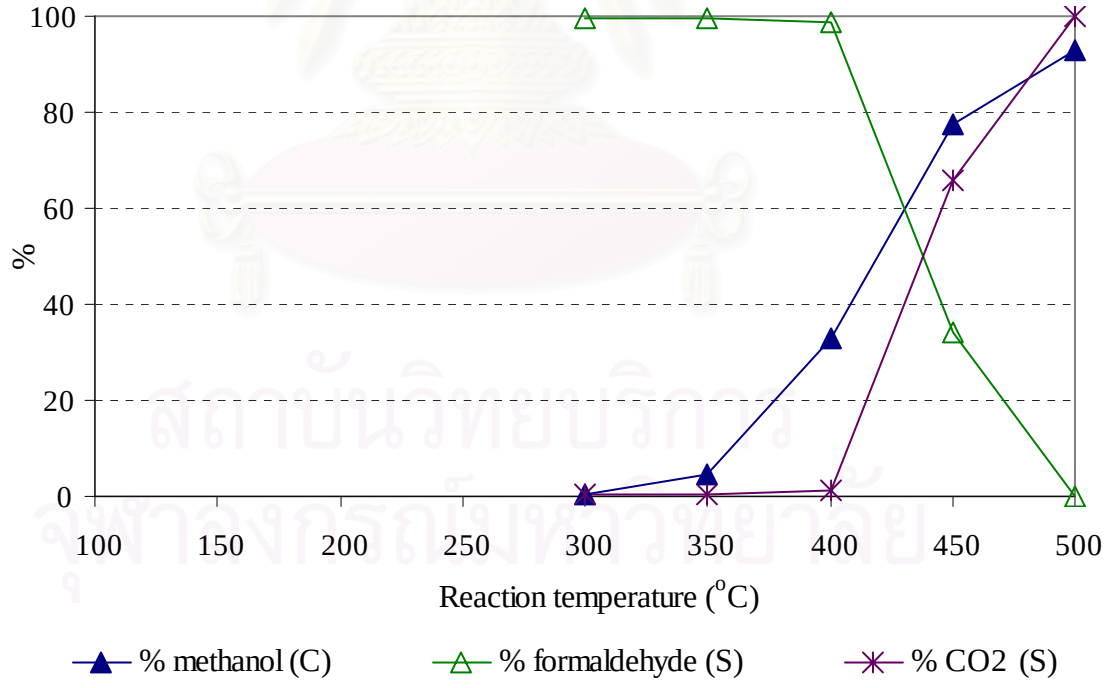

Figure 5.16d Product selectivities of methanol over TS-1 for 21 vol% O_2 system (C-Conversion, S-Selectivity)

The Schematic pathway of product formation in methanol oxidation reaction can be summarized and shown in Figure 5.17 below:

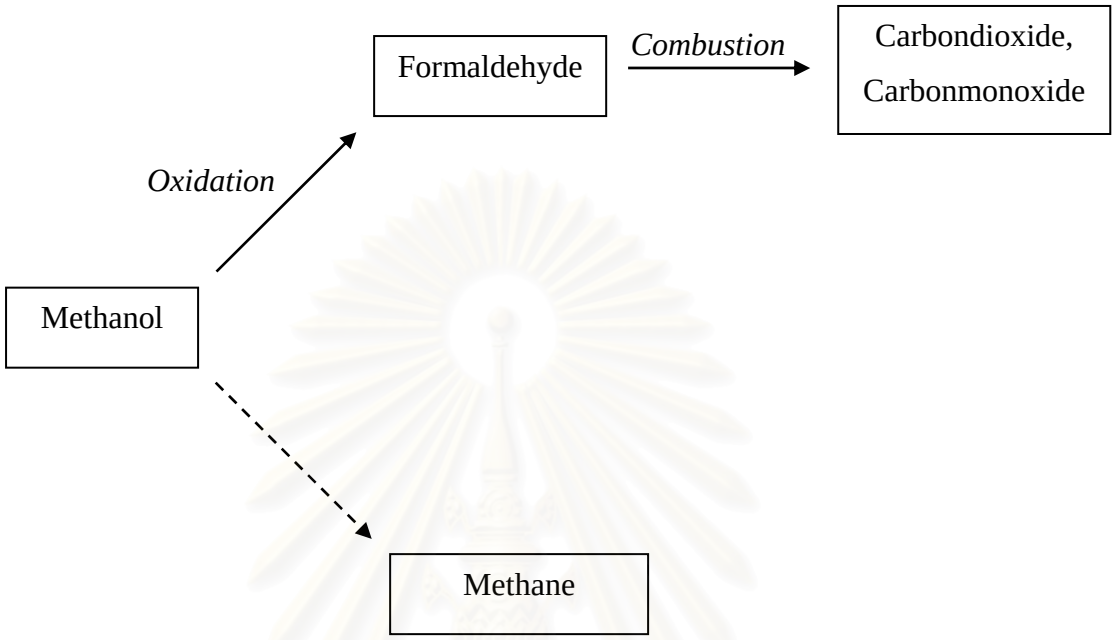

Figure 5.17 Schematic pathway of product formation in methanol oxidation reaction
(⟶ = main route, ⇢ = possible or not likely route)

CHAPTER VI

CONCLUSIONS AND RECOMMENDATIONS

6.1 Conclusions

The conclusions of the present research are the following:

1. The TS-1 plays role as an effective catalyst and high stability to be used for alcohol oxidation reactions in gas phase.

2. For the oxidation reaction, the oxidation property of the TS-1 catalyst depends on type of reactant.

3. For no oxygen system, 2-propanol, 1-propanol and ethanol oxidations show that the dehydration reaction mainly takes place which produces alkenes.

4. The present and amount of oxygen concentration in the feed gas affect the oxidation of alcohols both catalytic activity and product selectivities. At low reaction temperature, the oxidation of 1-propanol and 2-propanol yields acetone while the oxidation of ethanol yields acetaldehyde.

5. For all the systems which react with oxygen, at high reaction temperature the TS-1 catalyst plays role as a combustion catalyst.

6. The influence of reaction temperature on the conversion and product selectivities is more than the influence of oxygen concentration.

6.2 Recommendations for future studies

From the previous conclusions, the following recommendations for future studies are proposed.

1. Due to the amount of oxygen affecting the activity of alcohol oxidation reactions at low oxygen concentration, adding less oxygen in the feed gas should be carried out to see the effect of O_2 concentration.

2. Because the acid property influences the catalytic property, therefore the role of Brønsted/Lewis acid sites (during the oxidation process) should be further studied.

3. Because the TS-1 catalyst is an effective catalyst for alcohol oxidation reactions of methanol, ethanol, 1-propanol and 2-propanol which are in class of primary and secondary alcohols, so it will be interesting to further study the oxidation of higher primary and secondary alcohols such as 1-butanol, 1-pentanol, 2-butanol and 2-pentanol.

4. For the alcohol oxidation reactions, it will be interesting to study the effect of the other basic metal such as Au and Pt loading on the oxidation property of the TS-1 catalyst.

REFERENCES

Amato, G., Arcoria, A., Ballistreri, F. P., Tomaselli, G. A., Bortolini, O., Conte, V., Di Furia, F., Modena, G. and Valle, G., "Oxidations with peroxotungsten complexes: rates and mechanism of stoichiometric olefin epoxidations", *J. Mol. Cat.*, **37**, (1986):165-175.

Centi, G., Cavani, F. and Trifiro, F., "Selective oxidation in the liquid phase with solid micro- or Mesoporous materials", *Selective Oxidation by Heterogeneous Catalysis*, Plenum Pub Corp, (2001):287-299.

Davies, L.J., Mcmorn, P., Bethell, D., Bulman P., P.C., King, F., Hancock, F.E. and Hutchings, G.J., "Oxidation of crotyl alcohol using Ti-β and Ti-MCM-41 catalysts", *J. Mol. Cat. A.*, **165**, (2001):243-247.

Duprey, E., Beaunier, P., Springuel-Huet, M.-A., Bozon-Verduraz, F., Fraissard, J., Manoli, J.-M. and Brégeault, J.-M., "Characterization of catalysts based on titanium silicalite, TS-1 by physicochemical techniques", *J. Catal.*, **165**, (1997):22-32.

Huybrechts, D. R. C., Vaesen, I., Li, H. X. and Jacobs, P. A., "Factors influencing the catalytic activity of titanium silicalites in selective oxidations", *Catal. Lett.*, **8**, (1991):237-244.

Kraushaar-Czarnetzki, B. and van Hooff, J. H. C., "A test reaction for titanium silicalite catalysts", *Catal. Lett.*, **2**, (1989):43-48.

Mongkhonsi, T., Pimanmas, P., Praserthdam, P., "Selective Oxidation of ethanol and 1-propanol over V-Mg-O/TiO_2 catalyst", *Chem. Lett.*, (2000):968-969.

Mongkhonsi, T., Youngwanishsate, W., Kittikerdkulchai, S. and Praserthdam, P., "Selective oxidation of alcohols over Co-Mg-O catalyst", *J. Chin. Inst. Chem. Engrs.*, **32**, (2001):183-186.

Mongkhonsi, T., Chaiyasit, N. and Praserthdam, P., "Selective oxidation of 1-propanol and 2-propanol over supported Co-Mg-O catalysts", *J. Chin. Inst. Chem. Engrs.*, **33**, (2002):365-372.

Notari, B., " Synthesis and catalytic properties of titanium containing zeolites", *Stud. Surf. Sci. Catal.*, **37**, (1989):413-425.

Ozkan, U.S., Kueller, R.F. and Moctezuma, E., "Methanol oxidation over Nonprecious Transition Metal Oxide Catalysts", *Ind. Eng. Chem. Res*., **23**, **(**1990):1136-1142.

Perego, G., Bellussi, G., Corno, C., Taramasso, M., Buonomo, F. and Esposito, A., "Titanium-silicalite: a noval derivative in the pentasil family", *Stud. Surf. Sci. Catal.*, **28**, (1986):129-136.

Pestryakov, A.N. and Lunin, V.V.,"Physicochemical study of active sites of metal catalysts for alcohol partial oxidation", *J. Mol. Cat. A.*, **158**, (2000):325-329.

Rekoske, J. E. and Barteau, M. A., "Kinetics and selectivity of 2-propanol conversion on oxidized anatase TiO_2", *J. Catal.*, **165**, (1997):57-72.

Sato, S., Takahashi, R., Sodesaws, T., Honda, N. and Shimizu, H., "Selective dehydration of diols to allylic alcohols catalyzed by ceria", *Catalysis Communications*, **4**, (2003):77-81.

Schuster, W., Niederer, J.P.M. and Hoelderich, W.F., "The gas oxidative dehydrogenation of propane over TS-1", *Appl. Catal. A.*, **209**, (2001):131-143.

Scirè, S., Minicò, S., Crisafulli, C., Satriano, C. and Pistone, A., "Catalytic combustion of volatile organic compounds on gold/cerium oxide catalysts", *Appl. Catal. B.*, **40**, (2003):43-49.

Sheldon, R. A., "Synthetic and mechanistic aspects of metal-catalysed epoxidations with hydroperoxides", *J. Mol. Cat.*, **7**, (1980):107-126.

Taramasso, M., Perego, G. and Notari, B., "Preparation of porous crystalline synthetic material comprised of silicon and titanium oxides", *United States Patent*, **4410501**, (1983).

Unnikrishnan, R.P., and Endalkachew, S.D., "Selective Oxidation of Alcohols in Gas Phase Using Light-Activated Titanium Dioxide", *J. Catal*., **211**, (2002):434-444.

Van der Pol, A. J. H. P., Verduyn, A. J. and van Hooff, J. H. C., "Why are some titanium silicalite-1 samples active and others not?", *Appl. Catal. A*, **92**, (1992):113-130.

Wang, R., Guo, X., Wang, X., and Hao, J., "Gas-phase epoxidation of propylene over Ag/Ti-containing catalysts", *Catal. Today*, **93-95**, (2004):217-222.

Wang, R., Guo, X., Wang, X., Hao, J., Li, G., and Xiu, J., "Effect of preparation conditiona and reaction conditions on the epoxidation of propylene with molecular oxygen over Ag/TS-1 in the presence of hydrogen", *Appl. Catal. A.*, **261**, (2004):7-13.

Yao, Y-F. Y., "Catalytic Oxidation of Ethanol at Low Concentrations", *Ind. Eng. Chem. Res.***, 23,** (1984):60-67.

Yap, N., Andres, R.P. and Delgass, W.N., "Reactivity and stability of Au in and on TS-1 for epoxidation of propylene with H_2O_2", *J. Catal.*, **226**, (2004):156-170.

APPENDICES

APPENDIX A

CALCULATION FOR CATALYST PREPARATION

Calculation of Si/Ti Atomic Ration for TS-1

The calculation is based on weight of tetraethyl orthosilicate (TEOS, $Si(OC_2H_5)_4$) for Si source.

Molecular Weight of Si = 28.0855

Molecular Weight of TEOS = 208.330

Weight percent of Si in TEOS = 98

Using TEOS 17.208 g

$$\text{mole of Si used} = \text{wt.} \times \frac{(\%)}{100} \times \frac{(\text{M.W. of Si})}{(\text{M.W. of } SiO_2)} \times \frac{(1\,\text{mole})}{(\text{M.W. of Si})}$$

$$= 17.208 \times (98/100) \times (1/208.330)$$

$$= 0.0809$$

For example, to prepare TS-1 at Si/Ti atomic ratio of 34 by using tetraethyl orthotitanate (TEOT, $C_8H_{20}O_4Ti$) for Ti source.

Molecular Weight of Ti = 47.88

Molecular Weight of TEOT = 228.15

Weight percent purity of TEOT = 95

Si/Ti atomic ratio 34

mole of TEOT required = 0.0809/34

$= 2.37 \times 10^{-3}$ mole

amount of TEOT = $2.37 \times 10^{-3} \times 228.15\ (100/95)$

= 0.569 g

which used in Topic 4.1.2.1.

APPENDIX B

CALCULATION OF DIFFUSIONAL LIMITATION EFFECT

External diffusion limitation

The alcohol oxidation reactions are considered to be an irreversible first order reaction occurred on the pore surface of catalyst particles in a fixed bed microreactor. Assume isothermal operation for the reaction.

In the experiment, 5 vol% alcohols, 0-21 vol% oxygen balance with nitrogen were investigated, in this case using 5 vol% 1-propanol, 8 vol% oxygen and balance with nitrogen was used as an example system calculation. Molecular weight of 1-propanol, nitrogen and oxygen (8 vol%) are 60.09, 28.02 and 31.98 respectively. Thus, the average molecular weight of the gas mixture was calculated as follows:

$$M_{AB} = (0.05\times60.09) + 0.95\times((0.92\times28.02)+(0.08\times31.98))$$
$$= (0.05\times60.09) + (0.95\times28.34)$$
$$= 29.928 \text{ g mol}^{-1}$$

Calculation of reactant gas density

Consider the 1-propanol oxidation is operated at low pressure and high temperature. We assume that the gases are respect to ideal gas law. The density of such gas mixture reactant at various temperatures is calculated in the following.

$$\rho = \frac{PM}{RT} = \frac{1.0\times10^{5}\times29.928\times10^{-3}}{8.314T}$$

We obtained : $\rho = 0.761$ kg m^{-3} at T = 200°C

$\rho = 0.688$ kg m^{-3} at T = 250°C

ρ = 0.628 kg m^{-3} at T = 300ºC

ρ = 0.578 kg m^{-3} at T = 350ºC

Calculation of the gas mixture viscosity

The simplified methods for determining the viscosity of low pressure binary are described anywhere [Reid (1988)]. The method of Wilke is chosen to estimate the gas mixture viscosity.

For a binary system of 1 and 2,

$$\mu_m = \frac{y_1\mu_1}{y_1 + y_2\Phi_{12}} + \frac{y_2\mu_2}{y_2 + y_1\Phi_{21}}$$

Where, μ_m = viscosity of the mixture

μ_1, μ_2 = pure component viscosity

y_1 , y_2 = mole fractions

$$\phi_{12} = \frac{\left[1+\left(\frac{\mu_1}{\mu_2}\right)^{1/2}\left(\frac{M_1}{M_2}\right)^{1/4}\right]^2}{\left[8\left(1+\frac{M_1}{M_2}\right)\right]^{1/2}}$$

$$\phi_{21} = \phi_{12}\left(\frac{\mu_2}{\mu_1}\right)\left(\frac{M_1}{M_2}\right)$$

Where, M_1, M_2 = molecular weight

Let 1 refer to 1-propanol and 2 to air (O_2 8%)

M_1 = 60.09 and M_2 = 28.34

From Perry the viscosity of pure 1-propanol at 200ºC, 250ºC, 300ºC and 350ºC are 0.0124, 0.0135, 0.015 and 0.0162 cP, respectively. The viscosity of pure air at 200ºC, 250ºC, 300ºC and 350ºC are 0.0248, 0.0265, 0.0285 and 0.030 cP, respectively.

At 200ºC :

$$\phi_{12} = \frac{\left[1+\left(\frac{0.0124}{0.0248}\right)^{1/2}\left(\frac{28.34}{60.09}\right)^{1/4}\right]^2}{\left[8\left(1+\frac{60.09}{28.34}\right)\right]^{1/2}} = 0.503$$

$$\phi_{21} = 0.503\left(\frac{0.0248}{0.0124}\right)\left(\frac{60.09}{28.34}\right) = 2.133$$

$$\mu_m = \frac{0.05\times 0.0124}{0.05+0.95\times 0.503} + \frac{0.95\times 0.0248}{0.95+0.05\times 2.133} = 0.0235cP = 2.35\times 10^{-5}\,kg(m\sec)^{-1}$$

At 250ºC :

$$\phi_{12} = \frac{\left[1+\left(\frac{0.0135}{0.0265}\right)^{1/2}\left(\frac{28.34}{60.09}\right)^{1/4}\right]^2}{\left[8\left(1+\frac{60.09}{28.34}\right)\right]^{1/2}} = 0.507$$

$$\phi_{21} = 0.507\left(\frac{0.0265}{0.0135}\right)\left(\frac{60.09}{28.34}\right) = 2.110$$

$$\mu_m = \frac{0.05\times 0.0135}{0.05+0.95\times 0.507} + \frac{0.95\times 0.0265}{0.95+0.05\times 2.110} = 0.0251cP = 2.51\times 10^{-5}\,kg(m\sec)^{-1}$$

At 300ºC :

$$\phi_{12} = \frac{\left[1+\left(\frac{0.015}{0.0285}\right)^{1/2}\left(\frac{28.34}{60.09}\right)^{1/4}\right]^2}{\left[8\left(1+\frac{60.09}{28.34}\right)\right]^{1/2}} = 0.513$$

$$\phi_{21} = 0.513\left(\frac{0.0285}{0.015}\right)\left(\frac{60.09}{28.34}\right) = 2.067$$

$$\mu_m = \frac{0.05 \times 0.0150}{0.05 + 0.95 \times 0.513} + \frac{0.95 \times 0.0285}{0.95 + 0.05 \times 2.067} = 0.0271cP = 2.71 \times 10^{-5}\, kg\left(m\sec\right)^{-1}$$

At 350ºC : $$\phi_{12} = \frac{\left[1 + \left(\frac{0.0162}{0.030}\right)^{1/2}\left(\frac{28.34}{60.09}\right)^{1/4}\right]^2}{\left[8\left(1 + \frac{60.09}{28.34}\right)\right]^{1/2}} = 0.518$$

$$\phi_{21} = 0.518\left(\frac{0.030}{0.0162}\right)\left(\frac{60.09}{28.34}\right) = 2.034$$

$$\mu_m = \frac{0.05 \times 0.0162}{0.05 + 0.95 \times 0.518} + \frac{0.95 \times 0.0300}{0.95 + 0.05 \times 2.034} = 0.0286cP = 2.86 \times 10^{-5}\, kg\left(m\sec\right)^{-1}$$

Calculation of diffusion coefficients

Diffusion coefficients for binary gas system at low pressure calculated by empirical correlation are proposed by Reid (1988). Wilke and Lee method is chosen to estimate the value of D_{AB} due to the general and reliable method. The empirical correlation is

$$D_{AB} = \frac{\left(3.03 - \frac{0.98}{M_{AB}^{1/2}}\right)\left(10^{-3}\right)T^{3/2}}{PM_{AB}^{1/2}\sigma_{AB}^2\Omega_D}$$

Where, D_{AB} = binary diffusion coefficient, $cm^2\ s^{-1}$

T = temperature, K

M_A, M_B = molecular weights of A and B, $g\ mol^{-1}$

$$M_{AB} = 2\left[\left(\frac{1}{M_A}\right)+\left(\frac{1}{M_B}\right)\right]^{-1}$$

Where, P = pressure, bar

σ = characteristic length, Å

Ω_D = diffusion collision integral, dimensionless

The characteristic Lennard-Jones energy and length, ε and σ , of air and propanol are as follows: (Reid,1988)

For C_3H_7OH : σ (C_3H_7OH) = 4.549 Å, ε/k = 576.7

For air : σ (air) = 3.711 Å, ε/k = 78.6

The sample rules are usually employed.

$$\sigma_{AB} = \frac{\sigma_A + \sigma_B}{2} = \frac{4.549 + 3.711}{2} = 4.13$$

$$\varepsilon_{AB}/k = \left(\frac{\varepsilon_A \varepsilon_B}{k^2}\right)^{1/2} = (576.7 \times 78.6)^{1/2} = 212.9$$

Ω_D is tabulated as a function of kT/ε for the Lennard-Jones potential. The accurate relation is

$$\Omega_D = \frac{A}{(T^*)^B} + \frac{C}{\exp(DT^*)} + \frac{E}{\exp(FT^*)} + \frac{G}{\exp(HT^*)}$$

where $T^* = \frac{kT}{\varepsilon_{AB}}$, A = 1.06036 , B = 0.15610 , C = 0.19300 , D = 0.47635 , E = 1.03587 , F = 1.52996 , G = 1.76474 , H = 3.89411

Then, $T^* = \frac{473}{212.9} = 2.222$ at 200°C

$$T^* = \frac{523}{212.9} = 2.456 \text{ at } 250^oC$$

$$T^* = \frac{573}{212.9} = 2.691 \text{ at } 300^oC$$

$$T^* = \frac{623}{212.9} = 2.926 \text{ at } 350^oC$$

$$\Omega_D = \frac{1.06036}{(T^*)^{0.15610}} + \frac{0.19300}{\exp(0.47635T^*)} + \frac{1.03587}{\exp(1.52996T^*)} + \frac{1.76474}{\exp(3.89411T^*)}$$

Ω_D = 1.038 ; 200ºC

Ω_D = 1.006 ; 250ºC

Ω_D = 0.979 ; 300ºC

Ω_D = 0.956 ; 350ºC

With Equation of D_{AB},

$$\underline{\text{At } 200^oC} : D(C_3H_7OH\text{-air}) = \frac{\left(3.03 - \frac{0.98}{30.24^{0.5}}\right)(10^{-3})473^{3/2}}{1 \times 30.24^{0.5} \times 4.13^2 \times 1.038}$$

$$= 3.01 \times 10^{-5} \quad m^2 s^{-1}$$

$$\underline{\text{At } 250^oC} : D(C_3H_7OH\text{-air}) = \frac{\left(3.03 - \frac{0.98}{30.24^{0.5}}\right)(10^{-3})523^{3/2}}{1 \times 30.24^{0.5} \times 4.13^2 \times 1.006}$$

$$= 3.62 \times 10^{-5} \quad m^2 s^{-1}$$

$$\underline{\text{At } 300^oC} : D(C_3H_7OH\text{-air}) = \frac{\left(3.03 - \frac{0.98}{30.24^{0.5}}\right)(10^{-3})573^{3/2}}{1 \times 30.24^{0.5} \times 4.13^2 \times 0.979}$$

$$= 4.26 \times 10^{-5} \quad m^2 s^{-1}$$

$$\underline{\text{At } 350^{o}\text{C}}\ :\ D(C_3H_7OH\text{-air}) = \frac{\left(3.03-\frac{0.98}{30.24^{0.5}}\right)(10^{-3})623^{3/2}}{1\times 30.24^{0.5}\times 4.13^{2}\times 0.956}$$

$$= \quad 5.04\times 10^{-5} \quad m^2\ s^{-1}$$

Reactant gas mixture was supplied at 100 ml/min in tubular microreactor used in the 1-propanol oxidation system at 30ºC

1-propanol flow rate through reactor = 100 ml/min. at 30ºC

The density of 1-propanol , $\rho = \frac{1.0\times 10^{5}\times 29.928\times 10^{-3}}{8.314(273+30)} = 1.188\ \text{kg m}^{-3}$

Mass flow rate = $1.188\left(\frac{100\times 10^{-6}}{60}\right) = 1.98\times 10^{-6}$ kg s^{-1}

Diameter of quartz tube reactor = 8 mm

Cross-sectional area of tube reactor = $\frac{\pi(8\times 10^{-3})^{2}}{4} = 5.03\times 10^{-5}$ m^2

Mass Velocity , $G = \frac{1.98\times 10^{-6}}{5.03\times 10^{-5}} = 0.039$ kg $m^{-2}s^{-1}$

Catalyst size = 40-60 mesh = 0.178-0.126 mm

Average catalyst size = (0.126+0.178)/2 = 0.152 mm

Find Reynolds number, Re_p, which is well known as follows:

$$Re_p = \frac{d_p G}{\mu}$$

We obtained,

$$\underline{\text{At } 200^{o}\text{C}}\ : \qquad Re_p = \frac{(0.152\times 10^{-3}\times 0.039)}{2.35\times 10^{-5}} = 0.252$$

$$\underline{\text{At } 250^{o}\text{C}}\ : \qquad Re_p = \frac{(0.152\times 10^{-3}\times 0.039)}{2.51\times 10^{-5}} = 0.236$$

At 300ºC : $Re_p = \frac{(0.152\times10^{-3}\times0.039)}{2.71\times10^{-5}} = 0.219$

At 350ºC : $Re_p = \frac{(0.152\times10^{-3}\times0.039)}{2.86\times10^{-5}} = 0.207$

Average transport coefficient between the bulk stream and particles surface could be correlated in terms of dimensionless groups, which characterize the flow conditions. For mass transfer the Sherwood number, $k_m\rho/G$, is an empirical function of the Reynolds number, d_pG/μ, and the Schmit number, $\mu/\rho D$. The j-factors are defined as the following functions of the Schmidt number and Sherwood numbers:

$$j_D = \frac{k_m\rho}{G}\left(\frac{a_m}{a_t}\right)\left(\frac{\mu}{\rho D}\right)^{2/3}$$

The ratio (a_m/a_t) allows for the possibility that the effective mass-transfer area a_m, may be less than the total external area, a_t, of the particles. For Reynolds number greater than 10, the following relationship between j_D and the Reynolds number well represents available data.

$$j_D = \frac{0.458}{\varepsilon_B}\left(\frac{d_pG}{\mu}\right)^{-0.407}$$

Where, G = mass velocity(superficial) based upon cross-sectional area of empty reactor ($G = u\rho$)

d_p = diameter of catalyst particle for spheres

μ = viscosity of fluid

ρ = density of fluid

ε_B = void fraction of the interparticle space (void fraction of the bed)

D = molecular diffusivity of component being transferred

Assume $\varepsilon_B = 0.5$

<u>At 200ºC</u> ; $j_D = \frac{0.458}{0.5}(0.252)^{-0.407} = 1.605$

<u>At 250ºC</u> ; $j_D = \frac{0.458}{0.5}(0.236)^{-0.407} = 1.649$

<u>At 300ºC</u> ; $j_D = \frac{0.458}{0.5}(0.219)^{-0.407} = 1.699$

<u>At 350ºC</u> ; $j_D = \frac{0.458}{0.5}(0.207)^{-0.407} = 1.739$

A variation of the fixed bed reactor is an assembly of screens or gauze of catalytic solid over which the reacting fluid flows. Data on mass transfer from single screens has been reported by Gay and Maughan. Their correlation is of the form

$$j_D = \frac{\varepsilon k_m \rho}{G}\left(\frac{\mu}{\rho D}\right)^{2/3}$$

Where ε is the porosity of the single screen.

Hence, $k_m = \left(\frac{j_D G}{\mu}\right)\left(\frac{\mu}{\rho D}\right)^{2/3}$

$$k_m = \left(\frac{0.458G}{\varepsilon_B \rho}\right)\mathrm{Re}^{-0.407}\, Sc^{-2/3}$$

Find Schmidt number, Sc : $Sc = \frac{\mu}{\rho D}$

<u>At 200ºC</u> : $Sc = \frac{2.35*10^{-5}}{0.761*3.01*10^{-5}} = 1.026$

At 250ºC : $Sc = \frac{2.51*10^{-5}}{0.688*3.62*10^{-5}} = 1.008$

At 300ºC : $Sc = \frac{2.71*10^{-5}}{0.628*4.26*10^{-5}} = 1.013$

At 350ºC : $Sc = \frac{2.86*10^{-5}}{0.578*5.04*10^{-5}} = 0.982$

Find k_m : At 200ºC, $k_m = \left(\frac{1.605 \times 0.039}{0.761}\right)(1.026)^{-2/3} = 0.081\,\text{m s}^{-1}$

At 250ºC, $k_m = \left(\frac{1.649 \times 0.039}{0.688}\right)(1.008)^{-2/3} = 0.093\,\text{m s}^{-1}$

At 300ºC, $k_m = \left(\frac{1.699 \times 0.039}{0.628}\right)(1.013)^{-2/3} = 0.105\,\text{m s}^{-1}$

At 350ºC, $k_m = \left(\frac{1.739 \times 0.039}{0.578}\right)(0.982)^{-2/3} = 0.119\,\text{m s}^{-1}$

Properties of catalyst

Density = 12.102 g/ml catalyst

Diameter of 40-60 mesh catalyst particle = 0.152 mm

Weight per catalyst particle = $\frac{\pi(0.152 \times 0^{-1})^3 \times 12.102}{6} = 2.225 \times 10^{-5}$ g/particle

External surface area per particle = $\pi(0.152 \times 10^{-3})^2 = 7.258 \times 10^{-8}$ m^2/particle

$a_m = \frac{7.258 \times 10^{-8}}{2.225 \times 10^{-5}} = 3.262 \times 10^{-3}$ m^2/gram catalyst

Volumetric flow rate of gaseous feed stream = 100 ml min^{-1}

Molar flow rate of gaseous feed stream = $\frac{(1 \times 10^5)\left(\frac{100 \times 10^{-6}}{60}\right)}{8.314(273+30)} = 6.616 \times 10^{-5}\,\text{mol s}^{-1}$

1-propanol molar feed rate = $0.05 \times 6.616 \times 10^{-5} = 3.308 \times 10^{-6}$ mol s^{-1}

1-propanol conversion (experimental data): 0.07 % at 200ºC
0.45 % at 250ºC
44.49 % at 300ºC
74.40 % at 350ºC

The estimated rate of 1-propanol oxidation reaction is based on the ideal plug flow reactor which there is no mixing in the direction of flow and complete mixing perpendicular to the direction of flow (i.e., in the radial direction). The rate of reaction will vary with reaction length. Plug flow reactors are normally operated at steady state so that properties at any position are constant with respect to time. The mass balance around plug flow reactor becomes

$\{\text{rate of i into volume element}\} - \{\text{rate of i out of volume element}\}$
$+ \{\text{rate of production of i within the volume element}\}$
$= \{\text{rate of accumulation of i within the volume elecment}\}$

$$F_{Ao} = F_{Ao}(1-x) + (r_W W)$$
$$(r_W W) = F_{Ao} - F_{Ao}(1-x) = F_{Ao} = F_{Ao}x$$

$$r_W = \frac{F_{Ao}x}{W} = \frac{3.308 \times 10^{-6} \times 0.0007}{0.1} = 2.316 \times 10^{-8} \text{ mol } s^{-1}\text{gram})^{-1} \text{ catalyst at 200ºC}$$

$$r_W = \frac{F_{Ao}x}{W} = \frac{3.308 \times 10^{-6} \times 0.0045}{0.1} = 1.489 \times 10^{-5} \text{ mol } s^{-1}\text{gram}^{-1} \text{ catalyst at 250ºC}$$

$$r_W = \frac{F_{Ao}x}{W} = \frac{3.308 \times 10^{-6} \times 0.4449}{0.1} = 1.472 \times 10^{-5} \text{ mol } s^{-1}\text{gram}^{-1} \text{ catalyst at 300ºC}$$

$$r_W = \frac{F_{Ao}x}{W} = \frac{3.308 \times 10^{-6} \times 0.7440}{0.1} = 2.461 \times 10^{-5} \text{ mol } s^{-1}\text{gram}^{-1} \text{ catalyst at 350ºC}$$

At steady state the external transport rate may be written in terms of the diffusion rate from the bulk gas to the surface. The expression is:

$$R_{obs} = k_m a_m (C_b - C_s)$$

$$= \frac{1\text{-propanol converted (mole)}}{(\text{time})(\text{gram of catalyst})}$$

Where, C_b and C_s are the concentrations in the bulk gas and at the surface, respectively.

<u>At 200ºC</u>, $(C_b - C_s) = \frac{r_{obs}}{k_m a_m} = \frac{2.316 \times 10^{-8}}{0.081 \times 3.262 \times 10^{-3}} = 8.765 \times 10^{-5}$ mol m^{-3}

<u>At 250ºC</u>, $(C_b - C_s) = \frac{r_{obs}}{k_m a_m} = \frac{1.489 \times 10^{-7}}{0.093 \times 3.262 \times 10^{-3}} = 4.908 \times 10^{-4}$ mol m^{-3}

<u>At 300ºC</u>, $(C_b - C_s) = \frac{r_{obs}}{k_m a_m} = \frac{1.472 \times 10^{-5}}{0.105 \times 3.262 \times 10^{-3}} = 4.298 \times 10^{-2}$ mol m^{-3}

<u>At 350ºC</u>, $(C_b - C_s) = \frac{r_{obs}}{k_m a_m} = \frac{2.461 \times 10^{-5}}{0.110 \times 3.262 \times 10^{-3}} = 6.859 \times 10^{-2}$ mol m^{-3}

From C_b (1-propanol) = 2.25 mol m^{-3}

Consider the difference of the bulk and surface concentration is small. It means that the external mass transport has no effect on the 1-propanol oxidation reaction rate.

APPENDIX C

CALCULATION OF SPECIFIC SURFACE AREA

From Brunauer-Emmett-Teller (BET) equation

$$\frac{p}{n(1-p)} = \frac{1}{n_m C} + \frac{(C-1)p}{n_m C} \qquad (C1)$$

Where, p = Relative partial pressure of adsorbed gas, P/P_0

P_0 = Saturated vapor pressure of adsorbed gas in the condensed state at the experimental temperature, atm

P = Equilibrium vapor pressure of adsorbed gas, atm

n = Quantity of gas adsorbed at pressure P, ml at the NTP/g of sample

n_m = Quantity of gas adsorbed at monolayer, ml at the NTP/g of sample

C = Exp $[(H_C - H_l)/RT]$

H_C = Heat of condensation of adsorbed gas on all other layers

H_l = Heat of adsorption into the first layer

For the single point method, the graph must pass through the origin. Therefore, the value of C must be assumed to be infinity.

$C \rightarrow \infty$, then equation C1 is reduced to

$$\frac{p}{n(1-p)} = \frac{p}{n_m}$$

$$n_m = n(1 - p) \qquad (C2)$$

The surface area of the catalyst, S, is given by

$$S = S_b \times n_m \qquad (C3)$$

Where, S_b = Surface area of nitrogen gas

From the gas law

$$\frac{P_b V}{T_b} = \frac{P_t V}{T_t} \qquad \text{(C4)}$$

Where, P_b = Pressure at 0°C

P_t = Pressure at t°C

T_b = Temperature at 0°C = 273.15 K

T_t = Temperature at t°C = (273.15 + t) K

V = Constant volume

Then, $P_b = (273.15/ T_t) \times P_t = 1$ atm

Partial pressure

$$P = \frac{[\text{Flow of } (He + N_2) - \text{Flow of } He]}{\text{Flow of } (He + N_2)} \qquad \text{(C5)}$$

$$= 0.3 \text{ atm}$$

For nitrogen gas, the saturated vapor pressure equals to

$$P_0 = 1.1 \text{ atm}$$

then, $p = P/P_0 = 0.3/1.1 = 0.2727$

To measure the volume of nitrogen adsorbed, n

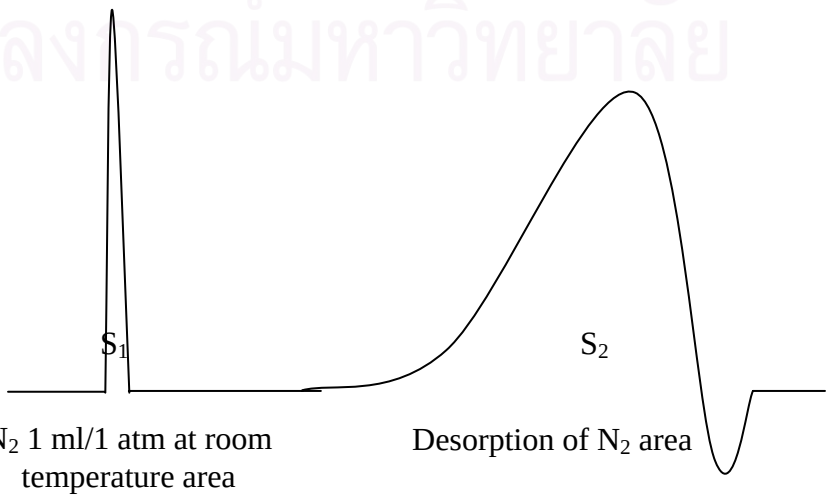

$$n = \frac{S_2}{S_1} \times \frac{1}{W} \times \frac{273.15}{T} \text{ ml g}^{-1} \text{ of catalyst} \quad \text{(C6)}$$

Where, S_1 = N_2 1 ml/1 atm at room temperature area

S_2 = Desorption of N_2 area

W = Sample weight, g

T = Room temperature, K

From C2, $n_m = n(1-p)$

Therefore,

$$n_m = \frac{S_2}{S_1} \times \frac{1}{W} \times \frac{273.15}{T} \times (1-p)$$

$$n_m = \frac{S_2}{S_1} \times \frac{1}{W} \times \frac{273.15}{T} \times 0.7272 \quad \text{(C7)}$$

Whereas, the surface area of nitrogen gas from literature equal to

S_b = 4.373 m^2 ml^{-1} of nitrogen gas

From C3, $S = S_b \times n_m$

Then,

$$S = \frac{S_2}{S_1} \times \frac{1}{W} \times \frac{273.15}{T} \times 0.7272 \times 4.343$$

$$S = \frac{S_2}{S_1} \times \frac{1}{W} \times \frac{273.15}{T} \times 3.1582 \text{ m}^2 \text{ g}^{-1} \quad \text{(C8)}$$

APPENDIX D

CALIBRATION CURVES

Flame ionization detector gas chromatograph, model 8A, was used to analyze the concentrations of oxygenated compounds. Methanol, 1-propanol, 2-propanol, methane, propylene, formaldehyde, isopropyl ether and acetone were analyzed by GC model 8A with using 15% Carbowax 1000, while ethanol, ethylene and acetaldehyde were analyzed by GC model 8A with using Carbopack B/3% SP-1500.

Gas chromatograph with the thermal conductivity detector, model 8A, was used to analyze the concentration of CO, CO_2 by using Molecular Sieve 5A and Porapak-Q columns respectively.

The calibration curves of methanol, ethanol, 1-propanol, 2-propanol, methane, ethylene, propylene, formaldehyde, acetaldehyde, isopropyl ether, acetone, CO and CO_2 are illustrated in the following figures.

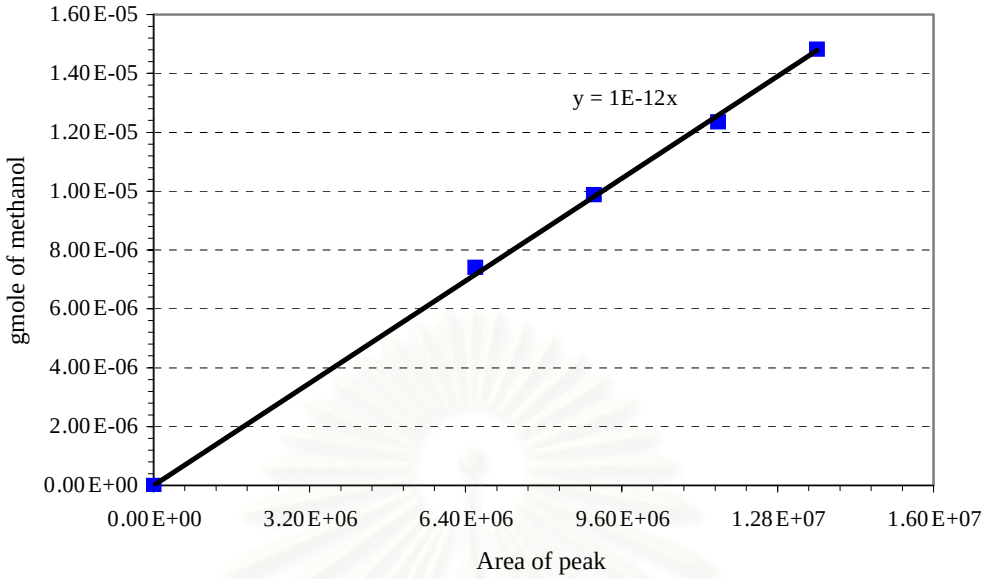

Figure D1 The calibration curve of methanol

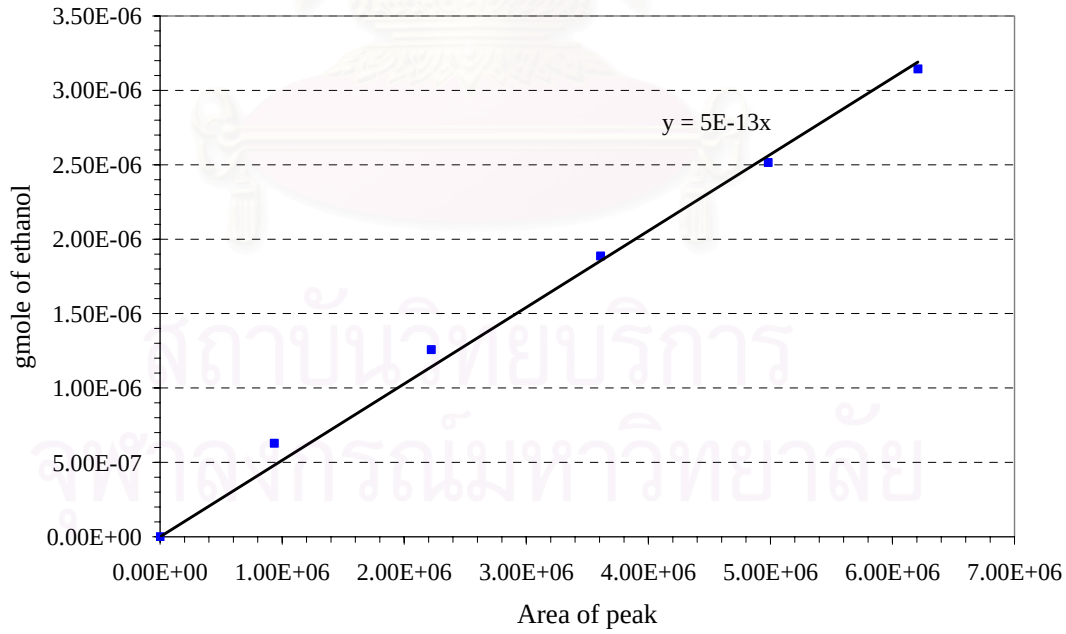

Figure D2 The calibration curve of ethanol

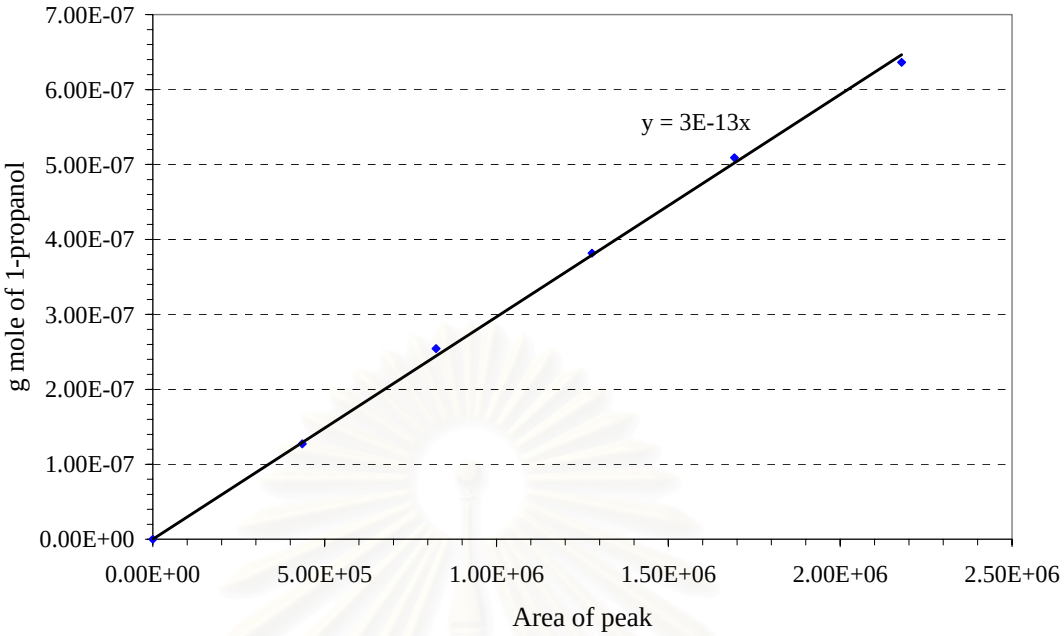

Figure D3 The calibration curve of 1-propanol

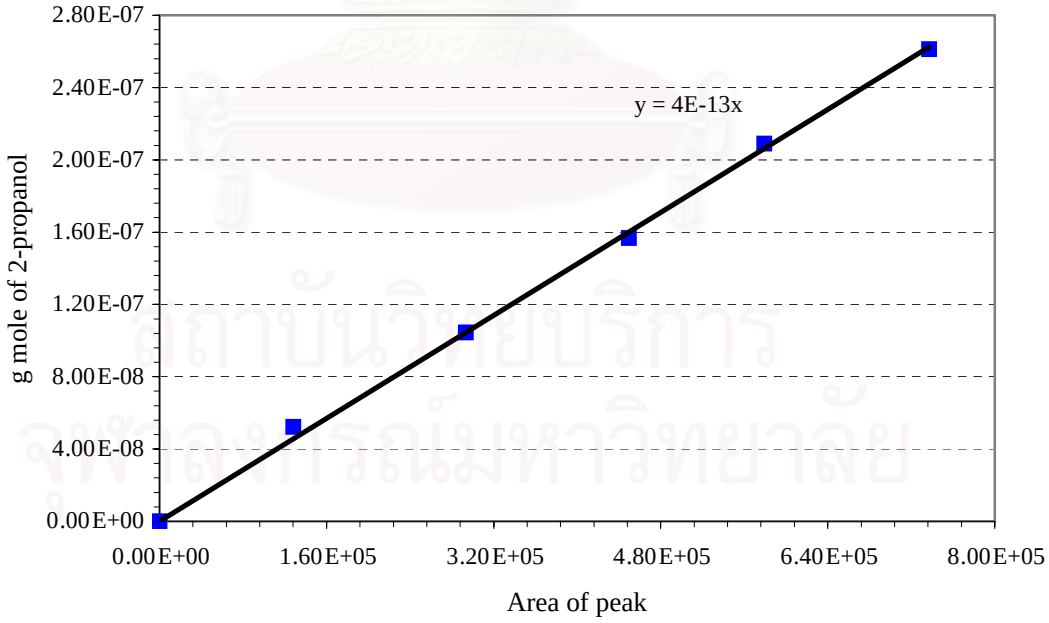

Figure D4 The calibration curve of 2-propanol

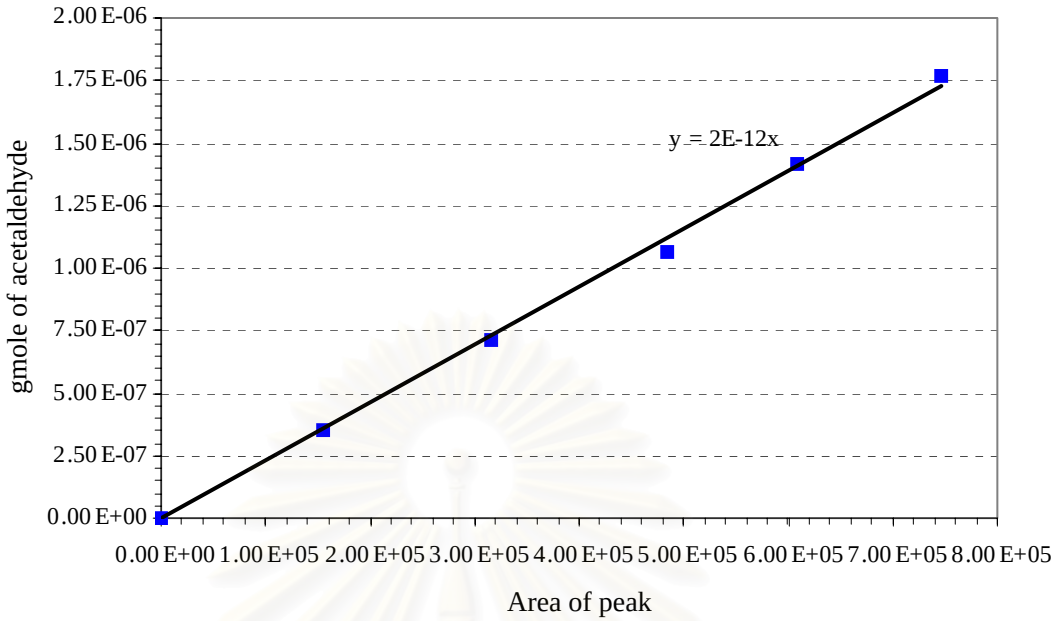

Figure D5 The calibration curve of methane

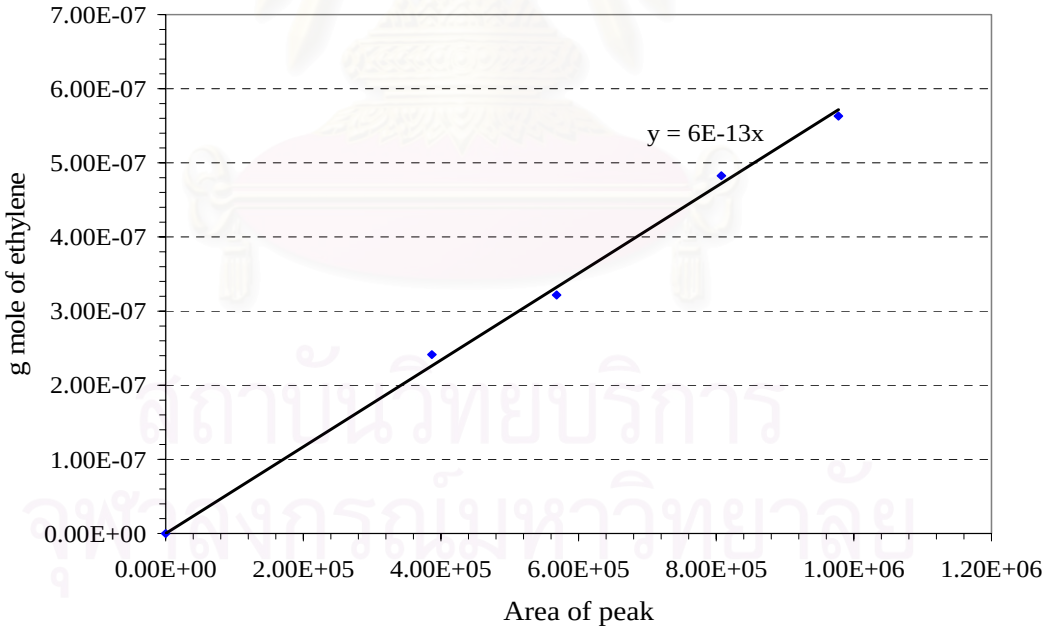

Figure D6 The calibration curve of ethylene

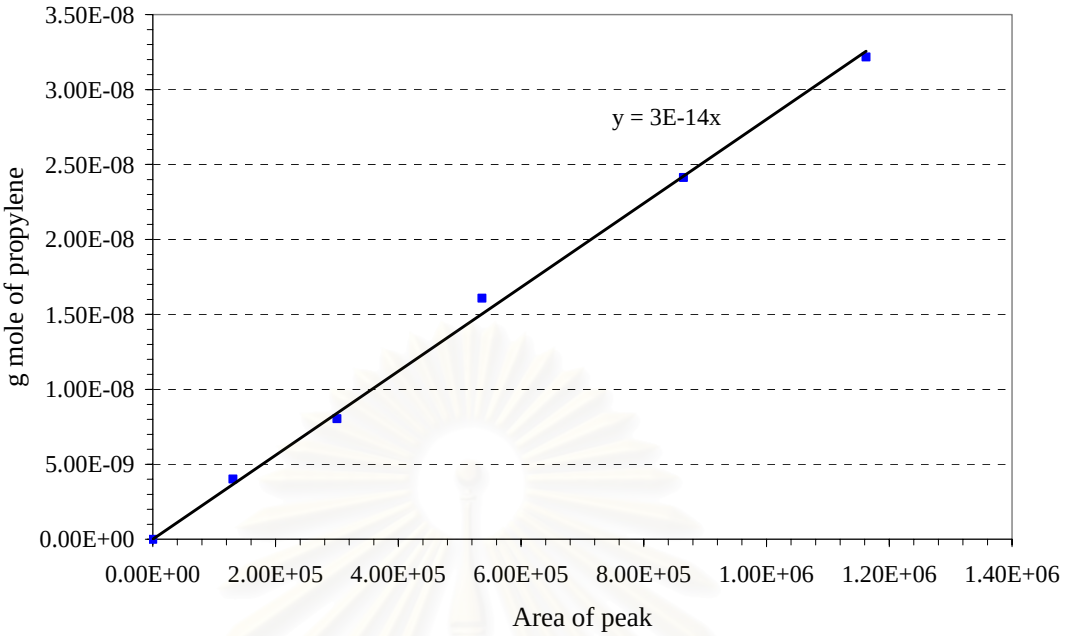

Figure D7 The calibration curve of propylene

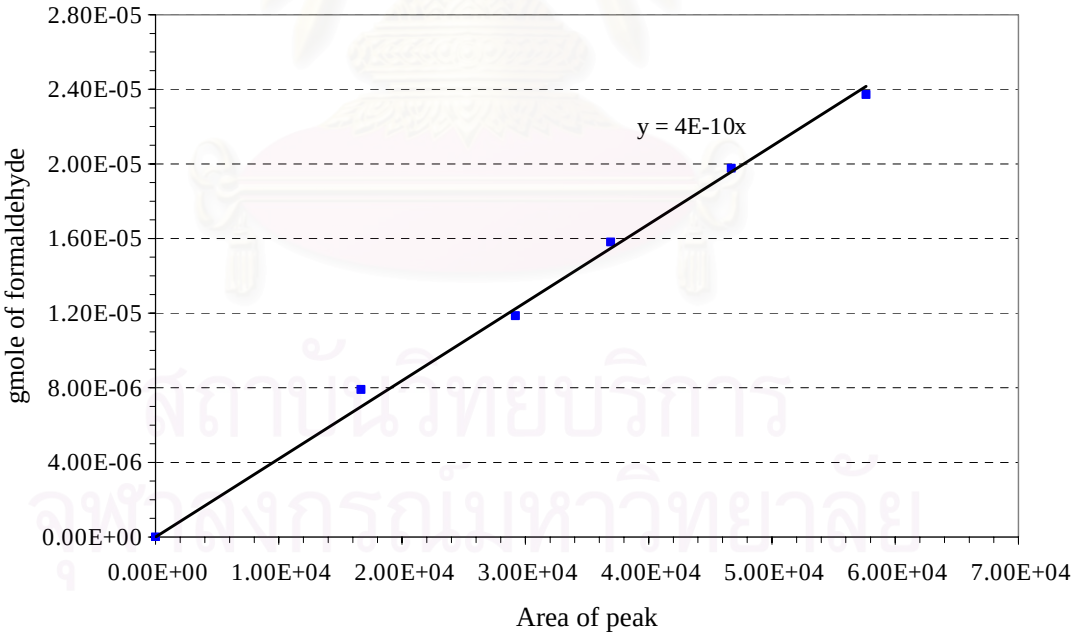

Figure D8 The calibration curve of formaldehyde

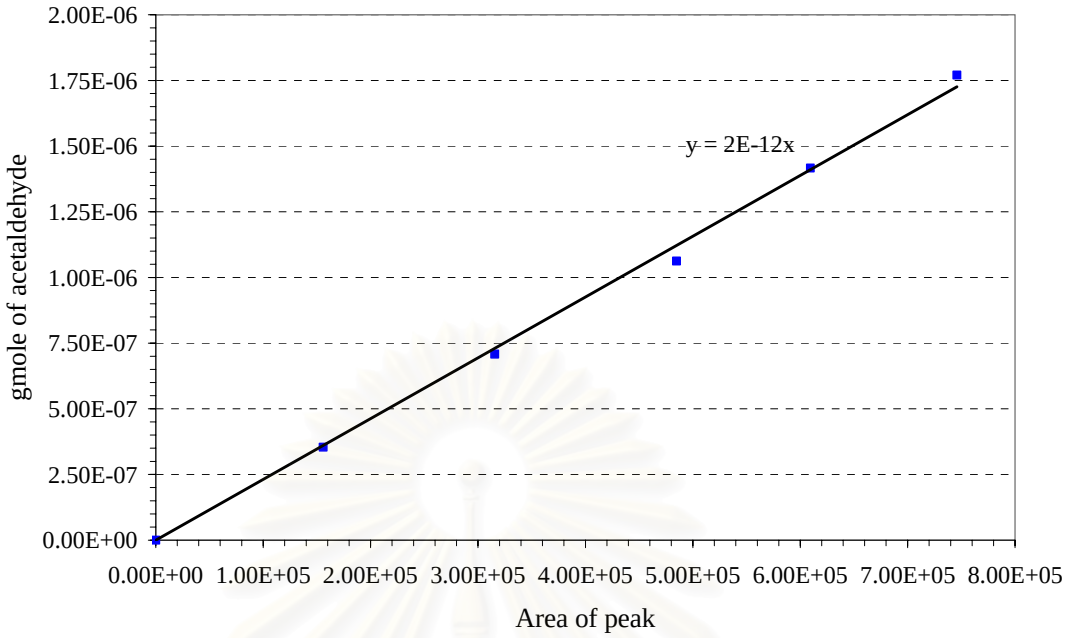

Figure D9 The calibration curve of acetaldehyde

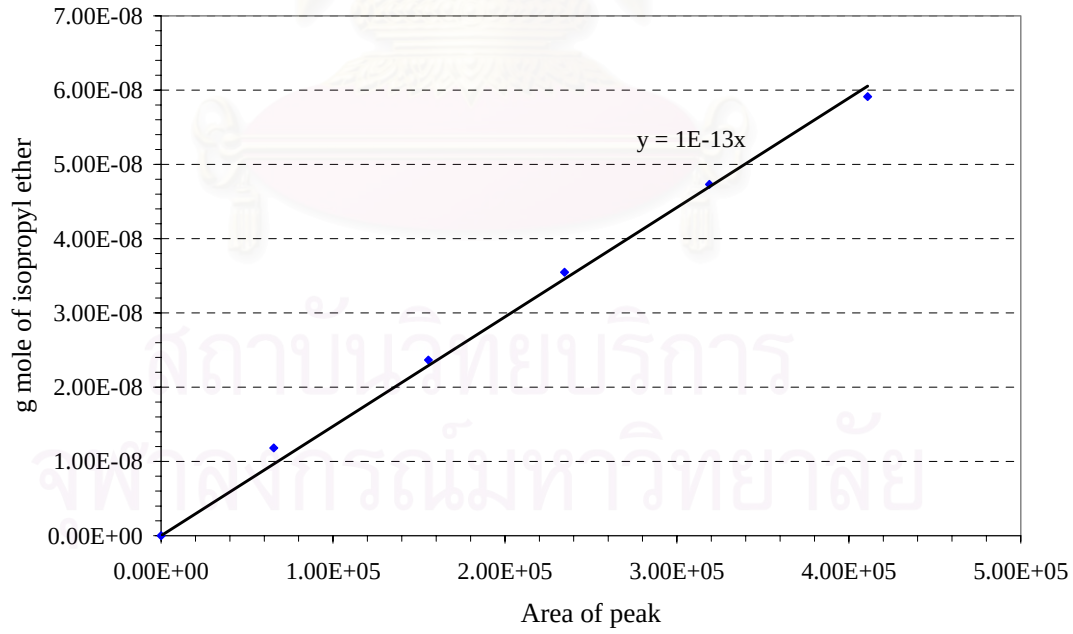

Figure D10 The calibration curve of isopropyl ether

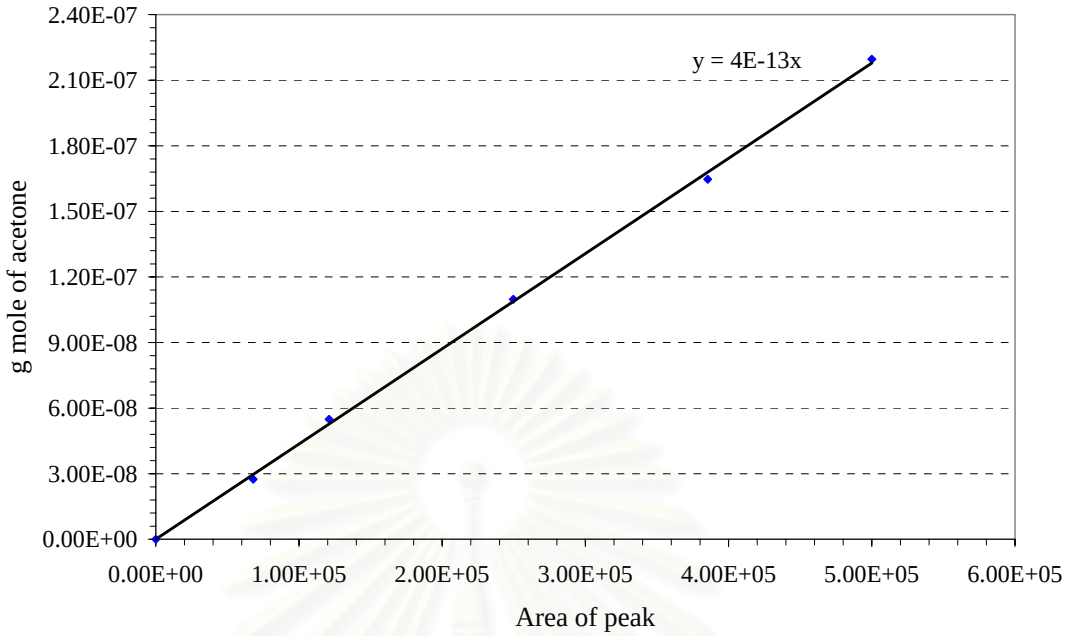

Figure D11 The calibration curve of acetone

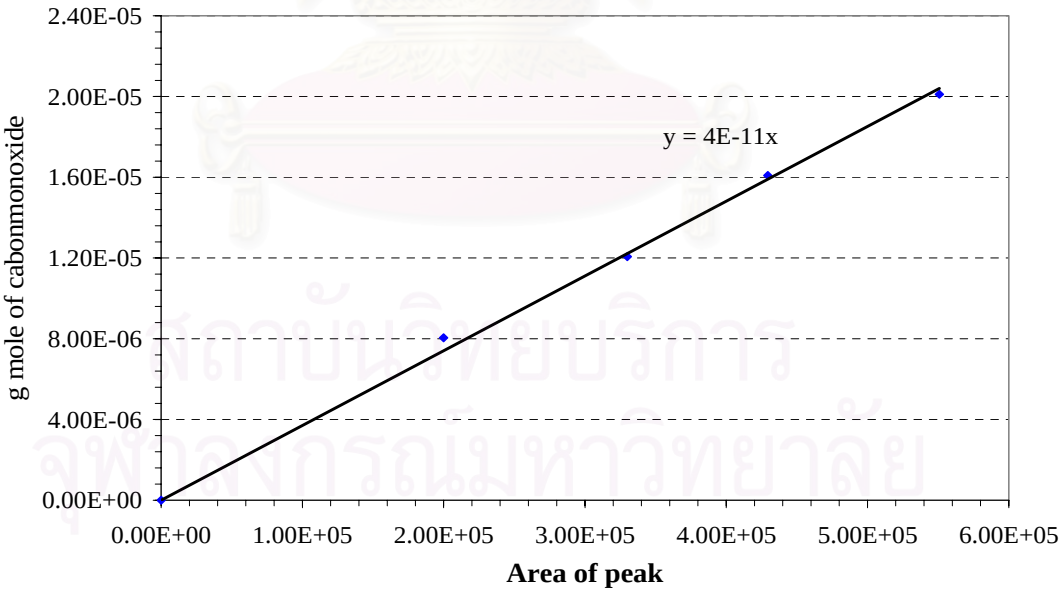

Figure D12 The calibration curve of carbonmonoxide

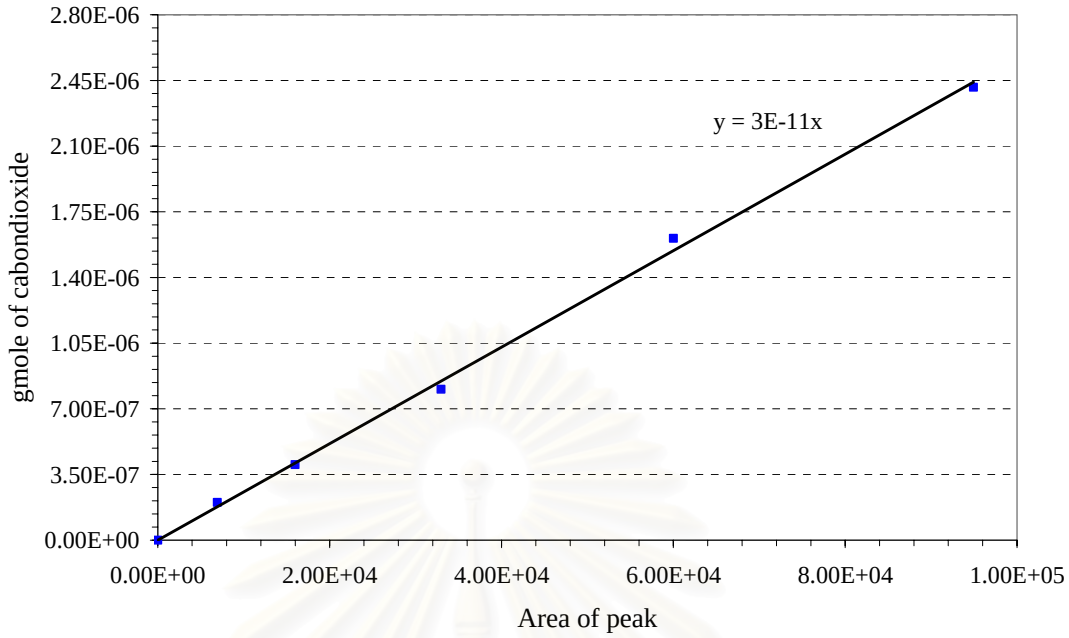

Figure D13 The calibration curve of carbondioxide

APPENDIX E

DATA OF EXPERIMENTS

Table E1 Data of Figure 5.5

Reaction temperature (°C)	Component				
	% 2-propanol (C)	%propylene (S)	% isopropyl ether (S)	% acetone(S)	% CO_2(S)
100	0.00	0.00	0.00	0.00	0.00
150	0.00	0.00	0.00	0.00	0.00
200	0.00	0.00	0.00	0.00	0.00
250	0.00	0.00	0.00	7.61	0.00
300	0.00	0.00	0.00	46.29	0.00
350	0.72	3.75	0.00	96.25	0.00
400	3.22	7.17	0.00	92.83	0.00
450	11.08	21.56	0.00	78.44	0.00
500	21.30	25.70	0.00	74.30	0.00

Table E2 Data of Figure 5.6a

Reaction temperature (°C)	Component				
	% 2-propanol (C)	%propylene (S)	% isopropyl ether (S)	% acetone(S)	% CO_2(S)
100	0.00	0.00	0.00	0.00	0.00
150	0.00	0.00	0.00	0.00	0.00
200	0.28	99.48	0.00	0.52	0.00
250	37.82	99.08	0.00	0.92	0.00
300	85.46	97.92	0.00	2.08	0.00
350	95.97	88.49	0.00	11.51	0.00
400	99.24	79.60	0.00	20.40	0.00
450	99.81	80.34	0.00	19.66	0.00
500	99.97	72.83	0.00	27.17	0.00

Table E3 Data of Figure 5.6b

Reaction temperature (°C)	Component				
	% 2-propanol (C)	%propylene (S)	% isopropyl ether (S)	% acetone(S)	% CO_2(S)
100	0.00	0.00	0.00	0.00	0.00
150	0.00	0.00	0.00	0.00	0.00
200	0.39	0.03	0.07	99.96	0.00
250	30.60	0.03	0.05	99.97	0.00
300	51.89	0.26	0.51	99.72	0.03
350	95.60	0.38	0.76	99.12	0.50
400	99.18	3.58	7.16	83.75	12.67
450	99.09	5.62	11.23	1.69	92.69
500	97.95	1.00	2.00	1.33	97.67

Table E4 Data of Figure 5.6c

Reaction temperature (°C)	Component				
	% 2-propanol (C)	%propylene (S)	% isopropyl ether (S)	% acetone(S)	% CO_2(S)
100	0.00	0.00	0.00	0.00	0.00
150	0.00	0.00	0.00	0.00	0.00
200	0.16	0.02	0.00	99.96	0.01
250	1.58	0.32	0.00	99.68	0.00
300	15.55	0.62	0.00	99.37	0.01
350	74.15	0.99	0.01	98.88	0.13
400	99.11	1.63	0.13	96.40	1.85
450	99.87	30.44	0.15	3.92	65.49
500	99.95	11.41	0.00	0.12	88.46

Table E5 Data of Figure 5.6d

Reaction temperature (°C)	Component				
	% 2-propanol (C)	%propylene (S)	% isopropyl ether (S)	% acetone(S)	% CO_2(S)
100	0.00	0.00	0.00	0.00	0.00
150	0.01	0.00	0.00	99.98	0.01
200	0.36	0.20	0.00	99.80	0.00
250	4.09	1.23	0.00	98.77	0.00
300	51.72	1.23	0.00	98.71	0.07
350	97.42	0.92	0.00	97.87	1.21
400	99.25	17.60	0.73	7.13	74.54
450	96.06	4.54	0.00	0.01	95.44
500	91.05	0.25	0.00	1.63	98.13

Table E6 Data of Figure 5.7

Reaction temperature (°C)	Component			
	% propylene (C)	% acetone (S)	% isopropyl ether (S)	% CO_2 (S)
100	0.00	0.00	0.00	0.00
150	0.00	0.00	0.00	0.00
200	0.00	0.00	0.00	0.00
250	0.00	0.00	0.00	0.00
300	0.04	100.00	0.00	0.00
350	2.75	99.87	0.13	0.00
400	12.29	96.69	1.09	2.22
450	29.97	96.23	0.93	2.84
500	32.79	90.87	5.04	4.09

Table E7 Data of Figure 5.9

Reaction temperature (°C)	Component				
	% 1-propanol (C)	%propylene (S)	% isopropyl ether (S)	% acetone(S)	% CO_2(S)
100	0.00	0.00	0.00	0.00	0.00
150	0.00	0.00	0.00	0.00	0.00
200	0.00	0.00	0.00	0.00	0.00
250	0.04	0.03	0.00	99.96	0.01
300	0.39	0.05	0.00	99.94	0.01
350	0.77	0.39	0.00	99.60	0.01
400	2.53	0.58	0.00	99.41	0.01
450	5.90	0.47	0.00	99.53	0.00
500	27.02	0.63	0.00	99.36	0.00

Table E8 Data of Figure 5.10a

Reaction temperature (°C)	Component				
	% 1-propanol (C)	%propylene (S)	% isopropyl ether (S)	% acetone(S)	% CO_2(S)
100	0.00	0.00	0.00	0.00	0.00
150	0.00	0.00	0.00	0.00	0.00
200	0.00	0.00	0.00	0.00	0.00
250	0.01	59.14	0.00	40.86	0.00
300	0.54	44.10	0.00	55.90	0.00
350	14.89	89.54	0.00	10.46	0.00
400	94.31	95.20	0.00	4.80	0.00
450	97.98	92.57	0.00	7.43	0.00
500	99.67	86.40	0.00	13.60	0.00

Table E9 Data of Figure 5.10b

Reaction temperature (°C)	Component				
	% 1-propanol (C)	%propylene (S)	% isopropyl ether (S)	% acetone(S)	% CO_2(S)
100	0.00	0.00	0.00	0.00	0.00
150	0.00	0.00	0.00	0.00	0.00
200	0.07	83.37	0.15	16.46	0.02
250	0.45	15.63	0.20	83.99	0.18
300	45.42	6.96	1.11	91.25	0.68
350	99.60	0.38	3.19	91.88	4.55
400	99.52	3.80	0.00	0.02	96.18
450	99.50	3.78	0.00	0.00	96.22
500	99.66	3.76	0.00	0.00	96.24

Table E10 Data of Figure 5.10c

Reaction temperature (°C)	Component				
	% 1-propanol (C)	%propylene (S)	% isopropyl ether (S)	% acetone(S)	% CO_2(S)
100	0.00	0.00	0.00	0.00	0.00
150	0.00	0.00	0.00	0.00	0.00
200	0.00	0.00	0.00	0.00	0.00
250	0.59	52.91	0.55	45.85	0.69
300	53.56	20.97	2.62	75.66	0.75
350	97.23	6.02	11.75	68.55	13.67
400	99.87	4.08	0.08	40.73	55.12
450	100.00	5.85	0.00	3.70	90.45
500	100.00	7.70	0.00	0.19	92.11

Table E11 Data of Figure 5.10d

Reaction temperature (°C)	Component				
	% 1-propanol (C)	%propylene (S)	% isopropyl ether (S)	% acetone(S)	% CO_2(S)
100	0.00	0.00	0.00	0.00	0.00
150	0.00	0.00	0.00	0.00	0.00
200	0.01	97.67	0.64	0.00	1.69
250	0.33	86.66	2.65	10.55	0.14
300	47.28	48.44	1.10	50.02	0.44
350	92.30	16.06	8.42	73.91	1.61
400	99.90	1.41	3.88	94.30	0.41
450	99.31	12.08	0.09	59.42	28.41
500	99.57	9.87	0.00	1.53	88.60

Table E12 Data of Figure 5.12

Reaction temperature (°C)	Component					
	%ethanol (C)	%methane (S)	%ethylene (S)	%acetaldehyde (S)	%acetone (S)	%CO_2 (S)
100	0.00	0.00	0.00	0.00	0.00	0.00
150	0.00	0.00	0.00	0.00	0.00	0.00
200	0.04	0.00	0.00	100.00	0.00	0.00
250	3.09	0.00	0.00	100.00	0.00	0.00
300	2.58	0.00	0.04	99.96	0.00	0.00
350	4.23	0.00	1.54	98.46	0.00	0.00
400	4.24	0.00	3.81	96.19	0.00	0.00
450	5.84	0.00	3.88	96.12	0.00	0.00
500	10.51	0.01	7.74	92.25	0.00	0.00

Table E13 Data of Figure 5.13a

Reaction temperature (°C)	Component					
	%ethanol (C)	%methane (S)	%ethylene (S)	%acetaldehyde (S)	%acetone (S)	%CO_2 (S)
100	0.00	0.00	0.00	0.00	0.00	0.00
150	0.00	0.00	0.00	0.00	0.00	0.00
200	0.00	0.00	0.00	0.00	0.00	0.00
250	0.01	0.00	100.00	0.00	0.00	0.00
300	0.40	0.00	85.92	14.07	0.00	0.00
350	28.45	0.00	98.15	1.85	0.00	0.00
400	89.41	0.00	99.73	0.27	0.00	0.00
450	98.48	0.00	99.86	0.14	0.00	0.00
500	99.61	0.00	99.75	0.25	0.00	0.00

Table E14 Data of Figure 5.13b

Reaction temperature (°C)	Component					
	%ethanol (C)	%methane (S)	%ethylene (S)	%acetaldehyde (S)	%acetone (S)	%CO_2 (S)
100	0.00	0.00	0.00	0.00	0.00	0.00
150	0.00	0.00	0.00	0.00	0.00	0.00
200	0.00	0.00	0.00	0.00	0.00	0.00
250	0.13	0.00	0.69	99.29	0.00	0.02
300	4.12	0.00	0.88	99.06	0.01	0.05
350	57.57	0.00	6.91	92.14	0.60	0.35
400	98.22	0.06	15.54	80.14	2.62	1.65
450	99.03	7.00	58.89	0.48	0.12	31.31
500	99.29	4.35	43.96	0.04	0.00	49.49

Table E15 Data of Figure 5.13c

Reaction temperature (°C)	Component					
	%ethanol (C)	%methane (S)	%ethylene (S)	%acetaldehyde (S)	%acetone (S)	%CO_2 (S)
100	0.00	0.00	0.00	0.00	0.00	0.00
150	0.00	0.00	0.00	0.00	0.00	0.00
200	0.05	0.01	0.03	99.96	0.00	0.00
250	0.84	0.00	0.35	99.24	0.00	0.41
300	8.47	0.00	1.75	98.03	0.00	0.22
350	57.38	0.00	6.44	93.39	0.10	0.07
400	99.30	0.01	14.29	83.04	1.55	1.12
450	99.77	1.50	76.17	0.61	0.22	21.19
500	99.83	1.28	74.26	0.01	0.00	24.14

Table E16 Data of Figure 5.13d

Reaction temperature (°C)	Component					
	%ethanol (C)	%methane (S)	%ethylene (S)	%acetaldehyde (S)	%acetone (S)	%CO_2 (S)
100	0.00	0.00	0.00	0.00	0.00	0.00
150	0.00	0.00	0.00	0.00	0.00	0.00
200	0.02	0.03	0.05	99.88	0.00	0.04
250	0.58	0.01	1.38	98.20	0.00	0.41
300	12.38	0.00	1.65	98.22	0.01	0.12
350	85.28	0.00	52.95	46.73	0.16	0.23
400	97.99	0.05	46.23	49.86	3.39	2.16
450	99.56	3.54	74.57	0.40	0.87	21.06
500	100.00	5.24	52.71	0.00	0.00	42.05

Table E17 Data of Figure 5.15

Reaction temperature (°C)	Component				
	% methanol (C)	% methane (S)	% formaldehyde (S)	% CO (S)	% CO_2 (S)
100	0.00	0.00	0.00	0.00	0.00
150	0.00	0.00	0.00	0.00	0.00
200	0.00	0.00	0.00	0.00	0.00
250	0.00	0.00	0.00	0.00	0.00
300	0.31	0.04	99.80	0.00	0.16
350	0.35	6.38	91.35	0.16	2.11
400	0.75	73.98	21.54	1.39	3.10
450	0.79	65.08	27.36	4.73	2.83
500	1.19	47.19	26.84	24.31	1.65

Table E18 Data of Figure 5.16a

Reaction temperature (°C)	Component				
	% methanol (C)	% methane (S)	% formaldehyde (S)	% CO (S)	% CO_2 (S)
100	0.00	0.00	0.00	0.00	0.00
150	0.00	0.00	0.00	0.00	0.00
200	0.00	0.00	0.00	0.00	0.00
250	0.00	0.00	0.00	0.00	0.00
300	0.00	0.00	0.00	0.00	0.00
350	0.09	67.91	0.00	0.00	32.09
400	0.13	24.12	0.00	13.50	62.38
450	34.73	0.66	0.00	95.32	4.02
500	99.50	0.32	0.00	95.43	4.25

Table E19 Data of Figure 5.16b

Reaction temperature (°C)	Component				
	% methanol (C)	% methane (S)	% formaldehyde (S)	% CO (S)	% CO_2 (S)
100	0.00	0.00	0.00	0.00	0.00
150	0.00	0.00	0.00	0.00	0.00
200	0.03	0.00	99.90	0.00	0.10
250	0.02	0.00	94.00	2.49	3.52
300	1.03	0.00	98.38	0.14	1.48
350	10.60	0.00	97.33	0.37	2.30
400	33.18	0.24	1.65	9.92	88.20
450	78.53	4.33	0.00	2.53	93.14
500	97.90	1.36	0.00	0.62	98.02

Table E20 Data of Figure 5.16c

Reaction temperature (°C)	Component				
	% methanol (C)	% methane (S)	% formaldehyde (S)	% CO (S)	% CO_2 (S)
100	0.00	0.00	0.00	0.00	0.00
150	0.00	0.00	0.00	0.00	0.00
200	0.07	0.00	99.90	0.00	0.10
250	0.07	0.00	90.00	0.00	10.00
300	0.27	0.00	88.67	0.00	11.33
350	5.63	0.00	97.88	0.31	1.82
400	29.19	0.00	46.66	3.93	49.41
450	71.63	0.00	0.00	2.81	97.19
500	92.24	0.00	0.00	0.43	99.57

Table E21 Data of Figure 5.16d

Reaction temperature (°C)	Component				
	% methanol (C)	% methane (S)	% formaldehyde (S)	% CO (S)	% CO_2 (S)
100	0.00	0.00	0.00	0.00	0.00
150	0.00	0.00	0.00	0.00	0.00
200	0.00	0.00	0.00	0.00	0.00
250	0.02	0.00	99.77	0.00	0.22
300	0.32	0.00	99.73	0.00	0.27
350	4.38	0.00	99.70	0.00	0.30
400	32.81	0.00	98.84	0.00	1.16
450	77.67	0.00	34.14	0.00	65.86
500	92.99	0.00	0.00	0.00	100.00

APPENDIX F

MATERIAL SAFETY DATA SHEET

1-Propanol

Safety data for 1-Propanol

General

Synonyms: n-Propyl alcohol

Molecular formula: C_3H_8O

Chemical formula: $CH_3CH_2CH_2OH$

Physical data

Melting point: -127°C

Boiling point: 96.5-98 °C

Ignition temperature: 360°C

Flash point: 15°C

Explosion limits: 2.1 % - 13.5 %

Vapor pressure: 14 mm (14.7°C)

Relative vapor density: 2.1

Density: 0.80 g cm^{-3} (20°C)

Solubility in water: miscible in all proportions (20°C)

Stability

Conditions to be avoided: Strong heating.

Substances to be avoided: alkali metals, alkaline earth metals, alcoholates, and strong oxidizing agents.

Further information: highly inflammable, explosive with air in a vaporous/gaseous state.

Toxicology

Further toxicological information

After inhalation: Irritations of the mucous membranes, coughing, dyspnoea, Drowsiness

After skin contact: Slught irritations.

After eye contact: Irritations, risk of serious damage to eyes.

After swallowing: rapid absorption, headache, dizziness, inebriation, unconsciousness, narcosis and risk of aspiration upon vomiting

After uptake of large quantities: respiratory paralysis, coma

Personal protection

Personal protective equipment: Protective clothing should be selected specifically for the working place, depending on concentration and quantity of the hazardous substances handled. The resistance of the protective clothing to chemicals should be ascertained with the respective supplier.

Industrial hygiene: Immediately change contaminated clothing. Apply Skin-protective barrier cream. Wash hands and face after working with substance. Work under hood. Do not inhale substance.

2-Propanol

Safety data for 2-Propanol

General

Synonyms: Isopropanol, Isopropyl alcohol

Molecular formula: C_3H_8O

Chemical formula: $CH_3CH(OH)CH_3$

Physical data

Melting point: -89.5°C

Boiling point: 82.4 °C

Ignition temperature: 425°C

Flash point: 12°C

Explosion limits: 2 % - 12.7 %

Vapor pressure: 31.68 mm (14.7°C)

Relative vapor density: 2.07

Density: 0.786 g cm^{-3} (20°C)

Solubility in water: soluble (20°C)

Stability

Conditions to be avoided: Strong heating.

Substances to be avoided: alkali metals, alkaline earth metals, aluminium in powder form, oxidizing agent, organic nitro compounds, aldehydes, amines, fuming sulfuric acid, phosgene.

Hazardous decomposition products: no information available.

Further information: highly inflammable; hygroscopic, explosive with air in a vapor/gas state.

Toxicology

Further toxicological information

After inhalation: Irritation symptoms in the respiratory tract Drowsiness

After skin contact: degreasing effect on the skin possibly followed by secondary inflammation.

After eye contact: Irritations.

After swallowing: after accidental swallowing the substance may pose a risk of aspiration. Passage into the lung can result in a condition resembling pneumonia

After absorption: headache, dizziness, inebriation

After uptake of large quantities: respiratory paralysis, coma.

Personal protection

Personal protective equipment: Protective clothing should be selected specifically for the working place, depending on concentration and quantity of the hazardous substances handled. The resistance of the protective clothing to chemicals should be ascertained with the respective supplier.

Industrial hygiene: Change contaminated clothing. Application of Skin-protective barrier cream recommended. Should be wash hands after working with substance.

Methanol

Safety data for Methanol

General

Synonyms: Methyl alcohol

Molecular formula: CH_4O

Chemical formula: CH_3OH

Physical data

Melting point: -98 °C

Boiling point: 64.5 °C

Ignition temperature: 455 °C

Flash point: 11 °C c.c.

Explosion limits: 5.5 % - 36.5 %

Relative vapor density: 1.11

Density: 0.79 g cm^{-3} (20 °C)

Solubility in water: soluble (20 °C)

Stability

Conditions to be avoided: Heating.

Substances to be avoided: acid halides, alkali metals, alkaline earth metals, oxidizing egent (i.a. perchloric acid, perchlorates, salts of oxyhalogenic acids, CrO_3, halogen oxides, nitric acid, nitrogen oxides, nonmetallic oxides, chromosulfuric acid), hydrides, zinc diethyl, halogens.

Hazardous decomposition products: no information available.

Further information: highly inflammable, hygroscopic

Toxicology

Further toxicological information

After inhalation of vapors: Irritation symptoms in the respiratory tract.

After skin contact: slow absorption.

After eye contact: Slight Irritations. Mucosal irritations.

After swallowing: absorption.

After absorption: nausea, vomiting, headache, dizziness, inebriation, impaired vision, blindness (Irreversible damage of the optical nerve).

Systemic effects: acidosis, drop in blood pressure, agitation, spasms, narcosis, coma Symptoms may occur after a latency period has elapsed.

Personal protection

Personal protective equipment: Protective clothing should be selected specifically for the working place, depending on concentration and quantity of the hazardous substances handled. The resistance of the protective clothing to chemicals should be ascertained with the respective supplier. Immediately change contaminated clothing. Apply Skin- protective barrier cream. Wash hands and face after working with substance. Work under hood. Do not inhale substance. Under no circumstances eat or drink at workplace.

Ethanol

Safety data for Ethanol

General

Synonyms: Ethyl alcohol

Molecular formula: C_2H_6O

Chemical formula: C_2H_5OH

Physical data

Melting point: -114.5 °C

Boiling point: 78.3 °C

Ignition temperature: 425 °C

Flash point: 12 °C c.c.

Explosion limits: 3.5 % - 15 %

Relative vapor density: 1.6

Density: 0.790-0.793 g cm^{-3} (20 °C)

Solubility in water: soluble (20 °C)

Stability

Conditions to be avoided: Heating.

Substances to be avoided: alkali metals, alkaline earth metals, alkali oxides, strong oxidizing agent, halogen-halogen compounds, CrO_3, chromyl chloride, ethylene oxide, fluorine, perchlorates, potassium permanganate / sulfuric acid, perchloric acid, permanganic acid, phosphorus oxides, nitric acid, nitrogen dioxide, uranium hexafluoride, hydrogen peroxide.

Hazardous decomposition products: no information available.

Further information: highly inflammable.

Toxicology

Further toxicological information

After inhalation of vapors: slight mucosal irritations. Risk of absorption.

After skin contact: After long-term exposure to the chemical: dermatitis.

After eye contact: Slight Irritations.

After swallowing of large amounts: nausea and vomiting.

Systemic effects: euphoria.

After absorption of large quantities: dizziness, inebriation, narcosis, respiratory paralysis.

Personal protection

Personal protective equipment: Protective clothing should be selected specifically for the working place, depending on concentration and quantity of the hazardous substances handled. The resistance of the protective clothing to chemicals should be ascertained with the respective supplier. Change contaminated clothing. Application of Skin- protective barrier cream recommended. Should be wash hands after working with substance.

APPENDIX G

LIST OF PUBLICATION

Chairat, K. and Mongkhonsi, T., “Application of the titanium silicalite-1 catalyst on the selective oxidation of alcohols”, *Regional Symposium on Chemical Engineering 2004*:NS-068

Application of the titanium silicalite-1 catalyst on the selective oxidation of alcohols

Kedsuda Chairat, Tharathon Mongkhonsi*
Center of Excellence on Catalysis and Catalytic Reaction Engineering
Department of Chemical Engineering, Faculty of Engineer, Chulalongkorn University,
Bangkok 10330, Thailand.
**e-mail: kedsuda_541@chula.com*

Abstract

The reactivity of TS-1 catalyst in the gas phase oxidation of 1-propanol and 2-propanol under inlet conditions of 0, 8, 16 and 21 vol% O_2 was studied by using a microreactor at temperature ranging from 373 to 773 K and atmospheric pressure. The results of 1-propanol reaction show that the major product was acetone while the major product of 2-propanol was propylene. Moreover, the reaction temperature affected the product selectivity.

1. Introduction

Selective oxidation is an important reaction that widely used in several processes to produce chemical intermediates of use in many industries. In recent years, selective oxidation of alcohols using different catalysts is interested. In particular, research has been studied to develop suitable heterogeneous catalysts that can be used. Most attention has been given to noble metal and to transition metal oxide catalysts is effective for oxidation of alcohols. Previous studies discovered that unsupported Co-Mg-O and supported Co-Mg-O systems can selectively oxidise alcohols (Mongkhonsi et al., 2001; Mongkhonsi et al., 2002). In the last decade, titanium silicalite-1 (TS-1), which has very interesting properties as a catalyst for several important oxidation reactions such as the olefin epoxidation, the phenol hydroxylation and the liquid phase oxidation of alcohol is attended. The gas phase oxidation of organic reactants using TS-1 has yet to be explored.

The present study investigates the oxidation properties of TS-1 for the oxidation of alcohols, such as methanol, ethanol, 1-propanol and 2-propanol. In addition, the concentration of oxygen is studied to determine the effect of oxygen concentration on the conversion of alcohols and product selectivities.

2. Experimental

2.1 Catalyst preparation and characterization

TS-1 was prepared according to the hydrothermal procedure. Tetraethyl orthotitanate was added dropwise to tetraethyl othorsilicate and the mixture was stirred at 35°C. To the clear solution, tetrapropyl ammonium hydroxide was added with stirring and then heating at 80°C for 1 hr. The clear gel was stirred at 80°C for 3 hrs to aid hydrolysis; during the procedure, the volume was maintained by addition of deionized water. The resulting solution was heated in a Teflon-lined stainless steel autoclave at 175°C for 4 days. The crystalline material was recovered by centrifuging washed with deionized water, dried at 110°C for 1 day, and calcined in air at 550°C for 6 hrs.

The composition of TS-1 was determined by Atomic Adsorption Spectroscopy and the catalyst was characterized by using x-ray diffraction, N_2-adsorption and FT-IR.

2.2 Reaction system

The catalytic test reaction was performed in a microreactor, using 0.1 g of catalyst at 100-500 ^{0}C. The reactant was fed to the reactor by flowing a part of the N_2 stream through a saturator containing the alcohol and then mixing with air and N_2 before reaching the catalyst. The total flow rate was 100 ml/min.

The composition of alcohol in the feed and product stream was analyzed by a Shimadzu GC 8A gas chromatograph equipped with a FID. A Shimadzu GC 8A gas chromatograph equipped with a TCD was used to analyze permanent gases and water. A MS-5A column is used to analyze O_2 and CO while a Porapak-Q was used to analyze CO_2 and H_2O.

3. Result and Discussion

3.1 Catalyst Characterization

The result of mole ratio of Si/Ti and BET surface area of TS-1 are 34.26 and 160 m^2/g, respectively. The x-ray diffraction is a technique which can identify the crystal structure. The XRD pattern indicated similarly six main peaks at 2θ as 8, 8.8, 14.8, 23.1, 24 and 26.7. The pattern obtained is the pattern typical for a crystalline zeolite having a MFI structure.

IR spectrum shows that Ti has entered the silicalite lattice, since an additional band typical for tetrahedral group $Ti(OSi)_4$ appears in the silicalite spectrum at 960 cm^{-1}.

3.2 Catalytic activity of TS-1

3.2.1 *1-propanol oxidation*

Figure 1 shows the conversions of 1-propanol at the feed gas contained 0 vol% O_2, 8 vol% O_2, 16 vol% O_2 and 21 vol% O_2. At the concentration of oxygen in feed gas was 0 vol% O_2, from 250-300 ^{0}C the 1-propanol conversion increased from 0.18% to 3.53 % before rapidly increased to nearly 100% at 400 ^{0}C. It is also observed that the O_2 concentration of 8, 16 and 21 vol% exhibited similar behavior for the oxidation of 1-propanol. In the reaction temperature range 250-350 ^{0}C, the conversion rose quickly to 100% followed by a rapid decreased in the temperature range 350-400 ^{0}C.

In the low reaction temperature region (100-300 ^{0}C), the main product was acetone with selectivity higher than 90% for all oxygen concentration used. Also, there was some formation of propylene, isopropyl ether and CO_2. When the temperature is further increased to 500 ^{0}C, the main product became CO_2, Table 1.

3.2.2 *2-propanol oxidation*

The conversions of 2-propanol are showed in figure 2. At low temperature (100-300°C) of 0 vol% O_2, the conversion of 2-propanol slightly rose followed by rapid increase in the temperature range 300-500°C to 100%. When oxygen in the feed was around 8 vol%, the conversion of 2-propanol gradually increased at reaction temperature range 100-200°C before rapidly rose to about 100% at 300°C. It was found that 16 vol% O_2 and 21 vol% O_2 systems showed similar behavior, the conversion of 2-propanol quickly reached to 100% at a reaction temperature of around 200°C and dropped to 75% at 500°C for 21 vol% O_2 system.

Product selectivities of 2-propanol oxidation are presented in Table 2. The result for the 0 vol% O_2 system showed that the main products were propylene and acetone. An increase of reaction temperature caused selectivity to approach 100% both of propylene and acetone. At the low reaction temperature of 8 vol% of O_2, the major product was propylene with selectivity from 6.24% to 100% followed by rapid decrease in the temperature range 300-400°C. Beyond 100 ^{0}C, the CO_2 selectivity was 31.25% before fell to 0% at 150 ^{0}C. In case of 16 vol% O_2, the propylene selectivity quickly rose from 0% to 90.92% at 150°C. In the temperature range 100-250°C, the main product was propylene with trace of acetone. In the region (250-400°C), acetone selectivity increased from 0.64% to 72.63% before dropped very fast at 450°C. As presented in Table 2, the selectivity to propylene of 21vol% O_2 reached 100% at 100°C while the selectivity to acetone rose to reach a maximum value about 100% at 250°C. Trace of isopropyl ether was detected in the range 350-400°C.

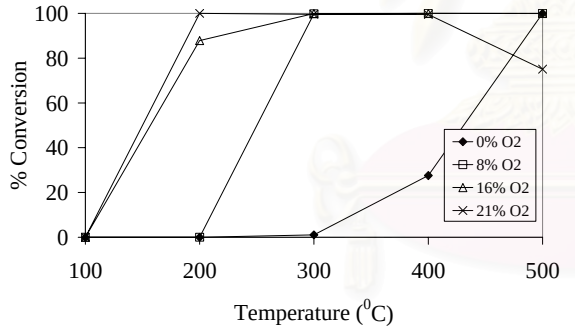

Fig. 1 The catalytic activity for 1-propanol oxidation.

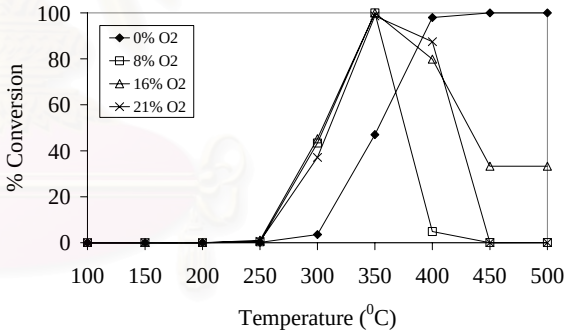

Fig. 2 The catalytic activity for 2-propanol oxidation.

Table 1 Product selectivities of 1-propanol oxidation

Temp.	0 vol% O_2	8 vol% O_2				16 vol% O_2				21 vol% O_2			
(^{0}C)	C_3H_6O	C_3H_6	$C_6H_{14}O$	C_3H_6O	CO_2	C_3H_6	$C_6H_{14}O$	C_3H_6O	CO_2	C_3H_6	$C_6H_{14}O$	C_3H_6O	CO_2
100	100.0	0.0	0.0	0.0	0.0	0.0	0.0	0.0	0.0	0.0	0.0	0.0	0.0
150	100.0	0.0	0.0	100.0	0.0	0.0	0.0	100.0	0.0	0.0	0.0	100.0	0.0
200	100.0	0.0	0.9	99.6	0.0	0.0	1.7	99.1	0.0	0.0	0.4	99.8	0.0
250	100.0	0.0	0.2	99.9	0.0	0.0	0.4	99.8	0.0	0.0	0.4	99.8	0.0
300	100.0	0.0	1.2	99.4	0.0	0.0	2.0	99.0	0.0	0.0	1.6	99.2	0.0
350	100.0	0.0	3.4	98.3	0.0	0.0	12.5	93.7	0.0	0.0	12.8	93.6	0.0
400	100.0	0.0	0.0	98.8	0.4	0.0	0.0	100.0	0.0	0.0	0.0	100.0	0.0
450	100.0	1.3	0.0	0.0	32.9	2.2	0.0	0.0	32.6	10.4	0.0	0.0	29.9
500	100.0	1.3	0.0	0.0	32.9	2.5	0.0	0.0	32.5	3.1	0.0	0.0	32.3

Table 2 Product selectivities of 2-propanol oxidation

Temp.	0 vol% O_2	8 vol% O_2				16 vol% O_2				21 vol% O_2			
(^{0}C)	C_3H_6O	C_3H_6	$C_6H_{14}O$	C_3H_6O	CO_2	C_3H_6	$C_6H_{14}O$	C_3H_6O	CO_2	C_3H_6	$C_6H_{14}O$	C_3H_6O	CO_2
100	100.0	0.0	0.0	0.0	0.0	0.0	0.0	0.0	0.0	0.0	0.0	0.0	0.0
150	100.0	0.0	0.0	100.0	0.0	0.0	0.0	100.0	0.0	0.0	0.0	100.0	0.0
200	100.0	0.0	0.9	99.6	0.0	0.0	1.7	99.1	0.0	0.0	0.4	99.8	0.0
250	100.0	0.0	0.2	99.9	0.0	0.0	0.4	99.8	0.0	0.0	0.4	99.8	0.0
300	100.0	0.0	1.2	99.4	0.0	0.0	2.0	99.0	0.0	0.0	1.6	99.2	0.0
350	100.0	0.0	3.4	98.3	0.0	0.0	12.5	93.7	0.0	0.0	12.8	93.6	0.0
400	100.0	0.0	0.0	98.8	0.4	0.0	0.0	100.0	0.0	0.0	0.0	100.0	0.0
450	100.0	1.3	0.0	0.0	32.9	2.2	0.0	0.0	32.6	10.4	0.0	0.0	29.9
500	100.0	1.3	0.0	0.0	32.9	2.5	0.0	0.0	32.5	3.1	0.0	0.0	32.3

4. Conclusions

1. Product selectivity of the reaction depends on the reactant and the reaction temperature range.
2. The increase oxygen concentration in the feed gas would increase the % conversion of alcohol.

5. References

Mongkhonsi, T., Youngwanishsate, W., Kittikerdkulchai, S., Praserthdam, P., Selective oxidation of alcohols over Co-Mg-O catalyst, J. Chin. Inst. Chem. Engrs., **32** (2001): 183-186

Mongkhonsi, T., Chaiyasit, N., Praserthdam, P., Selective oxidation of 1-propanol and 2-propanol over supported Co-Mg-O catalysts, J. Chin. Inst. Chem. Engrs., **33** (2002): 365-372

VITA

Miss Kedsuda Chairat was born on September 4th, 1981 in Bangkok, Thailand. She finished high school from Satriwitthaya 2 School, Bangkok in 1999, and received the bachelor's degree of Chemical Technology from Faculty of Science, Chulalongkorn University in 2003. She continued her master's study at Department of Chemical Engineering, Faculty of Engineering, Chulalongkorn University in June, 2003.